Pergamon

Prog. Energy Combust. Sci. Vol. 20, pp. 149–202, 1994

0360–1285/94 $26.00

0360–1285(94)00006–9

NITROUS OXIDE BEHAVIOR IN THE ATMOSPHERE, AND IN COMBUSTION AND INDUSTRIAL SYSTEMS

JOHN C. KRAMLICH*† and WILLIAM P. LINAK††

†Department of Mechanical Engineering, FU-10, University of Washington, Seattle, WA 98195, U.S.A.
††Combustion Research Branch, U.S. Environmental Protection Agency, MD-65, Air and Energy Engineering Research Laboratory, Research Triangle Park, NC 27711, U.S.A.

Received 19 April 1994

Abstract—Tropospheric measurements show that nitrous oxide (N_2O) concentrations are increasing over time. This demonstrates the existence of one or more significant anthropogenic sources, a fact that has generated considerable research interest over the last several years. The debate has principally focused on (1) the identity of the sources, and (2) the consequences of increased N_2O concentrations. Both questions remain open, to at least some degree.

The environmental concerns stem from the suggestion that diffusion of additional N_2O into the stratosphere can result in increased ozone (O_3) depletion. Within the stratosphere, N_2O undergoes photolysis and reacts with oxygen atoms to yield some nitric oxide (NO). This enters into the well known O_3 destruction cycle. N_2O is also a potent absorber of infrared radiation and can contribute to global warming through the greenhouse effect.

A major difficulty in research on N_2O is measurement. Both electron capture gas chromatography and continuous infrared methods have seen considerable development, and both can be used reliably if their limitations are understood and appropriate precautions are taken. In particular, the ease with which N_2O is formed from NO in stored combustion products must be recognized; this can occur even in the lines of continuous sampling systems.

In combustion, the homogeneous reactions leading to N_2O are principally $NCO + NO \rightarrow N_2O + CO$ and $NH + NO \rightarrow N_2O + H$, with the first reaction being the most important in practical combustion systems. Recent measurements have resulted in a revised rate for this reaction, and the suggestion that only a portion of the products may branch into $N_2O + CO$. Alternatively, recent measurements also suggest a reduced rate for the $N_2O + OH$ destruction reaction. Most modeling has been based on the earlier kinetic information, and the conclusions derived from these studies need to be revisited.

In high-temperature combustion, N_2O forms early in the flame if fuel-nitrogen is available. The high temperatures, however, ensure that little of this escapes, and emissions from most conventional combustion systems are quite low. The exception is combustion under moderate temperature conditions, where the N_2O is formed from fuel-nitrogen, but fails to be destroyed. The two principal examples are combustion fluidized beds, and the downstream injection of nitrogen-containing agents for nitrogen oxide (NO_x) control (e.g., selective noncatalytic reduction with urea).

There remains considerable debate on the degree to which homogeneous vs heterogeneous reactions contribute to N_2O formation in fluidized bed combustion. What is clear is that the N_2O yield is inversely proportional to bed temperature, and conversion of fuel-nitrogen to N_2O is favored for higher-rank fuels. Fixed-bed studies on highly devolatilized coal char do not indicate a significant role for heterogeneous reactions involving N_2O destruction. The reduction of NO at a coal char surface appears to yield significant N_2O only if oxygen (O_2) is also present. Some studies show that the degree of char devolatilization has a profound influence on both the yield of N_2O during char oxidation, and on the apparent mechanism. Since the char present in combustion fluidized beds will likely span a range of degrees of devolatilization, it becomes difficult to conclusively sort purely homogeneous behavior from potential heterogeneous contributions in practical systems.

Formation of N_2O during NO_x control processes has primarily been confined to selective noncatalytic reduction. Specifically, when the nitrogen-containing agents urea and cyanuric acid are injected, a significant portion (typically >10%) of the NO that is reduced is converted into N_2O. The use of promoters to reduce the optimum injection temperature appears to increase the fraction of NO converted into N_2O. Other operations, such as air staging and reburning, do not appear to be significant N_2O producers. In selective catalytic reduction the yield of N_2O depends on both catalyst type and operating condition, although most systems are not large emitters.

Other systems considered include mobile sources, waste incineration, and industrial sources. In waste incineration, the combustion of sewage sludge yields very high N_2O emissions. This appears to be due to the very high nitrogen content of the fuel and the low combustion temperatures. Many industrial systems are largely uncharacterized with respect to N_2O emissions. Adipic acid manufacture is known to produce large amounts of N_2O as a by-product, and abatement procedures are under development within the industry.

* Author to whom correspondence should be addressed.

CONTENTS

1. INTRODUCTION

Nitrous oxide (N_2O) was long neglected as a pollutant species in comparison to the attention given to the other nitrogen oxides (NO_x). Unlike other NO_x species, N_2O is known to be extremely inert in the troposphere. This inertness suggested that there was little environmental consequence associated with N_2O emission, so it was easy to consider it a nonpollutant.

The well-known toxicological (i.e., anesthetic) response in humans appears only when N_2O is administered in high concentration, typically 80%, with the balance being oxygen to prevent asphyxiation. The concentrations encountered in nature and in industrial emissions are so far below the level needed to elicit an immediate toxicological response that N_2O cannot be considered a pollutant on this basis.

In a more practical vein, the difficulty involved in obtaining N_2O measurements probably contributed to its neglect for many years. At times when NO_x measurements were being routinely made on many sources, N_2O was still a specialty measurement requiring return of batch samples to the laboratory, followed by a difficult gas chromatographic analysis.

Interest in N_2O emissions was largely started by atmospheric chemists, who observed that the tropospheric concentration was increasing with time at a rate of approximately 0.25%/yr. This increase suggested the existence of at least one unknown, substantial anthropogenic source. It also triggered interest in the consequences of this increased tropospheric N_2O burden.

Examination of the global N_2O budget shows that, while its source (natural and anthropogenic) is through ground level emissions into the troposphere, its primary sink occurs through diffusion to the stratosphere. Here, the N_2O is finally destroyed by either photolysis or reaction with singlet oxygen atoms. The result is that a portion of the N_2O is converted into nitric oxide, which enters the ozone destruction cycle. Thus, increased tropospheric N_2O concentrations can lead to increased O_3 removal rates. (It is critical to remember that considerable N_2O is made naturally, and this represents a major contribution to *natural* O_3 destruction in the stratosphere. The concern is that increased anthropogenic N_2O will accelerate this natural rate. This differs from the chlorofluorocarbon (CFC) problem where the natural tropospheric concentration is zero.)

The actual influence of the additional N_2O flux on stratospheric O_3 is itself an issue. In particular, chemical mechanisms have been proposed by which N_2O acts to lessen the O_3 destruction tendencies of CFCs. Thus, the problem presented by N_2O towards stratospheric O_3 remains a cause for debate.

In addition to its impact on stratospheric O_3, N_2O contributes to global warming. The N_2O molecule is a strong absorber of infrared radiation at wavelengths where carbon dioxide (CO_2) is transparent. Although the concentration of N_2O is much less than that of CO_2, it is a much stronger absorber on a molecule-by-molecule basis. This suggests that increased N_2O concentrations in the troposphere could lead to more retention of long-wavelength radiation emitting from the surface of the Earth.

The search for anthropogenic sources has concentrated on (1) industrial processes that may emit globally significant quantities of N_2O, and (2) biological processes that may produce N_2O on a widespread basis. Although there has been extensive work in both of these areas, the work has been hampered by measurement difficulties. Nonetheless, a substantially improved picture of the global N_2O budget has emerged. Based on this understanding, steps are being taken to modify the processes that generate anthropogenic N_2O.

Certain features have come to be recognized as contributing to N_2O emissions from combustion systems. First and foremost is the oxidation of fuel-nitrogen under relatively low-temperature conditions. This allows N_2O to form, and to avoid subsequent destruction. Thus, any system in which nitrogen in a combined form is oxidized under relatively low temperatures can lead to N_2O emissions. Practical examples include combustion fluidized beds, and NO_x control processes that involve the downstream injection of nitrogen-containing compounds, such as urea. In most combustion systems, however, the flame temperature is sufficiently high that any N_2O formed in the flame zone is destroyed before the gases are emitted. Thus, most combustion systems do not emit much N_2O.

This entire area is relatively new and is continuing to evolve. The purpose of writing this review is twofold: (1) to identify the bulk of the work performed on N_2O to date, and (2) to attempt as fair a comparison of the frequently contradictory results as possible. The latter is particularly difficult because many investigators are simultaneously working on the same problem, and have not had an opportunity to resolve differing results. Thus, for example, reports of work on fluidized bed combustors frequently appear on initial impression to be contradictory. As is clear from the following discussion, many issues cannot yet be resolved in terms of simple mechanisms.

This review describes atmospheric behavior and measurement systems. The discussion of the behavior of N_2O in combustion systems includes homogeneous and heterogeneous flame chemistry, pulverized coal and fluid bed combustion systems, and thermal waste remediation. The review concludes with a review of information on N_2O behavior during NO_x control activities, N_2O from mobile sources, and N_2O from other industrial sources.

Notably missing is any discussion of N_2O from biological activities. Although this is an important component of the global N_2O budget, it falls outside of the scope of this review.

2. ATMOSPHERIC CHEMISTRY AND ENVIRONMENTAL CONSEQUENCES

2.1. *Role of N_2O in Global Warming*

With an effective surface temperature of approximately 6000 K, most of the sun's radiation is emitted within a spectral range of 100 to 3000 nm. These wavelengths include the visible region and portions

TABLE 1. Summary of key greenhouse gases (adapted from Ramanathan,[1] Levine,[2] and Houghton *et al.*[3])*

	CO_2	CH_4	Refrigerant-11 CCl_3F	Refrigerant-12 CCl_2F_2	CH_3CCl_3	CCl_4	N_2O
Pre-industrial atmospheric conc. (1750–1800)	275–280 ppm	0.7–0.8 ppm	0	0	0	0	285–288 ppb
Approximate current atmospheric conc. (1985–1990)†	345–353 ppm	1.72 ppm	220–280 ppt	380–484 ppt	130 ppt	120 ppt	304–310 ppb
Current rate of annual atmospheric accumulation	1.8 ppm (+0.46–0.5%)	0.015 ppm (+0.9–1.1%)	9.5 ppt (+4.0–10.3%)	17 ppt (+4–10.1%)	+15.5%	+2.4%	0.8 ppb (+0.25–0.35%)
Projected atmospheric conc. mid-21st century‡	400–600 ppm	2.1–4.0 ppm	700–3000 ppt	2000–4800 ppt			350–450 ppb
Atmospheric lifetime§	50–200 year	10 yr	65 yr	130 yr			150 yr

*% = percent by volume, ppm = parts per million by volume, ppb = parts per billion (10^9) by volume, ppt = parts per trillion (10^{12}) by volume.

†1990 concentrations are based on extrapolation of measurements reported for earlier years.

‡Mid-21st century concentrations are based on current annual rate of atmospheric accumulation, and do not consider activities aimed at reducing emissions.

§Atmospheric lifetime defined as the ratio of atmospheric content to the total rate of removal. CO_2 lifetime is a rough indication of the time necessary for CO_2 concentrations to adjust to changes in emissions.

of the ultraviolet and infrared spectra. The Earth's atmosphere is transparent to most of this incident radiation and, as this radiation reaches the Earth, it is either reflected back to space or absorbed to heat the surface. To maintain constant temperatures, heat gained by the sun's incident radiation must be balanced by heat losses through re-radiation. With an average temperature of approximately 300 K, the Earth emits most of its radiation at infrared wavelengths above 3000 nm. Unlike inicident solar radiation, the Earth's atmosphere is not entirely transparent to outgoing infrared radiation. Atmospheric gases such as water (H_2O), CO_2, methane (CH_4), N_2O, O_3, and more than 12 synthetic gases such as CFCs and chlorinated solvents, absorb the Earth's radiation. These gases then re-emit this energy. A portion is radiated towards space at cooler atmospheric temperatures, and another portion is radiated back to Earth's surface where it results in additional surface heating. The net result is increased surface temperatures. This "greenhouse" effect is necessary for the existence of life on Earth, and accounts for a temperature enhancement from 253 K (−4 °F), the calculated average surface temperature without a greenhouse effect, to 288 K (59 °F), the Earth's current average temperature.[1,2] Without the greenhouse effect, the Earth would be covered with ice.

While water vapor absorbs radiation across the entire spectrum, other predominant greenhouse gases absorb radiation in distinct bands. These absorption bands are for CO_2 (13,000 to 17,000 nm), CH_4 (7000 to 8000 nm), N_2O (8000 to 8500 nm), and O_3 (9000 to 10,000 nm). In the pre-industrial atmosphere, nearly 80% of the radiation emitted by the Earth was in the spectral range 7000–13,000 nm. This region was referred to as the "window" because of its relative transparency to outgoing radiation.[1] However, as the natural balances of these atmospheric gases are changed (i.e., increased) through human activities, and as previously unknown synthetic greenhouse species, such as CFCs, and chlorinated solvents, are introduced into the atmosphere, this balance is upset, resulting in increased absorption in the CO_2, CH_4, N_2O, and O_3 bands, and new absorption by synthetic gases which absorb strongly in the window region. This increased absorption decreases the Earth's heat loss, and increases the greenhouse effect and net global warming. Since surface temperatures also drive climate and hydrological cycles, the excess energy now available powers changes to weather and precipitation patterns. These effects cannot be easily predicted, however, because of the nonlinear interactions involved.[1]

Table 1 presents a summary of key greenhouse gas concentrations in the atmosphere.[1–3] Comparison is made between pre-industrial concentrations, determined through polar ice core analysis, and current ambient concentrations. The data indicate a trend of increasing atmospheric concentrations for these species. Ramanathan[1] suggests that atmospheric

increases in CH_4 and carbon monoxide (CO), such as those seen during the twentieth century, may have increased tropospheric O_3 concentrations by 20%. Levine[4] identifies the relative contribution of several atmospheric gases to global warming: CO_2 (49%), CH_4 (18%), CFCs (Refrigerant-11 and -12) (14%), N_2O (6%), and other trace gases (13%).

2.2 *Role of N_2O in Stratospheric O_3 Chemistry*

Approximately 85% of the Earth's atmosphere, including almost all of its water vapor, is associated with the troposphere, which extends from the surface to about 15 km. The remaining 15% is associated with the stratosphere, which extends from approximately 15 to 50 km above the Earth's surface. Over 90% of atmospheric O_3 resides in the stratosphere. Stratospheric O_3 acts to shield the earth from biologically lethal ultraviolet (UV) radiation (wavelengths below 310 nm). Most importantly, stratospheric O_3 shields the earth from UV-B radiation with incident wavelengths from 280 to 310 nm. These wavelengths are especially harmful because they lie in a regime where the solar spectrum and DNA (biological) susceptibility overlap.[5]

In recent years, ground-based, aircraft, and satellite measurements have examined stratospheric O_3 concentrations over the Antarctic. These measurements indicate that, during the early Antarctic spring (a 4–6 week period beginning in late September), total column O_3 has decreased by over 50% during the past 10 years. Currently, this behavior seems to be unique to the Antarctic due to spring weather patterns which prevent the transport of O_3 from the southern hemisphere mid-latitudes to the polar regions. As spring progresses, normal circulation patterns are re-established, and the missing O_3 is replenished.[2] In 1988, the Ozone Trends Panel formed by the National Aeronautics and Space Administration (NASA), the National Oceanographic and Atmospheric Administration (NOAA), the World Meteorological Organization, and the United Nations Environment Program concluded that global stratospheric O_3 concentrations had fallen several percent between 1969 and 1986.[2] The Panel found that, during this period, stratospheric O_3 decreased between 1.7 and 3.0% in the area between 30 and 64°N.[2] The Panel also attributed these decreases to increasing atmospheric concentrations of trace gases, primarily CFCs.

In 1929, Chapman[6] identified a "classical" mechanism to describe the formation and destruction of stratospheric O_3. According to this mechanism, the chemical production of O_3 is initiated by the photodissociation of molecular oxygen by solar radiation with wavelengths of 242.3 nm or less:

$$O_2 + h\nu \rightarrow O + O \qquad \lambda \leq 242.3\ \text{nm}. \quad (1)$$

Once dissociated, atomic oxygen may combine with O_2 and a third body, M [usually N_2 or O_2], to form O_3:

$$O + O_2 + M \rightarrow O_3 + M. \quad (2)$$

O_3 destruction can also occur through photodissociation:

$$O_3 + h\nu \rightarrow O + O_2 \quad (3)$$

or through reaction with atomic oxygen:

$$O_3 + O \rightarrow 2O_2. \quad (4)$$

At the time, these reactions were thought to fully describe the global stratospheric O_3 balance. However, over the past 20–30 years three other destruction routes were discovered involving reactions with hydroxyl radical (OH):

$$OH + O_3 \rightarrow HO_2 + O_2 \quad (5)$$

$$HO_2 + O_3 \rightarrow OH + 2O_2 \quad (6)$$

$$HO_2 + O \rightarrow OH + O_2 \quad (7)$$

chlorine:

$$Cl + O_3 \rightarrow ClO + O_2 \quad (8)$$

$$ClO + O \rightarrow Cl + O_2 \quad (9)$$

and NO:

$$NO + O_3 \rightarrow NO_2 + O_2 \quad (10)$$

$$NO_2 + O \rightarrow NO + O_2. \quad (11)$$

Most importantly, these three mechanisms are catalytic in nature, resulting in the destruction of O_3, without the net destruction of the OH, Cl or NO reactants. Thus, these species are recycled and remain available for numerous O_3 destruction steps. A review of the OH and NO chemistry is presented by Crutzen.[7]

2.2.1. *H_2O/OH chemistry*

In the stratosphere, the OH radical is produced through the photodissociation of water:

$$H_2O + h\nu \rightarrow OH + H \qquad \lambda \leq 242\ \text{nm} \quad (12)$$

and through the oxidation of water by excited atomic singlet D oxygen [$O(^1D)$]:

$$H_2O + O(^1D) \rightarrow 2OH. \quad (13)$$

Water reaches the stratosphere through diffusion from the troposphere, and through CH_4 oxidation in the stratosphere:

$$CH_4 + OH \rightarrow CH_3 + H_2O. \quad (14)$$

In addition to direct destruction reactions, the OH radical can also interfere with O_3 production indirectly by consuming atomic oxygen (see Eq. (2)):

TABLE 2. Selected trace gases, and trace nitrogen species in the atmosphere (adapted from Levine[2,8])

	Concentration
Major gases	
Nitrogen (N_2)	78.08%
Oxygen (O_2)	20.95%
Argon (Ar)	0.93%
Selected trace gases	
Water (H_2O)	0 to 2%
Carbon dioxide (CO_2)	353 ppm
Ozone (O_3)	
Tropospheric	0.02 to 0.1 ppm
Stratospheric	0.1 to 10 ppm
Methane (CH_4)	1.72 ppm
Refrigerant-12 (CF_2Cl_2)	0.48 ppb
Refrigerant-11 ($CFCl_3$)	0.28 ppb
Hydroxyl (OH)	
Tropospheric	0.15 ppt
Stratospheric	0.02 to 0.3 ppt
Trace nitrogen species	
Nitrous oxide (N_2O)	310 ppb
Ammonia (NH_3)	0.1 to 1.0 ppb
Nitric oxide (NO)†	
Tropospheric	0 to 1 ppb
Stratospheric	up to 0.02 ppm
Nitric acid (HNO_3)	50 to 1000 ppt
Hydrogen cyanide (HCN)	200 ppt
Nitrogen dioxide (NO_2)	10 to 300 ppt
Nitrogen trioxide (NO_3)‡	100 ppt
Peroxyacetyl nitrate ($CH_3CO_3NO_2$)	50 ppt
Dinitrogen pentoxide (N_2O_5)‡	1 ppt
Pernitric acid (HO_2NO_2)†	0.5 ppt
Nitrous acid (HNO_2)	0.1 ppt
Nitrogen aerosols	
Ammonium nitrate (NH_4NO_3)	10 ppt
Ammonium chloride (NH_4Cl)	0.1 ppt

*% = percent by volume, ppm = parts per million by volume, ppb = parts per billion (10^9) by volume, ppt = parts per trillion (10^{12}) by volume.

†Exhibits strong diurnal variation with maximum concentration during the day.

‡Exhibits strong diurnal variation with maximum concentration during the night.

$$OH + O \rightarrow H + O_2 \quad (15)$$

$$H + O_2 + M \rightarrow HO_2 + M \quad (16)$$

$$HO_2 + O \rightarrow OH + O_2. \quad (17)$$

Again, this catalytic reaction set results in the destruction of atomic oxygen but not in the net destruction of OH radical.

2.2.2. *CFC/Cl chemistry*

Chlorine is produced in the stratosphere through the photodissociation of CFCs:

$$CCl_3F + h\nu \rightarrow CCl_2F + Cl \quad \lambda \leq 265\,nm \quad (18)$$

$$CCl_2F_2 + h\nu \rightarrow CClF_2 + Cl \quad \lambda \leq 200\,nm. \quad (19)$$

These CFCs, Refrigerant-11 (CCl_3F) and Refrigerant-12 (CCl_2F_2), are not naturally occurring in the environment. Their presence in the stratosphere is the result of anthropogenic emissions and diffusion through the troposphere. These compounds are extremely stable in the troposphere and were widely used as propellants, refrigerants, blowing agents, and solvents. Table 1 indicates that Refrigerant-11 and -12 exhibit mean atmospheric lifetimes of approximately 65 and 130 years, respectively.[2] As a consequence of concern regarding stratospheric O_3 destruction, these compounds are being replaced. However, adequate substitutes are not always available, and those that are available, such as hydrochlorofluorocarbons (HCFCs) including Refrigerant-21 ($CHCl_2F$) and Refrigerant-22 ($CHClF_2$), also have the potential for O_3 destruction, although to a somewhat lesser extent. In addition to CFCs and HCFCs, other anthropogenic sources, such as solvents and pesticides, may contribute to the stratospheric chlorine loading.

2.2.3. *N_2O/NO chemistry*

The stratospheric formation of NO is the result of photolysis of N_2O and reaction with $O(^1D)$, via the reaction set:

$$N_2O + h\nu \rightarrow N_2 + O(^1D) \quad (20)$$

$$N_2O + O(^1D) \rightarrow 2NO \quad (21)$$

$$N_2O + O(^1D) \rightarrow N_2 + O_2. \quad (22)$$

Levine[2] identifies the photolysis reaction (Eq. (20)) as being responsible for approximately 90% of the N_2O destruction, while Eqs (21) and (22) each account for about 5% of its destruction. With an atmospheric lifetime of approximately 150 years (see Table 1), N_2O is extremely long-lived. N_2O is also very stable in the troposphere. Its destruction takes place only after its diffusion into the stratosphere.[2] The reaction in Eq. (21) leads to the production of stratospheric NO and to the subsequent chemical destruction of stratospheric O_3 through the reactions described in Eqs (10) and (11), with the net result:

$$O_3 + O \rightarrow 2O_2.$$

Note that, as with the OH radical and Cl reactions, NO is not destroyed during this mechanism, and is recycled for further reaction with O_3. Levine[2] identifies this catalytic NO cycle as responsible for about 70% of the global chemical destruction of stratospheric O_3. However, a large portion of this contribution is from natural sources of N_2O. With the exception of relatively minor emissions from high flying aircraft, Eq. (21) is the only known source of stratospheric NO. Other NO_x species released into the troposphere as a consequence of combustion and other industrial activities are quickly removed and do not have the atmospheric lifetimes necessary to reach the stratosphere. Table 2 summarizes the atmospheric concentrations of major gases, selected trace gases (including OH, CFCs, and NO), and trace nitrogen species compiled by Levine.[2,8] It should be

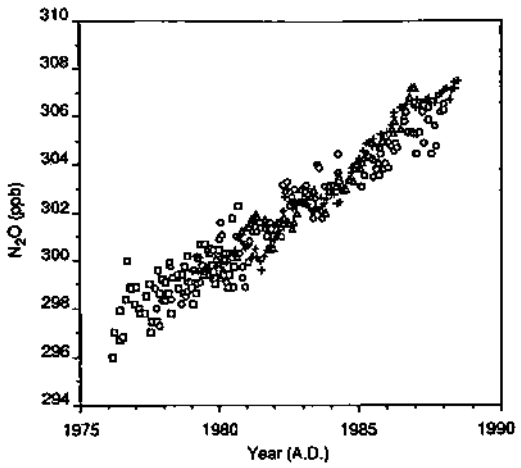

FIG. 1. Tropospheric measurements of N_2O from four independent sets of long-term investigations: □ Weiss,[9] ○ NOAA/GMCC,[11] + ALE-GAGE (Prinn *et al.*[12]), △ Khalil and Rasmussen[13] (adapted from Khalil and Rasmussen[13]).

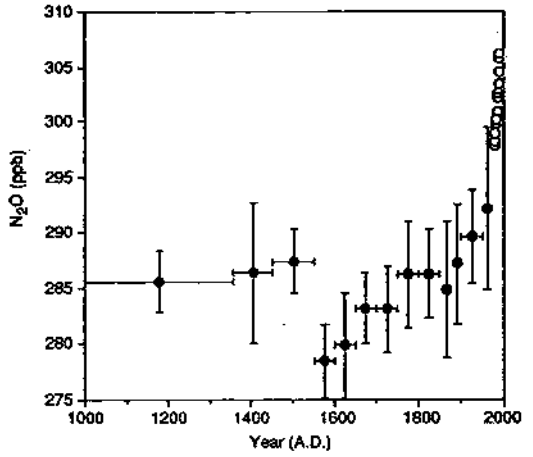

FIG. 2. Composite set of atmospheric concentrations of N_2O over the last 1000 years as determined from ice core air bubbles. Horizontal bars indicate time span over which data are averaged. Recent tropospheric measurements (as annual averages) are included in upper right corner (adapted from Khalil and Rasmussen[13]).

noted that N_2O is the second most abundant nitrogen species in the atmosphere after molecular nitrogen.

Stratospheric O_3 destruction is further complicated by potential interaction between chlorine monoxide (ClO) and nitrogen dioxide (NO_2):

$$ClO + NO_2 \rightarrow ClONO_2. \quad (23)$$

This reaction converts the chain carriers of two catalytic cycles to an "inert" product. Thus, as a result of this interaction, increased N_2O emissions may act to reduce stratospheric O_3 destruction by interfering with atomic chlorine reformation (Eq. (9)). Additionally, the converse is also true, increased CFC emissions may act to interfere with NO reformation (Eq. (11)). However, little is known about this reaction including a complete lack of rate data. Moreover, it is unknown how "inert" the product actually is.

This complex chemistry is further confused when interactions between stratospheric O_3 and the global heat balance are considered. These reactions are all temperature dependent and, by absorbing ultraviolet radiation, O_3 acts to control temperatures in the stratosphere. As stratospheric O_3 is depleted, more radiation reaches the Earth's surface, cooling the stratosphere. In addition, reductions in the Earth's radiative flux which reaches the stratosphere further affect temperatures and reaction rates.

2.3. *Tropospheric Measurements of N_2O*

Since the mid-1970s, systematic tropospheric measurements of N_2O have been made at locations worldwide.[9–12] These data, summarized by Khalil and Rasmussen[13] and presented in Fig. 1, show the atmospheric concentration of N_2O to be currently increasing at an average rate of approximately 0.80 ± 0.02 ppbv per year or approximately $0.27 \pm 0.01\%$ per year.[13] Based on these data, current (1993) atmospheric concentrations are estimated to be 310.5 ppbv. It is also interesting to note that Weiss[9] has determined that N_2O is unequally distributed between the northern and southern hemispheres, with the northern hemisphere higher by 0.83 ± 0.15 ppbv at the time that the measurements were made (1976–1980). This may be indicative of the larger land mass or larger population centers and industrial activity in the northern hemisphere.

Data by Pearman *et al.*,[14] Khalil and Rasmussen,[13,15] Ethridge *et al.*,[16] and Zardini *et al.*[17] examining N_2O concentrations in air bubbles trapped in polar ice core samples suggest that this temporal increase is a relatively recent phenomenon. In polar regions, where yearly snow falls do not melt, air associated with the snow is trapped in tiny bubbles as subsequent accumulation and pressure convert older snow to ice. Analysis of the air within these bubbles can yield information concerning the composition of gases in the atmosphere hundreds, thousands, or tens of thousands of years ago. These data, summarized for the past 1000 years by Khalil and Rasmussen[13] and presented in Fig. 2, include a composite set of measurements from 0–1820 A.D.,[15] 1600–1966 A.D.,[16] 1600–1900 A.D.,[17] and 1800–1900 A.D.[13] Understandably, these data are subject to much more uncertainty compared to the precise measurements of the past 15 years. Evident from Fig. 2 is the absence of any significant trend between 0 and 1500 A.D. At that time, however, concentrations were seen to suddenly drop and then rise again. Khalil and Rasmussen[13] suggest that this phenomenon was the result of the "little ice age" which reportedly occurred at this time and which may have resulted in reduced biological activity. For the period 1880–1960, the trend shows a steady increase of

TABLE 3. Estimates of global sources of N_2O (Tg N per year)*

	de Soete[19]†	Levine[2]	IPCC[20,21]	Elkins[23] and Mann *et al.*[24]‡	Khalil and Rasmussen[13]
Natural sources					
Soils					7.6
Tropical soils		3.7		3.7	
wet forests			2.2–3.7		
dry savannas			0.5–2.0		
Temperate soils		0.01–1.15		<0.5	
forests			0.05–2.0		
grasslands			NK§		
Oceans		1.4–2.6	1.4–2.6	1.4–2.6	1.9
Total natural sources		5.1–7.8	4.2–10.3	5.6–6.8	9.5
Anthropogenic sources					
Biomass burning	0.5 (0.4–0.6)	0.1–1.0	0.2–1.0	0.02–0.29	1.0 (0.1–1.9)
Sewage					1.0 (0.2–2.0)
Agriculture					
cattle operations					0.3 (0.2–0.6)
irrigation (ground water release)				0.5–1.1	0.5 (0.5–1.3)
use of nitrogen fertilizers	1.0 (0.7–1.3)		0.01–2.2	0.015–1.4	0.6 (0.3–1.9)
on agricultural fields		0.01–1.1			
leaching into groundwater		0.5–1.1			
land use changes (deforestation)		0.8–1.3		0.8–1.3	0.4
Fossil fuel combustion		0.1–0.3		<0.5	
stationary sources	0.2 (0.1–0.3)		0.1–0.3		0.0 (0.0–0.1)
mobile sources	0.4 (0.2–0.6)		0.2–0.6		0.5 (0.1–1.3)
Industrial activities					
adipic acid (nylon)			0.4–0.6		NK
nitric acid			0.1–0.3		
Global warming					0.2 (0.0–0.6)
Atmospheric formation (indirect)	NK				NK
Dry and wet deposition				0.13–5.0	
Total anthropogenic sources	2.1 (1.4–2.8)	1.5–4.8	1.0–5.0	2.0–9.6	4.5 (1.8–9.7)
Total	2.1 (1.4–2.8)	6.6–12.6	5.2–15.3	7.6–16.4	14.0 (11.3–19.2)

* 1 Tg = 1×10^6 tonnes = 1×10^{12} g.
† Anthropogenic sources only.
‡ Data presented in the review by Mann *et al.*[24] were taken from Elkins.[22]
§ NK, not known.

0.07 ± 0.01 ppbv per year. For comparison, the most recent atmospheric data (1976–1988) (see Fig. 1 and Table 1) have also been included, and show an even more expanded rate of increase (0.08 ± 0.02 ppbv). Khalil and Rasmussen[13] point out that the ice core data are often imprecise, ambiguous, and subject to potential errors. Moreover, the most recent ice core data (late 1800s–early 1900s) are subject to even greater uncertainties due to problems associated with resolving air bubble formation in ice over short time intervals. A review of the use of ice core data to resolve historical trends of greenhouse gases is presented by Raynaud *et al.*[18]

2.4. *Tropospheric N_2O Balance*

Major uncertainties exist concerning the identification and apportionment of the global sources of N_2O. It is known, however, that these global sources must balance the global rate of atmospheric destruction plus the rate of atmospheric accumulation. Rate data suggest that Eqs (20), (21), and (22) destroy approximately 10.5 ± 3.0 teragrams of nitrogen (in the form of N_2O) per year (Tg N per year). Also, the atmospheric accumulation described above requires the production of another 3.5 ± 0.5 Tg N per year. As a result, total global production of N_2O must be approximately 14 ± 3.5 Tg N per year to balance these destruction and accumulation terms.[2]

Table 3 presents estimates of the global sources of N_2O published by several groups in recent years.[2,13,19–24] The contributions from natural and anthropogenic sources have been grouped separately for comparison. Natural sources include nitrification and denitrification of nitrogen species in soils and oceans. Denitrification involves the chemical transformation of soil nitrate (NO_3^-) to molecular nitrogen

(N_2) and N_2O. Almost all of the N_2O produced by denitrification escapes into the atmosphere. Nitrification involves the oxidation of reduced soil nitrogen species (such as NH_4^+) to nitrite (NO_2^-) and nitrate (NO_3^-) with N_2O as an intermediate product. These same processes are responsible for N_2O production in oceans. However, it is uncertain whether denitrification in oxygen-deficient deep waters or nitrification in oxygen-rich surface waters is repsonsible.[2] Table 3 indicates general agreement among the four recent studies which have presented natural source data. The single exception is the soil source published by Khalil and Rasmussen,[13] which is notably higher than the other estimates.

Table 3 suggests that the global estimates of anthropogenic sources are highly variable, with values ranging from 1.0 to 9.3 Tg N per year. In addition, the different studies often do not include the same set of sources in their anthropogenic estimates. For example, Khalil and Rasmussen[13] include a sewage source that the others do not. IPCC[21] also includes estimates from adipic and nitric acid production which are notably significant. Several data sets[13,19,24] also suggest indirect N_2O formation through atmospheric transformations from NO_x precursors, or heterogeneous mechanisms involving atmospheric nitrates, although these sources are not well quantified. Of particular interest is the potential source identified by Khalil and Rasmussen,[13] which identifies climatic feedback and accelerated biogenic activity from CO_2 increases and global warming as being responsible for approximately 0.2 Tg N per year. This estimate was taken from ice core data and N_2O trends seen during the "little ice age." Evident from Table 3 is that not all global sources of N_2O have been identified, and that those which have been identified are subject to large error as indicated by the large range of estimates presented. However, we see that, while the magnitude of total global sources ranges widely (5.2–16.1 Tg N per year), they bracket the sum of the destruction and accumulation terms determined independently (14 ± 3.5 Tg N per year).

Table 3 indicates that N_2O emissions from fossil fuel combustion sources contribute a relatively small portion of the total anthropogenic source. However, this was not always believed to be true. Only recently, fossil fuel combustion, especially coal combustion, was believed to be the major contributor to measured increases in ambient N_2O concentrations. These increases also seemed to track measured increases in ambient CO_2 concentrations. Previous research[25] presented data indicating direct N_2O emissions from coal combustion exceeding 100 ppm, and an approximate average N_2O–N:NO_x molar ratio of 0.58:1. These data seemed to confirm earlier suggestions[26,27] that combustion of fossil fuels (and coal in particular) represented a dominant factor in the observed increase of N_2O. In addition, emission factors generated using N_2O stack concentrations of 100–200 ppm were adequate to close to global anthropogenic mass balance.

Additional combustion measurements, gathered by a number of research groups, however, did not always confirm the early results. These numerous studies often used various N_2O sampling and analytical methodologies including samples measured on-line and samples extracted into containers for subsequent analysis in a laboratory environment. An explanation for the resulting growing scatter in the data was proposed by Muzio and Kramlich[28] who suggested the presence of an N_2O sampling artifact. They presented evidence that indicated that N_2O was produced in sampling containers awaiting analysis. They further hypothesized a mechanism for this formation involving NO, SO_2, and H_2O. This evidence questioned the validity of all existing data which involved container sampling. Additionally, since secondary reactions converting NO to N_2O in the sample containers were found to occur easily at room temperature,[28–33] a new indirect relationship between anthropogenic NO emissions (including combustion) and global N_2O increases was suggested (see Table 3).[13,19] Although not yet characterized or quantified, this may include NO conversion in plumes, in the troposphere, or on surfaces.[34] Further discussion of the sampling artifact, and the application of sampling and analytical procedures to minimize its effect, is presented in Section 3.

Since the discovery of the sampling artifact, new research has sought to characterize N_2O emissions from fossil fuel combustion sources, and to determine the effect that modifications used to control NO_x has on N_2O emissions. A summary of these findings is presented in Table 4. For conventional stationary combustion sources (including coal combustion), recent measurements indicate average N_2O emissions less than 5 ppm. These values are more than a factor of 20 times less than emissions believed to be produced several years ago. Interestingly, fluidized bed combustors, and several of the thermal $DeNO_x$ and catalytic processes developed for NO_x control, also seem to contribute to increased levels of N_2O. At present, these technologies are not in widespread application, and the associated increases in N_2O emissions do not add significantly to the global flux. However, as these technologies are further developed, and their use becomes more common, they have the potential of affecting global emissions. Several of these technologies will be discussed further in later sections.

3. MEASUREMENT OF N_2O

N_2O from combustion sources has been measured using a variety of methods including both grab (container) sampling and on-line monitoring techniques. Once collected, grab samples are often analyzed using gas chromatography (GC). On-line monitoring

TABLE 4. N_2O emission from fossil fuel combustion (adapted from de Soete[19])

Uncontrolled combustion	N_2O emissions
Conventional stationary combustion (coal, oil, gas)	1–5 ppm
Fluidized bed combustion (depends on temperature, oxygen concentration, physical/chemical properties of fuel)	20–150 ppm
Diesel engines (value given for small passenger cars; heavy duty engine emissions may be higher)	0.03 g N per km
Gasoline engines	0.01–0.03 g N per km
NO_x control technology	**Effect on N_2O emissions**
Fuel staging for conventional stationary combustion	Up to 10 ppmv increase over uncontrolled combustion
Thermal DeNO$_x$ controls (SNCR)	
NH_3 injection	3–5% of NO_x reduction converted to N_2O
Urea or cyanuric acid injection	10–15% of NO_x reduction converted to N_2O
Catalytic processes	
Selective catalytic reduction (SCR)	Limited laboratory studies indicate increased emissions from some catalysts No field data available
Three-way catalysts (gasoline engines)	
New catalysts	3–5 times the uncontrolled emissions
Medium aged catalysts	10–16 times the uncontrolled emissions

methods include nondispersive infrared (NDIR), tunable diode infrared laser (TDIR), Fourier transform infrared (FTIR), and GC techniques. Each of these methods presents its own advantages and disadvantages. This section will present some of the history behind N_2O measurements, briefly describe some of the developing on-line techniques, and then focus in some detail on the configuration and operation of a gas chromatograph/electron capture detection (GC/ECD) method that can be used for on-line or sample container analysis.

3.1. *Atmospheric Analysis Procedures Applied to Combustion Samples*

The origins of most of the analytical procedures that have been applied to measure N_2O concentrations in combustion stack gases lie in the methods developed by atmospheric scientists to measure tropospheric and stratospheric gases including N_2O. These procedures, first developed in the 1960s, employed thermal conductivity GC.[35–37] More recent procedures, however, have used electron capture gas chromatography because of its extremely high sensitivity and specificity for N_2O.[9,26,38–41] In fact, the analytical procedure described in Section 3.4. can trace its origin to the work by Weiss.[9] In addition to the analytical procedures that were adapted from atmospheric sciences, combustion researchers also borrowed the container sampling procedures commonly used for atmospheric measurements. These involved the extractive sampling of flue gases directly into sampling bags or rigid bombs (glass or metal) and then subsequent analyses of these samples at some later time in a remote laboratory. Unfortunately, this procedure led to errors in efforts to establish a global N_2O database in the early to mid-1980s, causing incorrect conclusions concerning the contribution of combustion sources.

3.2. *N_2O Formation in Sampling Containers*

Grab sampling methods are appealing from cost and convenience considerations. However, as mentioned in Section 2, the integrity of samples taken in this manner may be easily compromised under many common combustion sampling conditions.[28,30,33] This sampling artifact has been observed when nitrogen oxides (NO_x), sulfur dioxide (SO_2), and moisture, present in many combustion samples, react in the sampling containers to produce N_2O. N_2O generation in grab sample containers approaching 200 ppm has been observed.[33] However, current research[42,43] is evaluating the use of modified sample conditioning techniques that minimizes or negates N_2O formation in contained samples. This container sampling technique uses calcium hydroxide ($Ca(OH)_2$) and phosphorus pentoxide (P_2O_5) sorbents to selectively remove the SO_2 and moisture. This procedure has been proven able to reduce N_2O formation to under 10 ppm for samples stored for up to 2 weeks with initial NO, SO_2, and moisture contents of 600 ppm, 1200 ppm, and 10%, respectively. The artifact chemistry has been investigated by Muzio *et al.*[30] and Lyon

TABLE 5. Chemical mechanism, rate constants, and equilibrium constants for model to predict N_2O formation in flue gas sampling containers (adapted from Muzio *et al.*[30] and Lyon and Cole[31])*

Gas-phase reaction	Rate constant†
$NO + NO + O_2 \rightarrow NO_2 + NO_2$	6.73×10^3
Liquid-phase reactions	Rate constant
$NO_2 + HSO_3^- \rightarrow NO_2^- + HSO_3$	3.00×10^5
$HSO_3 + HSO_3(+ H_2O) \rightarrow H_2SO_3 + H_2SO_4$	5.00×10^5
$2NO_2 + H_2O \rightarrow HNO_2 + HNO_3$	7.00×10^7
$HNO_2 + HSO_3^- \rightarrow NOSO_3^- + H_2O$	2.40×10^0
$NOSO_3^- + H^+(+ H_2O) \rightarrow HNO + H_2SO_4$	5.00×10^1
$NHO + HNO \rightarrow N_2O + H_2O$	3.00×10^4
$NOSO_3^- + HSO_3^- \rightarrow HNO(SO_3)_2^{-2}$	8.50×10^1
$HNO(SO_3)^{-2} + H^+(+H_2O) \rightarrow HONHSO_3^- + H^+ + HSO_4^-$	1.90×10^{-2}
$HNO(SO_3)^{-2} + H_2O \rightarrow HONHSO_3^- + H^+ + HSO_4^-$	1.50×10^{-6}
Equilibrium processes	Henry's law constant
$NO_2(gas) = NO_2(aq)$	$H = 0.01$ M/atm
$SO_2(gas) = SO_2(aq)$	$H = 1.3$ M/atm
	Equilibrium constant
$SO_2(aq) = H^+ + HSO_3^-$	$K = 1.54 \times 10^{-2}$ M
$HNO_2 = H^+ + NO_2^-$	$K = 5.10 \times 10^{-4}$ M
$HSO_4^- = H^+ + SO_4^{-2}$	$K = 1.20 \times 10^{-2}$ M

* Rate constants and equilibrium constants at 25 °C.
† Rate constants are in units l/mol/s or $l^2/mol^2/s$.

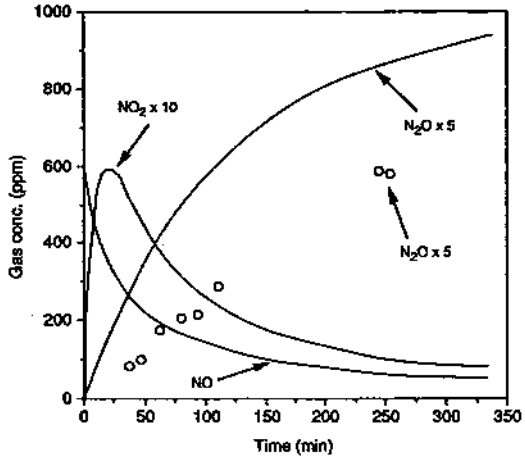

FIG. 3. Comparison of kinetic calculations (curves) and experimental data (○) of N_2O formation in sampling containers. Initial concentrations for model: $H_2O = 10\%$, $CO_2 = 11\%$, $O_2 = 4\%$, NO = 600 ppm, $SO_2 = 2000$ ppm. Experimental results are for an unnamed coal (adapted from Muzio *et al.*[30]).

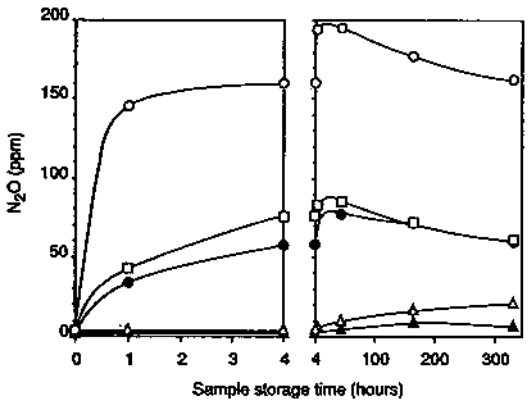

FIG. 4. N_2O formation in contained flue gas samples as a function of sample dryness. Pilot-scale measurements examined a Utah bituminous coal ($NO_i = 757$ ppm): △ dry P_2O_5, □ dry (refrigerated), ○ wet. Full-scale measurements examined a medium sulfur Alabama bituminous coal ($NO_i = 354$ ppm): ▲ dry P_2O_5, ● wet (adapted from Linak *et al.*[33]).

and Cole.[31] Both groups concluded that the mechanism involves the dissolution of NO_2 and SO_2 into condensed water followed by a complex set of liquid-phase reactions which produce N_2O as a by-product. This mechanism was summarized by both groups and is presented in Table 5. Using appropriate rate information and species concentrations, comparison can be made between model predictions and experimental results as shown in Fig. 3.

Figure 4 illustrates how quickly N_2O can be formed in sampling containers, and that condensed water is not necessary for the reaction to proceed. These data, taken from Linak *et al.*,[33] present results of time-resolved analyses of stack gases from selected laboratory and full-scale tests. Stainless steel sample containers were used during this study. Figure 4 (laboratory combustor data, open symbols) shows that N_2O is rapidly formed from an initial value of 4.2 ppm to a level approaching 200 ppm, when condensed water was present, to half that value when water was removed by a refrigerated knockout pot, and to less than 30 ppm when the sample was desiccated with P_2O_5. Data from glass containers showed similar asymptotes in N_2O, but a slower rate of increase at early times. This study also showed that the rise of N_2O is accompanied by a drop in gaseous SO_2 in the sample container, indicating the importance of sulfur as well as moisture on this low-temperature mechanism. Figure 4 also presents similar N_2O evolution data from a sample collected from a

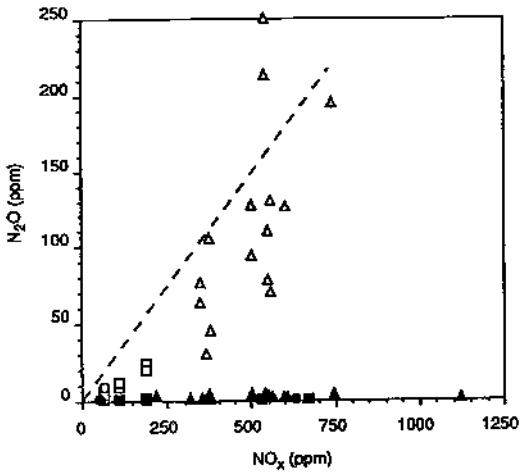

FIG. 5. Comparison of on-line N_2O flue gas measurements (solid symbols: ▲ pulverized coal, ■ fuel oil, ● natural gas) to measurements made from contained flue gas samples after 48 hours of sample hold time (open symbols: △ pulverized coal, □ fuel oil, ○ natural gas). The dashed line represents a previously proposed N_2O–N:NO_x correlation of 0.58:1 (adapted from Linak *et al.*[33]).

full-scale coal-fired utility boiler (solid symbols). It is interesting to note that both the sub-scale and full-scale N_2O data from wet or partially dry samples show rapid increases in the first minutes and hours after sampling. Smaller (but non-negligible) increases are seen in the dry samples. Maximum N_2O values from wet samples are seen after 24 hours. These values (200 and 75 ppm) are comparable to those presented by the historical data and the previously proposed N_2O–N:NO_x correlation. The data also indicate that the maximum N_2O concentration is related to the initial NO and SO_2 concentrations. Nitric oxide data show the rapid removal/reaction of this species (possibly forming NO_2) within 1–4 hours regardless of the moisture content of the samples. These results are consistent with data from other studies[28,29,44–46] and the model proposed above.[30,31] Similar data trends were observed for No. 5 and No. 2 fuel oils, and tests on natural gas combustion effluents indicated a measurable, albeit smaller, effect, even though SO_2 values were below detectable levels.

Figure 5 summarizes several sets of time-resolved data and shows how the maximum yield of N_2O formed in the sample container (after approximately 48 hours) depends on the initial NO in the flue gas.[33] These data (open symbols) can be compared to the previously accepted N_2O/NO_x emission ratio (dotted line). It is now generally accepted that high N_2O emissions from conventional combustion systems characterized by the historical database can be explained on the basis of this sample container artifact. The true N_2O emission levels, shown in Figure 5 as solid symbols, are independent of the initial NO concentration and never exceed 5 ppm for the combustion units tested.

3.3. *Continuous Infrared Spectrometry Approaches*

On-line, real-time N_2O analyzers are desirable; however, the commercial availability of these monitors has, until recently, been limited. In early systems, detection levels were insufficient, and elaborate sample conditioning systems were routinely required. Additionally, these systems were largely research-oriented,[47] requiring extensive operator attention and may not have been designed for field use. Several continuous, real-time monitoring techniques based on infrared radiation absorption have been developed and applied to N_2O combustion source monitoring.

A tunable diode infrared (TDIR) spectrometry analyzer has been developed by EPA's Air and Energy Engineering Research Laboratory (AEERL) to monitor N_2O emissions from its fossil fuel combustion test facilities.[48] TDIR systems offer excellent sensitivity, and are capable of detection levels in the parts per billion range. In addition, interferences from other IR radiation absorbing gases can be minimized by the TDIR analyzer's ability to isolate appropriate N_2O absorbing wavelengths with greater resolution. The main disadvantages of TDIR spectrometry are its complexity, high cost, short life span of laser diodes (1–2 years), and the necessity for cryogenic cooling.

FTIR spectrometry is another viable continuous N_2O monitoring method, it offers excellent wavelength resolution and sensitivity. In addition, FTIR spectrometry is capable of monitoring multiple wavelengths simultaneously, making the technique suitable for real-time, multi-component monitoring of combustion gases. The main disadvantages of FTIR systems are their complexity and high cost.

A less complex nondispersive infrared system has been developed at the University of California, Irvine (UCI) Combustion Laboratory.[49] NDIR analyzers are routinely used for the continuous measurement of CO, CO_2, and SO_2 from combustion sources. The UCI group conducted parametric investigations using a variable-wavelength infrared analyzer and simulated combustion gases to examine N_2O absorption and interference sensitivity around three N_2O absorbing infrared wavelengths (4500, 8000 and 17,000 nm). They concluded that the region between 7800 and 8500 nm was most suitable for measuring N_2O in combustion gases, and that NO_2 and SO_2 are the primary interfering species in this region. Based on this information, the UCI group adapted a Horiba Model VIA-500 NDIR analyzer with a 500 mm sample cell and a detector arrangement designed to electronically correct for a portion of the effects of interfering species. The prototype instrument responded linearly to N_2O concentrations ranging between 0 and 250 ppm. The UCI group also employed sodium sulfite and sodium carbonate solutions to scrub the sample gas to further minimize the effects of NO_2 and SO_2, respectively. They found

that these solutions effectively remove NO_2 and SO_2 from the sample without affecting N_2O. This system was then used to make measurements from two tangential-fired coal utility boilers. Results indicate that N_2O emissions from these units were consistently less than 1 ppm. They concluded that the NDIR system can provide continuous measurement capabilities and is capable of monitoring N_2O levels as low as several parts per million. However, the system is susceptible to interferences from other compounds present in combustion gases that absorb IR radiation at similar wavelengths to N_2O. These interferences can often be minimized through the use of elaborate conditioning systems as well as electronic background correction.

3.4. *On-line Gas Chromatography Approaches*

Currently, N_2O concentrations in combustion gases are most commonly monitored using gas chromatography. GC techniques, coupled with electron capture detection (ECD), offer excellent sensitivity with detection levels far less than ambient concentrations (approximately 350 ppb). Other detection methods such as thermal conductivity detection (TCD) and mass spectrometry (MS) have also been successfully used. An important limitation of GC methods is that they do not allow a continuous real-time measurement. Other disadvantages include analytical difficulties and detector desensitivity caused by interfering compounds present in the combustion gases. Conversely, in addition to excellent sensitivity, GC methods are typically easy to construct and operate, and relatively inexpensive. A GC analytical procedure suitable for N_2O measurement from combustion gases has been documented.[50,51]

In addition to a susceptibility to interferences present in the flue gases, GCs are prone to memory effects from moisture and SO_2 resulting in detector baseline instability as well as operational difficulties. These effects have direct impacts on detector sensitivity, often raising detection levels to values above the actual N_2O concentrations present in the flue gas streams to be measured. However, regardless of these limitations and the fact that this technique does not yield real-time information, the GC/ECD system offers the advantages of being highly sensitive, relatively inexpensive, widely available, and fairly simple to operate. The development of an acceptable GC/ECD analytical system and procedure suitable for the on-line measurement of N_2O from fossil fuel combustion sources requires negating the effects of interferences present in combustion process emissions, configuring the instrument for automated operation, and improving the linear working range of N_2O emission quantification.

The GC/ECD analytical system developed for use by EPA's Air and Energy Engineering Research Laboratory[50] uses a precolumn backflush method to isolate the interfering flue gas components. The system is automated by using the timed event commands associated with the GC operation/data acquisition system to control and activate the sampling–valving hardware. N_2O is quantified by relating integrated peak areas to a least-squares linear regression of logarithm-transformed calibration variables (peak area and N_2O concentration). The system requires that a particulate free, moisture conditioned, sample stream be delivered to the system under slight positive pressure. Figure 6 is a schematic diagram of the analytical system. The analytical conditions of the GC/ECD system are presented in Table 6.

Potential column contaminants are avoided by precolumn backflushing. This technique uses a single 10-port valve to divert–direct the flow of carrier gas and sample gas streams through the chromatograph system. A schematic diagram of a 10-port valve is presented in Fig. 7. The 10-port valve can be operated in two positions or modes. In the backflush position (Fig. 7a), the precolumn is backflushed by carrier 2 to a vent (ports 10, 9, 6, and 8 consecutively). The analytical column, supplied by carrier 1 (ports 5 and 7 consecutively), is connected to the ECD. A 1 cm^3 sample loop, bridging ports 3 and 4, can be charged with the sample stream (ports 1 and 2 consecutively). In the analyze position (Fig. 7b), the valve is aligned so that carrier 1 purges the sample loop to the precolumn (ports 5, 3, 4, and 6 consecutively). The effluent of the precolumn is routed to the analytical column and on to the detector (ports 9 and 7 consecutively). Carrier 2 is vented via ports 10 and 8. The sample stream is vented via ports 1 and 2. Once the analyte of interest (N_2O) has eluted from the precolumn onto the analytical column, the valve is returned to the backflush position: the flow through the precolumn is reversed and the interfering sample components are purged from the precolumn.

An electronically controlled air actuator is used to automate valve switching. The valving system is controlled by interfacing the GC and integrator to a timed event control module that converts digital commands from the integrator to time controlled electrical switches. To further aid in analytical system automation, a solenoid valve, installed upstream of the 10-port valve sample loop, allows continuous purging of the sample loop with sample gas until the time of analysis. The valve was controlled so that, just prior to analysis, the solenoid valve is closed, sample flow is stopped, and the sample loop is equilibrated to atmospheric pressure. Later, the 10-port valve is returned to the backflush position and the sample solenoid valve opened, restoring flow to the sample loop. The system is also configured for unattended, continuous operation by incorporating the programmed timed events into a separate program capable of automatically re-initiating the sequence of timed events.

The linearity of the GC/ECD system developed by

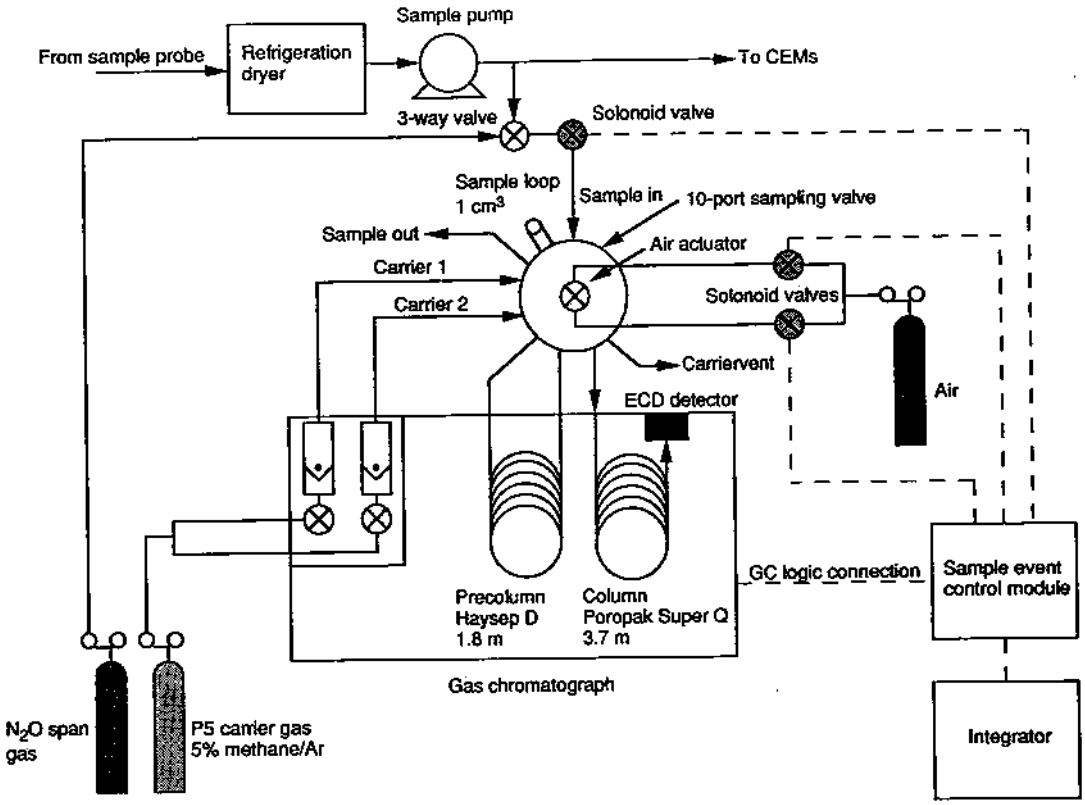

FIG. 6. Automated on-line GC/ECD system for N_2O analysis (adapted from Ryan and Linak[51]).

TABLE 6. GC/ECD analytical system equipment and conditions (adapted from Ryan and Linak[51])

Gas chromatograph	Hewlett-Packard model 5890A
Integrator	Hewlett-Packard model 3392A
Timed sample event controller	Hewlett-Packard model 19505A
Detector	^{63}Ni constant current cell electron capture detector maintained at 300 °C
GC oven temperature	Isothermal, 50 °C
Carrier gas	5 or 10% methane in argon (P5, P10)
Precolumn	6 ft (1.8 m) × 0.125 in. (0.32 cm) O.D. stainless steel, packed with HayeSep D, 100/120 mesh support
Precolumn carrier flow	30 cm³/min (head pressure ~30 psig, 308.2 kPa)
Analytical column	12 ft (3.7 m) × 0.125 in. (0.32 cm) O.D. stainless steel, packed with Porapak Super Q, 80/100 mesh support
Analytical column carrier flow	30 cm³/min (head pressure ~40 psig, 377.1 kPa)

TABLE 7. Two mathematical approaches to evaluate detector linearity (adapted from Ryan and Linak[51])*

	Linear regression			ln transformed linear regression			
N_2O (known)	Peak area	N_2O (calc.)	Bias %	ln (N_2O known)	ln (Peak area)	N_2O (calc.)	Bias %
0.514	6858	−3.11	−705.1	−0.66553	8.833171	0.47	−8.6
0.97	13153	−2.13	−319.6	−0.03045	9.484405	0.99	2.1
1.99	24199	−0.40	−120.1	0.688134	10.09406	2.02	1.5
5.03	56075	4.58	−8.9	1.615419	10.92444	5.36	6.6
9.85	99278	11.35	15.2	2.287471	11.50567	10.41	5.7
19.4	174880	23.18	19.5	2.965273	12.07185	20.11	3.7
40.4	318970	45.74	13.2	3.698829	12.67285	40.45	0.1
80.1	559344	83.36	4.1	4.383275	13.23451	77.74	−2.9
128	816984	123.68	−3.4	4.852030	13.61337	120.79	−5.6

*N_2O concentrations in ppmv.

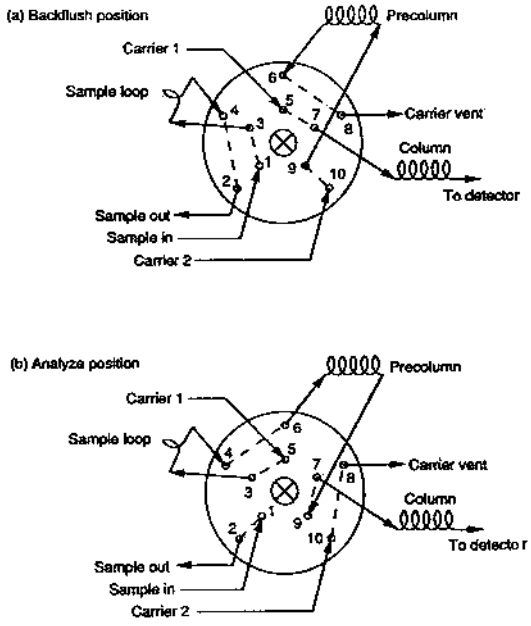

FIG. 7. Ten-port sampling valve configured for on-line N_2O analysis (adapted from Ryan and Linak[51]).

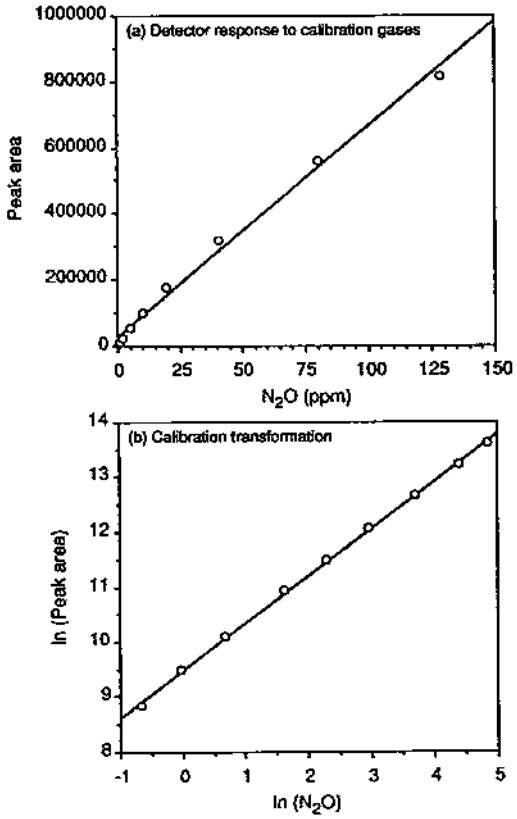

FIG. 8. ECD response to N_2O calibration gases (a) detector response to known calibration standards (O), peak area = 6389.233 (N_2O) + 26755.25, r^2 = 0.993537 (b) calibration transformation, ln(peak area) = 0.8597 ln(N_2O) + 9.491897, r^2 = 0.999238 (adapted from Ryan and Linak[51]).

AEERL was evaluated with varied concentration N_2O in nitrogen span gases ranging from 0.514 to 128 ppmv. The detector response to N_2O (area counts /ppm N_2O) exhibited decreasing sensitivity with increasing concentration. This effect tends to limit the linear working range of quantification. The linearity of the detector was evaluated using two mathematical approaches: a least-squares linear regression of the calibration variables, concentrations, and peak areas; and a least-squares linear regression based on transformed (natural logarithmic) calibration variables. A comparison of these two approaches is presented in Table 7 and Fig. 8. The approaches are compared by back-calculating the concentration of each calibration standard and determining the percentage bias from the known value. The linear regression of the transformed calibration variables (Fig. 8b) was effective in minimizing the relative error of calculated concentrations. Less than 10% bias was observed over the entire range. By calibrating in a narrower concentration range, more specific to anticipated emission concentrations, the relative error can be further reduced.

The automated, on-line GC/ECD system was evaluated extensively on a number of diverse fossil fuel and biomass fuel combustion test facilities. During on-line analyses, span or performance checks were conducted on a routine basis. These checks, used to evaluate method accuracy and precision, were conducted at various times during the measurement process. The accuracy and precision levels achieved during various on-line monitoring requirements were consistent. The type of combustion source monitored did not appear to affect method performance. Accuracy of span checks, expressed as percentage bias, was consistently less than 15%. The precision of replicate span checks, expressed as percent relative standard deviation (RSD), was consistently less than 10%. The method was found to be suitable for the quantification of N_2O concentrations ranging from 0.100 to 200 ppm. Using this method for on-line monitoring purposes allows an automated semicontinuous measurement approximately once every 8 minutes. The system can be easily incorporated into most continuous emission monitoring sample delivery–conditioning systems, the only requirements being the removal of particulates and moisture from the sample stream by a refrigeration condenser. The sample stream should be diverted to the analytical system prior to further moisture conditioning by a desiccant.

4. N_2O IN GAS-FIRED COMBUSTION

The goals of this section are (1) to review the critical reactions that govern the homogeneous chemistry of N_2O in combustion, and (2) to discuss the behavior of N_2O in gas flames. The literature clearly shows that N_2O can arise as an intermediate in the

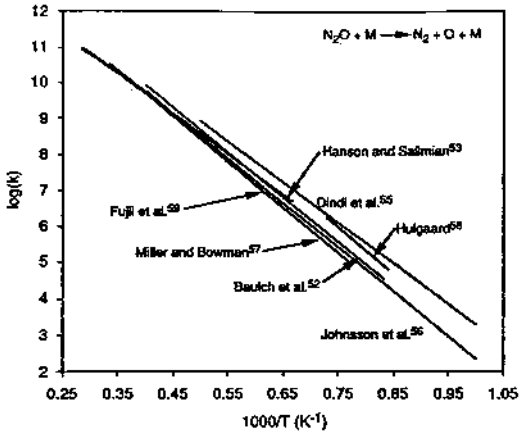

FIG. 9. Comparison of rate constants for $N_2O + M \rightarrow N_2 + O + M$ from reviews and recent data.

combustion of fuel-nitrogen. Once the fuel-nitrogen is consumed, however, fast destruction reactions ensure that little escapes the flame. Higher N_2O emissions can occur only if the flame is quenched, or the fuel nitrogen is introduced downstream of the flame zone. In both cases, N_2O destruction reactions are diminished.

Although the qualitative features of the flame behavior of N_2O are understood, quantitative prediction remains uncertain. In particular, recent measurements of the rate of the critical NCO + NO reaction indicate (1) that its rate is lower at high temperatures than previously thought, and (2) that, potentially, only a portion of the reaction branches to N_2O. In addition, recent measurements also suggest that the destruction reaction N_2O + OH is approximately 10 times slower than the rate used in most modeling studies. Since most kinetic modeling has used both the earlier, higher NCO + NO rate with a branching ratio into N_2O of unity, and the higher rate for N_2O + NO, these findings have the potential to upset current views of N_2O formation from cyano species.

4.1. *Elementary Reactions of N_2O Relevant to Gas Flames*

Reactions thought to be important to the behavior of N_2O in combustion systems include:

$$N_2O + M \rightarrow N_2 + O + M \quad (24)$$

$$N_2O + O \rightarrow N_2 + O_2 \quad (25)$$

$$\rightarrow NO + NO \quad (26)$$

$$N_2O + H \rightarrow N_2 + OH \quad (27)$$

$$N_2O + OH \rightarrow N_2 + HO_2 \quad (28)$$

$$NCO + NO \rightarrow N_2O + CO \quad (29)$$

$$\rightarrow N_2 + CO_2 \quad (30)$$

$$\rightarrow N_2 + CO + O \quad (31)$$

$$NH + NO \rightarrow N_2O + H. \quad (32)$$

The reactions governing NCO concentrations are also important to the problem. These include reactions forming NCO, and alternate destruction pathways that compete with Eq. (29) for available NCO. Rates for these reactions must be carefully selected with an awareness that the understanding is rapidly evolving. In contrast, the reactions and rates governing the concentration of the other precursor, NH, are more firmly established.

4.1.1. *$N_2O + M \rightarrow N_2 + O + M$*

The thermal destruction of N_2O via the reaction

$$N_2O + M \rightarrow N_2 + O + M \quad (24)$$

has been extensively studied. It is used as a source of oxygen atoms in fundamental experiments, where the reaction is generally recognized as producing triplet oxygen via a spin-hindered pathway.[52] The reaction is also one of the more easily studied thermal decomposition reactions, so it has become a prototype for testing both new experimental systems and theories. In addition, the reverse reaction has been implicated as a source of NO_x (via N_2O oxidation) under the moderate temperatures (*ca* 1600 K) characteristic of ultralean, premixed gas turbine operation. Kinetic studies reported before 1973 have been reviewed by Baulch *et al.*[52] and those since Baulch but before 1984 by Hanson and Salimian.[53] Data through to 1989 are discussed by Tsang and Herron.[54] We will comment only on recent rate determinations and their comparison with these reviews. A comparison of these rate expressions with more recent data is shown in Fig. 9 and Table 8.[52,53,55–59]

The Leeds review[52] suggests curvature in the Arrhenius plot above 2000 K. This is taken into account in the Hanson and Salimian review,[53] that proposes a modified Arrhenius rate for this reaction. At normal combustion temperatures the curvature is not very severe, and the rate expressions proposed by either of the authors, or by Miller and Bowman,[57] are adequate.

The very high activation energy of the reaction makes the rate quite slow at low temperatures (*ca* 1000–1500 K), where it is more difficult to obtain rate data without considering interfering reactions. One reason for studying the reaction at low and moderate temperatures is to obtain an accurate reverse rate for N_2O formation in low-temperature, lean, premixed combustion.[60,61] Johnsson *et al.*[56] and Hulgaard[58] were interested in this temperature range because of its similarity to fluidized bed operating temperatures. An improved knowledge of the homogeneous decomposition rate under fluidized bed

TABLE 8. Rate constants for $N_2O + M \rightarrow N_2 + O + M$

Reference	Rate expression	Comments
Baulch *et al.*[52]	$5.0 \times 10^{14} \exp(-29{,}000/T)$	Review, 1300–2500 K
Hanson and Salimian[53]	$6.9 \times 10^{23} T^{-2.5} \exp(32{,}710/T)$	Review, 1500–3600 K
Dindi *et al.*[55]	$3.5 \times 10^{14} \exp(-25{,}970/T)$	Flame, 1000–2000 K
Johnsson *et al.*[56]	$4.0 \times 10^{14} \exp(-28{,}230/T)$	See text
Miller and Bowman[57]	$1.6 \times 10^{14} \exp(-25{,}970/T)$	Review
Hulgaard[58]	$6.5 \times 10^{15} \exp(-30{,}250/T)$	Flow reactor, see text, 1190–1370 K
Fujii *et al.*[59]	$1.0 \times 10^{15} \exp(-30{,}190/T)$	Reactor, 1600–2500 K

conditions would help identify the relative importance of homogeneous vs heterogeneous destruction in these facilities.

Both Johnsson *et al.*[56] and Hulgaard[58] used flow reactors to characterize the $N_2O + M$ reaction in this moderate temperature range. The Hulgaard data[58] yield a higher rate than the consensus of the published data, although this is attributed to the presence of secondary reactions. Johnsson *et al.*[56] obtained data at 1000–1350 K, and combined these data with published higher temperature results to develop a rate expression very similar to those in the literature reviews. The recent data of Fujii *et al.*[59] also are in agreement with the reviews.

Dindi *et al.*[55] used a CO–N_2O flat flame, which allowed attention to be focused only on those reactions involving N_2O, NO, CO, and N_2. Their rate, and that derived from flow reactor data by Hulgaard,[58] both deviate from the published reviews at low temperatures. These deviations can become critical when these rates are used to calculate N_2O formation via the reverse reaction. As discussed by Tsang and Herron,[54] the variations in the rate constant at lower temperatures require additional work.

Although there is substantial scatter in the reports of chaperon efficiencies,[52] recent results suggest that $M(N_2) = 1.55\,M(Ar)$.[56] For helium, the chaperon efficiency varies with temperature, and has been approximated by the form: $M(He) = x\,M(Ar)$, where $x = 12.25 \exp(-2000/T)$.[56] These values agree, at least qualitatively, with other data,[56] and can be used both to correct fundamental data to a common basis, and for modeling. Additional measurements in the 1000–1400 K temperature range suggest the following efficiencies relative to Ar: O_2, 1.4 ± 0.3, CO_2, 3.0 ± 0.6, N_2, 1.7 ± 0.3, and H_2O, 12 ± 3.5.[62] The pressure dependence of $N_2O + M$ is well-characterized, and is discussed in Tsang and Herron.[54] Under combustion conditions it appears to always be in the fall-off regime.

4.1.2. $N_2O + O \rightarrow$ *products*

The reaction of N_2O with oxygen atoms has also been extensively studied. In general, the two product channels are found to be approximately equally favored over a wide temperature range

$$N_2O + O \rightarrow N_2 + O_2 \qquad (25)$$

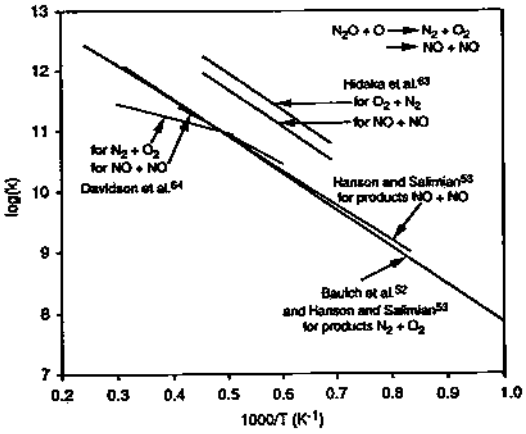

FIG. 10. Comparison of rate constants for $N_2O + O \rightarrow N_2 + O_2$ or NO + NO from reviews and recent data.

$$N_2O + O \rightarrow NO + NO. \qquad (26)$$

These rates are critical insofar as they determine the yield of NO from the destruction of N_2O; Eq. (26) is almost alone in yielding NO from N_2O destruction. These reactions were reviewed by Baulch *et al.*[52] for pre-1973, by Hansen and Salimian[53] for 1973–1984, and by Tsang and Herron[54] for 1984–1989. Some recent data are reviewed by Dindi *et al.*[55] In general, the more recent rate recommendations (Hanson and Salimian,[53] for Eq. (25)[57,58]) follow the expression recommended by Baulch *et al.*:[52]

$$k_{25} = k_{26} = 1.0 \times 10^{14} \exp(-14{,}100/T) \qquad 1200\text{–}2000\ \text{K} \qquad (33)$$

which is plotted in Fig. 10. These rates, along with those for the remaining N_2O destruction reactions discussed here, are summarized in Table 9.[52–55,57,58,63–67] Although some authors have suggested slightly different rates for these two reactions,[53] Fig. 10 shows that there is little difference between the consensus rate and the alternative proposed for the NO + NO product channel. Recent data on the product channel $N_2 + O_2$ suggest a reduced rate and lower activation energy at high temperature.[64]

Tsang and Herron[54] point out that the data of Hidaka *et al.*[63] are substantially higher than the consensus. They suggest that the participation of the $N_2O + OH$ reaction, which was not accounted for

TABLE 9. Rate constants for N_2O destruction reactions

Reference	Rate expression	Comments
$N_2O + O \rightarrow N_2 + O_2$		
Baulch *et al.*[52] Hanson and Salimian[53] Dindi *et al.*[55]	$1.0 \times 10^{14} \exp(-14{,}100/T)$	Reviews
Hidaka *et al.*[63]	$1.0 \times 10^{15} \exp(-14{,}100/T)$	Shock tube, 1450–2200 K
Davidson *et al.*[64]	$1.4 \times 10^{12} \exp(-5440/T)$	Shock tube, 1940–3340 K
$N_2O + O \rightarrow NO + NO$		
Baulch *et al.*[52] Dindi *et al.*[55]	$1.0 \times 10^{14} \exp(-14{,}100/T)$	Reviews
Hanson and Salimian[53]	$6.92 \times 10^{13} \exp(-13{,}400/T)$	Review
Hidaka *et al.*[63]	$5.6 \times 10^{14} \exp(-14{,}100/T)$	Shock tube, 1450–2200 K
Davidson *et al.*[64]	$2.9 \times 10^{13} \exp(-11{,}650/T)$	Shock tube, 1680–2430 K
$N_2O + H \rightarrow N_2 + OH$		
Baulch *et al.*[52] Hanson and Salimian[53]	$7.6 \times 10^{13} \exp(-7600/T)$	Reviews, 700–2500 K
Marshall *et al.*[65]	$3.31 \times 10^{10} \exp(-2380/T) + 4.4 \times 10^{14} \exp(-9690/T)$	390–1310 K
Marshall *et al.*[66]	$2.53 \times 10^{10} \exp(-2290/T) + 2.23 \times 10^{14} \exp(-8430/T)$	410–1230 K
Hidaka *et al.*[63]	$1.51 \times 10^{14} \exp(-7550/T)$	Shock tube, 1450–2200 K
Tsang and Herron[54]	$9.64 \times 10^{13} \exp(-7600/T)$	Review
Hulgaard[58]	$1.9 \times 10^{6} T^{2.42} \exp(-6794/T)$	Review
$N_2O + OH \rightarrow N_2 + HO_2$		
Miller and Bowman[57]	$2 \times 10^{12} \exp(-5030/T)$	Review
Martin and Brown[67]	$6 \times 10^{11} \exp(-3775/T)$	Review
Tsang and Herron[54]	$8.43 \times 10^{12} \exp(-5000/T)$	Review

in data analysis, may have increased the apparent rate of $N_2O + O$ reaction. This view is supported by Dindi *et al.*[55] whose use of a CO flame would have minimized the latter reaction. In this case, the data agree closely with the reviews. It must be remembered, however, that the rate of the $N_2O + OH$ reaction is imperfectly known at high temperatures, and that recent results described below suggest a much lower rate.

4.1.3. $N_2O + H \rightarrow N_2 + OH$

The reaction

$$N_2O + H \rightarrow N_2 + OH \qquad (27)$$

is a major sink for N_2O in flames. The rate recommended by the Leeds group[52] has generally been accepted by most recent reviews,[53,57] and is shown in Fig. 11. Two more recent determinations by Marshall *et al.*[65,66] show a marked curvature in the Arrhenius plot, although the simple Arrhenius expression suggested by the Leeds group appears to be adequate at higher temperatures. The rate recommended by Hulgaard[58] shows substantial curvature if extrapolated to higher temperatures, and suggests a higher rate, as do the measurements of Hidaka *et al.*[63]

The alternative product channel of NH + NO becomes more important at increased temperatures,[52] but remains minor even at high combustion temperatures.[65] Figure 11 shows the rate used in the Miller and Bowman[57] compilation (calculated from the reverse reaction), and the upper limit for the rate defined in Marshall *et al.*[65] Although this channel is not a significant sink for N_2O, it can be a major source of NH in flames using N_2O as the oxidizer, as will be discussed shortly.

4.1.4. $N_2O + OH \rightarrow N_2 + HO_2$

The removal of N_2O by hydroxyl radicals has received only limited attention:

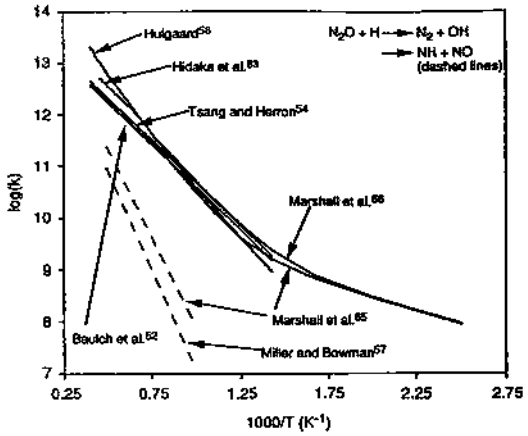

FIG. 11. Comparison of rate constants for $N_2O + H \rightarrow N_2 + OH$ or $NH + NO$ from reviews and recent data.

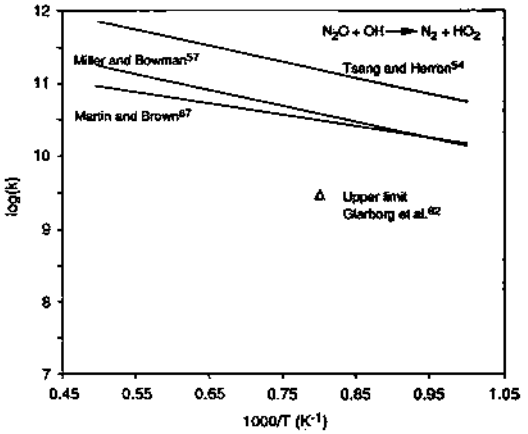

FIG. 12. Comparison of rate constants for $N_2O + OH \rightarrow N_2 + HO_2$ from reviews and recent data.

$$N_2O + OH \rightarrow N_2 + HO_2. \qquad (28)$$

The reaction has been studied at room temperature to determine the degree to which OH is capable of removing tropospheric N_2O. Figure 12 compares the rates suggested by Miller and Bowman[57] (based on the data of Biermann *et al.*[68]) with those proposed by Martin and Brown[67] (derived from Chang and Kaufmann[69]) and by Tsang and Herron.[54] Also included is a single measurement by Glarborg *et al.*,[62] which suggests the rate is at least an order of magnitude lower than those used in the compilations, something they attribute to a higher activation energy. The significant scatter shown in the plot is suggestive of the controversy over the importance of this reaction. Ignored in early modeling studies, its exclusion has been suggested as a source of error in some flame predictions.[70] As discussed in later sections, some modeling studies indicate major importance for this reaction under certain conditions. The low rate reported by Glarborg *et al.*[62] would, however, preclude this conclusion. Tsang and Herron[54] suggest a second possible product channel, into $HNO + NO$. If this channel is active, it provides an additional means for N_2O decomposition to lead to NO (the other major source being the $N_2O + O$ reaction discussed above). Clearly, more data are needed on this reaction.

4.1.5. $NCO + NO \rightarrow N_2O + CO$

The formation of N_2O in gas flames with added fuel nitrogen is thought to occur primarily through

$$NCO + NO \rightarrow N_2O + CO \qquad (29)$$

$$NH + NO \rightarrow N_2O + H. \qquad (32)$$

as well as the reverse of Eq. (24). NCO arises from reactions involving the decomposition of cyano species such as HCN and HNCO, as discussed in Section 4.1.7.

Equation (29) is projected to be the major pathway in both flames and post-flame processes involving cyano species. It appears to be a major source of N_2O when HCN is introduced into the gas phase downstream of the primary flame zone,[71] and in fluidized bed combustion.[24] It is also critical to the formation of N_2O when urea injection is used for NO_x control[72] and in the RapreNO_x process.[73–76] Due to its apparent importance, both the rate and product identification have been areas of recent interest in the literature.

At present, seven determinations of the rate have been identified from the literature, four at room temperature, and three at variable temperatures. These are summarized in Table 10[77–79] and Fig. 13.[57,73,77,79–83] The early determination of Fifer and Holmes[80] was estimated from kinetic modeling of a more complex system.[84] With the exception of Fifer and Holmes,[80] all the determinations are in excellent agreement at room temperature. All of the determinations at higher temperature also show remarkable consistency. The expression developed by Perry[77] lacks curvature on the Arrhenius plot, although this appears to be because his temperature range was not sufficiently large to make the curvature evident; his data are consistent with those of Atakan and Wolfrum.[78] For reference, the earlier rate recommended by Miller and Bowman[57] is included, primarily because it has been used extensively in recent modeling. This was based on an extrapolation of the Perry[77] expression before the more recent data were available,[78,79] and clearly it has been superseded.

Three product channels have been suggested:

$$NCO + NO \rightarrow N_2O + CO \qquad (29)$$

$$\rightarrow N_2 + CO_2 \qquad (30)$$

$$\rightarrow N_2 + CO + O. \qquad (31)$$

Perry[77] uses structural and energy arguments to suggest that the most likely products are $N_2O + CO$, although the other channels cannot be excluded. Zahniser *et al.*[83] established a lower bound on the

TABLE 10. Rate constants for NCO + NO reaction

Reference	Rate expression	Comments
Perry[77]	$1.02 \times 10^{13} \exp(196/T)$	Laser photolysis, 294–538 K
Atakan and Wolfrum[78]	$3.0 \times 10^{17} T^{-1.53} \exp(-260/T)$	Laser photolysis, 294–1260 K
Mertens *et al.*[79]	$1.4 \times 10^{18} T^{-1.73} \exp(-384/T)$	Shock tube, 2380–2660 K, rate expression developed for 294–2660 K

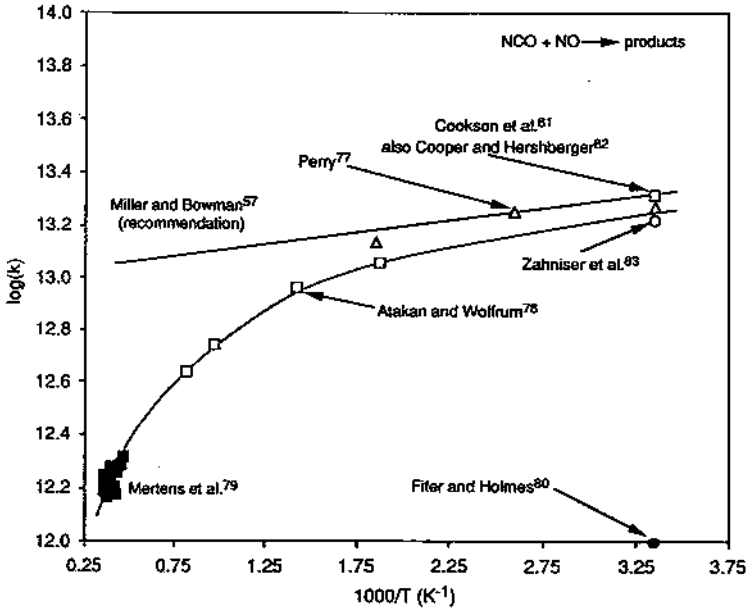

FIG. 13. Comparison of rate constants for NCO + NO → products from reviews and recent data.

TABLE 11. Room temperature branching ratios from the literature

Products	Branching ratio	
	Cooper and Hershberger[82]	Becker *et al.*[85]
$N_2O + CO$	0.33	0.35
$N_2 + CO_2$	0.44	0.65
$N_2 + CO + O$	0.23	0.0

N_2O channel of 0.4 relative to the overall rate of Eq. (29) at room temperature. Recently, Cooper and Hershberger[82] and Becker *et al.*[85] developed measurements of the branching ratios at room temperature. These branching ratios, presented in Table 11, were not anticipated based on kinetic arguments, and they suggest that the branching ratio into N_2O may also be less than unity at higher temperatures.

These findings have the potential to alter the present view that NCO + NO is the key pathway to N_2O in RapreNO$_x$ and urea injection, as well as in low-temperature oxidation of HCN and in fluidized bed combustion. The revised rate for NCO + NO at 1200 K is now a factor of 2.5 slower than the Miller and Bowman[57] extrapolation that has been used extensively in modeling. In addition, the yield of N_2O at high temperature may be only a fraction of the total products of this reaction. Although these findings suggest that other pathways may be important in generating N_2O, the picture is far from being resolved. For example, the curvature of the Arrhenius plot suggests a change in the mechanism with temperature,[78] which may also indicate a change in the branching ratio. In addition, Glarborg *et al.*[62] suggest that their new reduced rate for the destruction reaction $N_2O + OH$ may cancel the reduced formation from NCO + NO and prevent significant changes in model predictions. High-temperature measurements of the branching ratio would help resolve this issue and establish the importance of the NCO + NO reaction to the generation of N_2O in practical systems.

4.1.6. $NH + NO \rightarrow N_2O + H$

Equation (32) is a key route to the formation of N_2O in flames that lack cyano species. Data before 1985 have been reviewed,[53] as have more recent data.[57,84] We will comment on some of the more important points brought out in the reviews, as well as on some of the most recent data. BAC-MP4 calculations suggest that $N_2O + H$ predominate over $N_2 + OH$ as products because of a lower energy barrier between intermediate and product, in spite of greater exothermicity of the $N_2 + OH$ channel.[86] Miller and Melius[86] estimate that 19% of the reaction branches into $N_2 + OH$ at room temperature, and that this fraction rises to 30% at 3500 K.

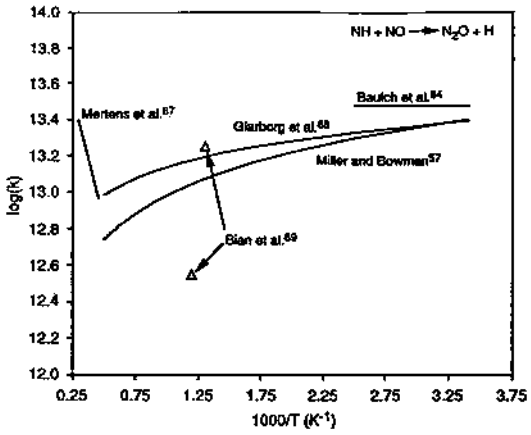

FIG. 14. Comparison of rate constants for NH + NO → N_2O + H from reviews and recent data.

Figure 14 compares recommended rates from the reviews and recent data.[57,84,87-89] Direct rate measurements at lower temperatures are in good agreement, while indirect measurements at higher temperatures show a wide variation (see discussion and plots in Miller and Bowman[57]). Miller and Bowman suggest a rate constant that extrapolates the low-temperature data in order to pass near the upper limit of the rate set in Morley.[90] The rate proposed by Glarborg *et al.*[88] yields a slightly higher rate at high temperatures. This rate produces better agreement with flame modeling.[67] Also, recent shock tube measurements support a higher rate.[87] The scatter in Fig. 14, as well as the significant scatter shown in the data plots in the review articles, illustrates the difficulty in resolving the high-temperature behavior of this reaction due to interfering reactions. Additional data will help to firmly establish the rate.

4.1.7. *Other NCO reactions*

The formation of N_2O from NCO depends not only on the rate and product distribution of the NCO + NO reaction, but also on the availability of NCO. The several reactions governing the formation, and particularly the destruction, of NCO have been shown through modeling to have a critical influence on N_2O yields.[91] The key destruction reactions include:

$$NCO + O \rightarrow NO + CO \quad (34)$$

$$\rightarrow CN + O_2 \text{ (minor)} \quad (35)$$

$$NCO + H \rightarrow NH + CO \quad (36)$$

$$NCO + OH \rightarrow HNCO + O \quad (37)$$

$$NCO + O_2 \rightarrow NO + CO_2. \quad (38)$$

Reviews of these reactions are available.[54,84] These reactions are areas of current research interest, and the understanding is continuing to evolve.[76,78,79] The formation of NCO occurs through the oxidation of both HCN and HNCO via reactions such as:

$$HCN + O \rightarrow NCO + H \quad (39)$$

$$HNCO + OH \rightarrow NCO + H_2O. \quad (40)$$

4.2. *Behavior of N_2O in Homogeneous Systems*

4.2.1. *Flame studies*

A number of flat-flame studies concerning N_2O have been performed. These include flames in which N_2O is the principal oxidizer, flames where N_2O is present as a trace species in the reactants, and cases where no N_2O enters the flame, but where it appears as an intermediate from added NO or other fixed nitrogen compounds.

All of the flames share certain features in common. First, if N_2O is present in the reactants, either as a major or minor species, it is rapidly removed by the flame. Only for relatively low-temperature combustion does significant N_2O persist beyond the primary flame. For those systems where a fixed nitrogen species other than N_2O is initially present (e.g., NH_3, HCN, NO), the N_2O appears early in the reaction zone as an intermediate, and is consumed by the end of the flame.

The use of N_2O as an oxidant in hydrocarbon flames has a long history.[92-95] Recent advances in combustion diagnostics and kinetic modeling have enabled comprehensive investigations of individual flames. Two recent exercises of note are by Habeebullah *et al.*[96] and Zabarnick.[97]

The experiments of Habeebullah *et al.*[96] examined low-pressure CH_4–N_2O flames. These focused on a broad range of issues in hydrocarbon and nitrogen chemistry. With respect to N_2O, most of the decomposition was attributed to $N_2O + M \rightarrow N_2 + O + M$, with a fraction due to N_2O + H. The appearance of imidogen (NH) is partially due to the reverse reaction of Eq. (32):

$$N_2O + H \rightarrow NH + NO.$$

Although only a small fraction of the N_2O is processed through this channel in this flame, the appearance of NH provides a fairly sensitive test of the pathways leading directly to NH. (Note that NH_2 was not detected, and thus by inference higher amines were not present.) The appearance of NH is consistent with a mechanism in which at least a portion of the N_2O + H reaction proceeds as shown in the reverse of Eq. (32), rather than exclusively into N_2 + OH. The analysis is, however, complicated by the presence of other formation channels in this hydrocarbon flame: CH + NO → NH + NO. Nonetheless, the NH peak height was adequately modeled using a rate for the reverse reaction of Eq. (32) based on the Leeds compilation.[52]

Zabarnick[97] studied a similar flame. Application of a detailed model provided good agreement for

most species, indicating that the most important kinetic pathways were adequately modeled by the kinetic set. The critical discrepancy was the prediction of too much NH by the model. In the model, the rate for $N_2O + H \rightarrow NH + NO$ was based on data from Miller and Bowman.[57] Figure 11 shows that the Miller and Bowman rate is somewhat below the upper limit recommended by Marshall *et al.*[65] The apparent uncertainty in this rate manifests itself as an uncertainty in predicted NH from these flames.

Roby and Bowman[98] examined rich, atmospheric pressure $H_2/O_2/Ar/NO$ flames, some of which were perturbed by the addition of C_2H_2. Approximately 1750 ppm NO was added, which yielded almost 100 ppm NH_3 early in the flame. As this NH_3 decayed, a transient peak of 15 ppm N_2O developed. It is clear that the source of the N_2O was NH + NO; the NH arises as a decomposition product of the NH_3. Detailed modeling was not, however, able to identify a source for NH_3 from the reactant NO. This issue has apparently remained unresolved as no later work has involved a flame under these very rich conditions. Nonetheless, simplified kinetic calculations using the measured NH_3 profile as input showed that the source of N_2O was NH + NO. The calculations also suggested that a significant amount of probe chemistry distorted the N_2O profiles, generally by reducing apparent N_2O concentrations below their actual flame values. The action of the probe was to freeze both the NH_i chemistry producing N_2O, and the destruction reaction involving $N_2O + H$. It is a little surprising that the N_2O levels were reduced in the probe, where the high-activation energy destruction reactions would be expected to preferentially slow first, yielding increased N_2O. Di Julio and Knuth[99] examined fuel-nitrogen conversion in an atmospheric pressure H_2 fueled flat flame. They observed N_2O as an intermediate early in the flame, but it was rapidly consumed.

In contrast to Roby and Bowman, Martin and Brown[100] examined N_2O behavior in lean premixed combustion (H_2 or CH_4, with NO, NH_3, or N_2O as a dopant). In general, they found that the amount of N_2O surviving varied inversely with temperature, which was a direct consequence of the high activation energy of the destruction step ($N_2O + H$) compared with that of the principal formation step (NH + NO). With N_2O as a dopant, they saw a small amount of NO formation, which was attributed to a partial branch of the $N_2O + H$ reaction into NO + NH. Alternatively, a portion of N_2O could form NO through $N_2O + O \rightarrow NO + NO$.

One of the most interesting observations was the appearance of an N_2O spike when the probe was passed radially through the shear layer at the edge of the flame.[100] At a constant distance from the flame, the passage through the shear layer increased the N_2O from an in-flame value of *ca.* 1 ppm to 28 ppm. This was attributed to a preferential loss of hydrogen atoms from the shear layer due to their high diffusivity. The gradient is maintained by the loss of hydrogen in the colder regions due to $H + O_2 + M \rightarrow HO_2 + M$. This suggests a mechanism that explains the small emissions of N_2O from industrial gas flames; i.e., via turbulent quenching.[100] A slightly different mechanism may be active in turbulent flame sheets under high Damköhler numbers.[101] Here, the thin flame sheets could become preferentially depleted in hydrogen atoms due to diffusion, and the small amount of N_2O that is formed near the flame zone may partially escape flame destruction.

Martin and Brown subsequently applied kinetic modeling to their data.[67] Sensitivity analysis showed that the most important reactions were the principal formation reaction, $NH + NO \rightarrow N_2O + H$; the principal sink reaction, $N_2O + H \rightarrow N_2 + OH$; and the principal reaction removing hydrogen atoms, $H + O_2 + M \rightarrow HO_2 + M$. The rate of the latter two are known with certainty. The sensitivity analysis, however, points out the need for (1) a more complete understanding of the rate of NH + NO, and (2) proper identification of the product channels for NH + NO and $N_2O + H$ at the temperatures of interest. Note that they were better able to fit their data using the slightly high rate for NH + NO of Glarborg *et al.*[88] than with the rate proposed by Miller and Bowman.[57]

Only very limited studies of N_2O in high-intensity stirred combustion have been made. Houser *et al.*[102-104] used this experimental format to study the decomposition of model fuel-nitrogen compounds, which will be discussed in the next section. Malte and Pratt[60] used a stirred reactor operating on CO near the lean blowout limit to investigate NO formation mechanisms appropriate for advanced, premixed gas-turbine combustion. Under these relatively cool conditions where thermal NO_x was well-reduced, they identified N_2O as an intermediate leading to NO_x,

$$N_2 + O + M \rightarrow N_2O + M$$
$$N_2O + O \rightarrow NO + NO. \qquad (26)$$

This was also recognized by Wolfrum.[105] Recent data from high-pressure flames show that this mechanism can be a significant contributor to gas-turbine NO_x, particularly under reduced temperature conditions designed to minimize thermal NO_x.[106] These results illustrate the value of obtaining accurate rate data for the reverse reaction of Eq. (24), or accurate data for the reverse rate in the correct temperature range if the rate is found from thermochemistry.

4.2.2. *Reaction of fuel-nitrogen*

As noted earlier, the addition of fuel-nitrogen to laminar flames leads to the appearance of N_2O as an

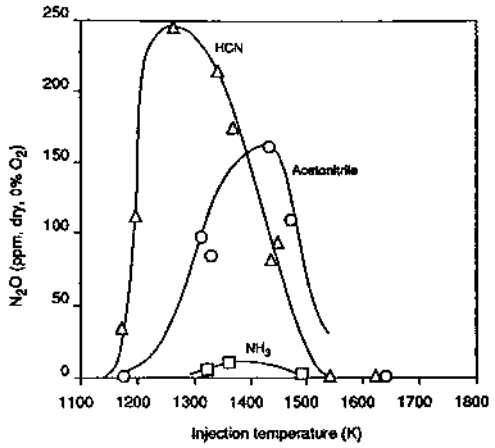

FIG. 15. Emissions of N_2O from a tunnel furnace with side-stream injection of: □ NH_3, △ HCN, and ○ acetonitrile at various temperatures (adapted from Kramlich *et al.*[71]).

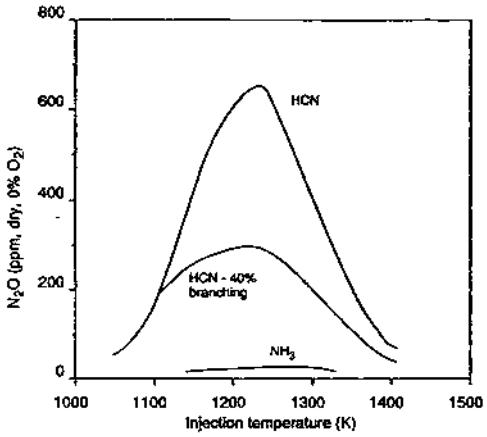

FIG. 16. Kinetic modeling of the experiment described by Fig. 15, including a case where only 40% of the NCO + NO reaction branches to N_2O + CO (adapted from Kramlich *et al.*[71]).

intermediate. Significant emissions occur, however, only for low-temperature flames (obtained either through a low adiabatic flame temperature or through high heat extraction at the burner). Also, addition of fuel-nitrogen to large turbulent flames yields no more N_2O in the exhaust than if no fixed nitrogen was included with the fuel.[71,107] Modeling efforts suggested that the reaction $N_2O + H \rightarrow N_2 + OH$ is sufficiently fast to be capable of removing all the N_2O formed in the flame zones, even if the N_2O formation rate is artificially augmented by unrealistically rapid char production rates. If N_2O is to be emitted from any fossil fuel systems, what could be the source?

One clue is provided by early data on the oxidative pyrolysis of fuel-nitrogen compounds. Researchers have recognized that, although nitrogen is bound into complex organic structures in coal, it appears in the devolatilization products almost exclusively as HCN and NH_3.[108–110] It is now known that the HCN and NH_3 arise from secondary tar cracking reactions after primary devolatilization, although the exact mechanism remains an area of research. Early studies on the pyrolysis[111] and oxidative pyrolysis[102–104,112] of model fuel-nitrogen compounds showed that under certain oxidizing, moderate-temperature regimes, compounds such as cyanogen, pyridine, and HCN could yield large amounts of N_2O.

Kramlich *et al.*[71] were able to generate large exhaust concentrations of N_2O in a tunnel furnace by the downstream injection of cyano species. The primary natural gas flame of this furnace was designed to generate 600 ppm NO. The post-flame gases were quenched by heat extraction at a rate of 350 K/s. A side-stream injector was used to introduce HCN into the furnace at various locations and temperatures. The results, shown in Fig. 15, indicate that between 1100 and 1500 K a significant fraction of the HCN was converted to N_2O. Similar results were obtained for an acetonitrile spray, with the maximum conversion temperature offset somewhat due to the time required for the evaporation of the spray. Ammonia, however, generated very little N_2O under these conditions.

Application of a plug-flow model (with distributed side-stream addition) to these results produced the predictions shown in Fig. 16. The major features of Fig. 15 are reproduced: a peak in N_2O emissions as a function of injection temperature, and the lack of N_2O production from NH_3. Sensitivity analysis showed that the N_2O behavior is governed by

$$HCN + O \rightarrow NCO + H \quad (39)$$

$$NCO + NO \rightarrow N_2O + CO \quad (29)$$

$$NH + NO \rightarrow N_2O + H \quad (32)$$

$$N_2O + H \rightarrow N_2 + OH. \quad (27)$$

Above the favorable temperature window, N_2O removal via Eq. (27) was rapid, and alternate pathways for the oxidation of HCN and its intermediates were opened. At lower temperatures, HCN failed to react within the time available. In the case of NH_3 injection, competing oxidation reactions within the temperature window prevented Eq. (32) from generating significant N_2O. One feature of the model was the overprediction of the conversion of HCN to N_2O. Use of a recommended reduced branching ratio[83] of 40% was entered into the model, which resulted in much more realistic N_2O predictions. This lends global support to the fractional branching ratios (see Table 11) recently reported.[82,85] However, it has been argued that this discrepancy is due to neglecting the N_2O + OH reaction, which would also act to suppress the N_2O concentrations.[91] The data of Glarborg *et al.*[62] suggest the N_2O + OH rate is too slow to contribute, which raises the specter that errors in both the N_2O + OH and NCO + NO reactions may cancel each other in modeling. Clearly, the uncertainty in the branching ratio and the rate of the

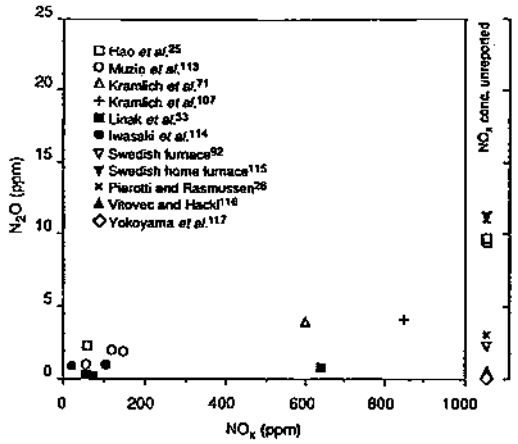

FIG. 17. Compilation of field data on N_2O emissions from gas-fired equipment.

N_2O + OH reaction prevent firm conclusions from being drawn at this time.

For such a mechanism to explain N_2O emissions in pulverized coal flames, a means of transporting volatile HCN to these cooler environments must be proposed. While late devolatilization or turbulent mixing limitations could provide some HCN within the appropriate temperature window, neither of these is likely to act as a major source in practical systems. This is consistent with the low N_2O emissions reported from coal-fired furnaces, as will be discussed shortly.

Houser *et al.*[104] studied HCN decomposition in moderate-temperature stirred reactors and plug-flow reactors. In the stirred reactor preignition mode, they found no NO generated, and N_2O as a major product. At higher temperatures the reactor contents ignite, and they found no N_2O in the products. Using these data, they conclude that the NCO + NO reaction cannot be a major source of N_2O. The key reactions are assumed to be

$$HCN + O \rightarrow NCO + H \quad (39)$$

$$NCO + O \rightarrow NO + CO \quad (34)$$

$$NCO + NO \rightarrow N_2O + CO \quad (29)$$

$$N_2O + H \rightarrow N_2 + OH. \quad (27)$$

Houser *et al.*[104] concluded that above the ignition temperature Eq. (27) is too slow to completely remove N_2O unless unrealistically high hydrogen atom concentrations are assumed. Thus, low N_2O emissions can be accounted for only by (1) the insignificance of Eq. (29), or (2) the predominance of Eq. (39) over Eq. (29). They concluded that the latter possibility requires an unrealistically high oxygen atom concentration, so by process of elimination, Eq. (29) must have an insignificant rate. An alternative proposed by Houser *et al.* is the reaction sequence:

$$CN + NCO \rightarrow CN_2 + CO \quad (41)$$

$$O_2 + CN_2 \rightarrow CO + N_2O. \quad (42)$$

Other N_2O destruction pathways may be active in this system with its very high fuel-nitrogen content that are not active in practical flames. A recent kinetic evaluation has been successful in reproducing the plug-flow nitrogen speciation data of Houser *et al.*[104] using the NCO + NO reaction as the source of the N_2O.[91]

4.3. *Industrial Gas Flame Data*

The emission of N_2O from industrial gas flames has always been found to be quite low. Figure 17 provides a compilation of data from large-scale, turbulent gas flames.[25,26,33,71,107,113–117] The left-hand half of the plot compares NO_x and N_2O data, while data in the right-hand panel do not have accompanying NO_x data. In general, emissions are so low as to be of little environmental consequence when it is remembered that the atmosphere contains approximately 0.3 ppm N_2O. Two of these data were obtained with NH_3 doping into the fuel,[71,107] but this failed to generate significant N_2O. The highest concentrations noted in Fig. 17 are associated with (1) a Swedish home heating furnace,[115] (2) early data by Hao *et al.*,[25] and (3) early data by Pierotti and Rasmussen.[26]

The home heating furnace likely involves lower overall flame temperatures and greater opportunity for quench of the flame. There is ample evidence that the quench of flames containing fuel-nitrogen will produce higher levels of N_2O,[100] although it has not been shown that this is true when fixed nitrogen species are absent from the fuel.

The data of Hao *et al.*[25] were obtained by collection in 50 cm^3 syringes that had an opportunity to age before analysis. Since SO_2 was not present in these gas flames to a significant extent, it is unlikely that a large amount of N_2O was generated in the sample.[28,30,31] However, there is evidence that the formation of N_2O within sample containers can proceed to a limited extent, and at a slower rate, in the absence of one of the necessary ingredients: SO_2 or moisture.[29] Although this question cannot be conclusively settled in retrospect, the large quantity of recent data from Austria[116] and Japan[117,118] suggests that most industrial gas equipment does not produce more than 2 ppm N_2O. Reported concentrations in excess of these values must be carefully examined to determine if special combustion conditions exist which give rise to emissions above the anticipated level.

4.4. *Summary of N_2O in Gas Flames*

Although N_2O is not emitted in significant concentrations from gas flames, research shows that it has

an active flame chemistry that is relevant to pulverized coal combustion and combustion fluidized beds. Flame studies suggest that N_2O is formed from other fixed-nitrogen compounds early in flames, but that it is rapidly and completely removed. Imposition of high-quench environments appears to preferentially deplete hydrogen atoms, thereby reducing the N_2O removal rate and leading to enhanced emission from flames containing fuel-nitrogen.

Clearly, the highest emissions occur in gas flames where cyano species are oxidized under moderate-temperature conditions. This situation can occur in practice in combustion fluidized beds and with downstream injection of cyanuric acid or urea for NO_x control. Present modeling shows that N_2O arises from the reaction NCO + NO. Recent data suggest, however, that this reaction is somewhat slower at 1000–1200 K than previously thought. Also, room-temperature product measurements show that only a portion of the reaction branches into N_2O, which may indicate that other product channels are active at higher temperatures. Certain kinetic studies have also suggested a role for the reaction N_2O + OH, although recent rate data on this very imperfectly known reaction tend to minimize its importance. These findings may alter current kinetic scenarios governing N_2O formation in combustion fluidized beds and during cyanuric acid and urea injection.

5. HETEROGENEOUS CHEMISTRY OF N_2O

The overall conclusion from Section 4 is that N_2O emissions from industrial gas flames are not significant. Only two situations were identified in which elevated N_2O emissions are possible. The first occurs when fuel-nitrogen is introduced downstream of the flame zone. Here relatively temperature-insensitive N_2O formation reactions occur, but the destruction reactions are suppressed. This situation can occur in practice when urea or cyanuric acid is injected into hot flue gas as a reagent for NO_x control (see Section 8). This situation may also occur in combustion fluidized beds, where volatile HCN enters the gas phase at relatively moderate temperatures.

The second scenario takes place when reacting gases containing NH_3 are quenched, which again suppresses the temperature-sensitive destruction reactions, but allows the temperature-insensitive formation reactions to occur for a time. In light of this recognition that gas flames do not present an environmental N_2O problem, the research community has focused on heterogeneous systems, although work continues to fully quantify the gas-phase mechanisms.

Research into the problems of N_2O formation in heterogeneous combustion has largely been driven by field measurements on practical units. These suggest that some types of combustion systems (e.g., pulverized coal flames or oil flames) do not emit significant N_2O. Other devices (e.g., fluidized bed combustors) have more substantial emissions. While this has served to focus research, it has not been interpreted as a license to ignore low-emission systems. Rather, the fact that certain heterogeneous systems do not yield much N_2O provides valuable clues on the mechanisms that are active, and on how N_2O can be suppressed in high-emission systems.

The importance of the heterogeneous contribution to N_2O is reflected by the fact that this and Sections 6 and 7 are largely devoted to it. This section reviews the fundamentals of heterogeneous N_2O chemistry. Section 6 focuses on pulverized coal combustion, while Section 7 is directed towards combustion fluidized beds. The heterogeneous chemistry covered in this section includes char reactions, and catalytic reactions associated with practical combustion systems (e.g., catalytic activity of alkaline compounds used for SO_2 control in combustion fluidized beds). Downstream catalytic processes will be covered in Section 8.4.

5.1. *Overview of Heterogeneous Chemistry*

The principal forms of heterogeneous reactions that have attracted research attention include:

(1) destruction of N_2O on char surfaces;
(2) reduction of NO on char surfaces to yield N_2O;
(3) oxidation of char-bound nitrogen to yield N_2O;
(4) heterogeneous generation of HCN from char nitrogen, which forms N_2O in the gas phase; and
(5) reactions of N_2O over alkaline surfaces, including catalytic destruction and catalytic formation from NO and NH_3.

These heterogeneous reactions are difficult to characterize in many experimental systems due to concurrent homogeneous chemistry. The gas-phase reactions can complicate both the qualitative and quantitative interpretations of the results.

5.2. *Destruction of N_2O on Char Surfaces*

de Soete has performed the most detailed study to date on the chemistry involving N_2O and char,[119] including N_2O destruction on char surfaces. His reactor system included a small packed bed (20 mm i.d. × 8 mm tall) containing 50–100 mg of highly devolatilized coal (35–50 μm in diameter) mixed with inert quartz beads. The reagent gases were passed through the bed while it was heated in an electric tube furnace. Measurements of product gas composition were used to develop heterogeneous kinetics under both steady-state and transient conditions.

Generally, N_2O was found to be more readily

TABLE 12. Arrhenius rate parameters for Eq. (45) (adapted from de Soete[120])

Coal	A (g/s/g(C)/Pa)	T^* (K)
Cedar Grove	0.9	13,900
Prosper	0.68	12,200
Eschweiler	0.14	10,000

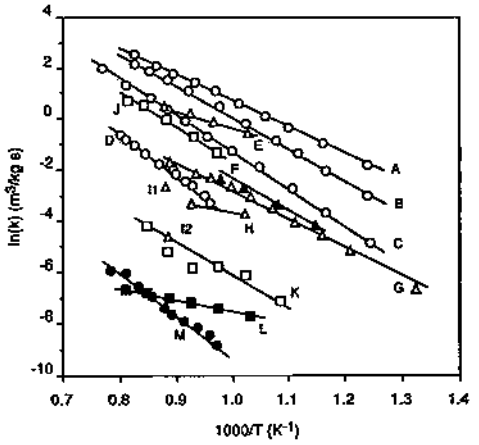

FIG. 18. Rate constants for heterogeneous N_2O reduction: ○ chars of graphite and bituminous coals, △ ▲ CaO and calcined limestone, □ $CaSO_4$ and sulfated limestone, ■ ● SiO_2 and quartz sand. The key to the references is Table 13 (adapted from de Soete[120]).

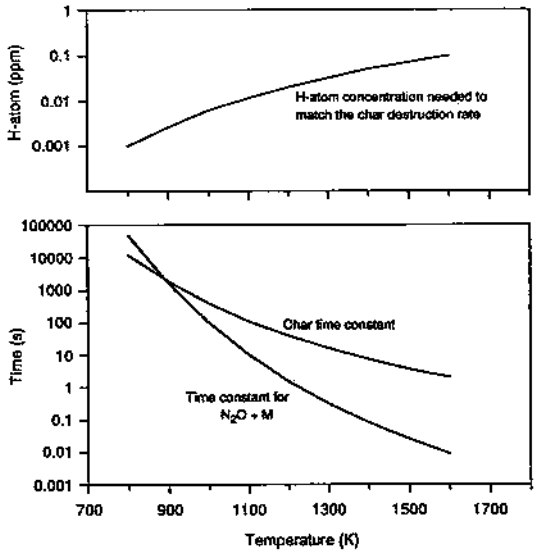

FIG. 19. Comparison of time constants for N_2O destruction due to various sources in a pulverized coal flame.

reduced on char surfaces than NO. Mechanistic arguments lead to the following as the dominant reaction:

$$N_2O + (-C) \rightarrow N_2 + (-CO) \qquad (43)$$

where the species in parentheses represents a surface site. Very little NO product was observed, which indicates that this is the major pathway, as opposed to:[120]

$$N_2O + (-CO) \rightarrow 2NO + (-C). \qquad (44)$$

de Soete tested three chars, and developed the kinetic expression:

$$N_2O \text{ destruction rate (g/s)} = A \exp(-T^*/T)\, m_C\, p_{N_2O} \qquad (45)$$

where A and T^* are Arrhenius rate parameters, m_C is the mass of carbon present in the char (g), and p_{N_2O} is the partial pressure of N_2O (Pa). The Arrhenius parameters, defined for each of the chars, are presented in Table 12.

Figure 18 summarizes recent data on the heterogeneous destruction of N_2O on various surfaces;[120] Table 13 describes the various data in Fig. 18.[120–124] The work on calcium surfaces will be discussed presently. Additional data on the destruction of N_2O over a char surface have been presented by Gulyurtlu *et al.*[125] Consistent with de Soete, these authors find that N_2 is the predominant product.

These rates provide sufficient information to perform a preliminary assessment of the heterogeneous contribution to N_2O destruction in pulverized coal flames. For this calculation, let us assume that pulverized coal is burned in 125% theoretical air. Half the coal mass is lost during devolatilization and burned to give combustion products. One mole of this product gas is accepted as the basis for the calculation, including its accompanying char. This allows the ratio of solids to gas to be correctly set. Given this, Eq. (45) can be integrated to establish a characteristic time constant for first-order N_2O decay due to heterogeneous reactions in this system (i.e., the time needed for $[1 - e^{-1}]$ or 63% of the original N_2O to be removed).

This characteristic time is plotted against temperature in Fig. 19, using data for the Cedar Grove char. It is clear that at moderate temperatures substantial time is needed to effect heterogeneous N_2O destruction at the suspension densities characteristic of pulverized coal firing. However, it must be remembered that this calculation sets an upper limit for N_2O destruction by char in pulverized coal flames because it does not allow for any reduction in char mass through oxidation. The corresponding time constant for the homogeneous removal of N_2O by the reaction:

$$N_2O + M \rightarrow N_2 + O + M \qquad (24)$$

is plotted for comparison. For all but the lowest temperature conditions the homogeneous mechanism predominates. Another means of comparing the heterogeneous rate to homogeneous destruction is to determine the hydrogen atom concentration that would be needed for the rate of the destruction reaction:

$$N_2O + H \rightarrow N_2 + OH \qquad (27)$$

TABLE 13. Key to heterogeneous destruction data reported in Fig. 18

A.	Char from Eschweiler bituminous coal	de Soete[120]
B.	Char from Prosper bituminous coal	de Soete[120]
C.	Char from Cedar Grove bituminous coal	de Soete[120]
D.	Graphite	de Soete[120]
E.	Calcined Ignaberga limestone, 300–500 μm	Santala *et al.*[121]
F.	Analytical grade CaO	Miettinen *et al.*[122]
G.	Calcined Pyrenees limestone, 80–160 μm	de Soete[120]
H.	Calcined limestone	Moritomi *et al.*[123]
I1.	Calcined crystalline limestone	Khan *et al.*[124]
I2.	Calcined amorphous limestone	Khan *et al.*[124]
J.	Calcined Ignaberga limestone, followed by 4 hr of sulfation	Santala *et al.*[121]
K.	Reagent grade $CaSO_4$	Miettinen *et al.*[122]
L.	Analytical grade quartz sand, 200–800 μm	Santala *et al.*[121]
M.	SiO_2, 100 μm	de Soete[120]

to match the heterogeneous rate. This is also shown in Fig. 19, which illustrates that very low levels of hydrogen atoms are needed to make this homogeneous reaction the dominant removal pathway.

These conservative calculations suggest that heterogeneous N_2O destruction on char surfaces is not a significant contributor to the overall destruction rate in pulverized coal firing. This conclusion is indirectly supported by Aho and Rantanen[126] who show that homogeneous N_2O removal was not enhanced by the addition of a peat dispersion to a homogeneous N_2O destruction experiment. Further evaluation would be necessary to establish the heterogeneous contribution in higher firing density situations (e.g., combustion fluidized beds).

5.3. *Reduction of NO on Char Surfaces to Yield N_2O*

With well-devolatilized char, de Soete[120] and Gulyurtlu *et al.*[125] saw very little conversion of NO to N_2O on char surfaces when no oxygen was present in the reactants (i.e., when no O_2 was available to generate N_2O through char-nitrogen oxidation). Other work, however, has been interpreted to suggest that, with oxygen present, N_2O becomes a major product of NO reduction over char.[127–129] Åmand *et al.*[130] invoke this reaction to explain their fluidized bed results. Here, N_2O yields dropped and NO concentrations increased when ash recirculation in their bed was stopped (presumably reducing the unburned char loading). As pointed out by Hulgaard,[58] there are other possible mechanisms that give rise to this. For example, the oxidation of HCN or NH_3 over fly ash could form N_2O, while at the same time NO could be reduced over the fly ash. An interruption in the ash flow to the bed could reduce N_2O formation and NO destruction.

Tullin *et al.*[131] burned small amounts of coal in an externally heated fluidized bed operating in a batch mode. They found that the fractional conversion to NO increased as the char approached final burnout. This suggests that NO is formed as the primary oxidation product, and that N_2O is formed by the reaction of some of this NO with char nitrogen. Near burnout, the amount of char surface available is diminished, and the N_2O formation reaction is stopped. This conclusion is supported by an increase in N_2O yields when additional NO is added to the experiment.[127] Mochizuki *et al.*[129] also conclude that the reaction between NO and nitrogen at the char surface is a major pathway to N_2O. One interpretation of the oxygen effect is that O_2 is required to continually expose fresh char-nitrogen for reaction with NO.[129,131] All of these data suggest that the surface absorption of NO, followed by reaction with another NO molecule to yield N_2O, is not an important path.

5.4. *Oxidation of Char-Bound Nitrogen to Yield N_2O*

de Soete's fixed bed experiments[120] represent the most quantitative approach to the oxidation of char-bound N_2 to yield N_2O to date. Although previous work examining 50 coals indicates that typically less than 20% of the char-nitrogen is converted to NO,[109] de Soete's experiments under steady-state condition suggest this conversion to be 30–70%, and that 1–6% of the char-nitrogen becomes N_2O. The amount of N_2O formed is proportional to the amount of carbon consumed. This suggests that N_2O formation is mechanistically linked with carbon oxidation. In fact, carbon oxidation and nitrogen burnout have previously been found to be proportional, and deviations from the proportionality have been attributed to late nitrogen devolatilization.[132]

The full mechanism proposed to account for the behavior is:[119]

$$O_2 + 2(-C) \rightarrow 2(-CO) \quad (46)$$

$$(-CO) \rightarrow CO + \text{free site} \quad (47)$$

$$2(-CO) \rightarrow CO_2 + (-C) + \text{free site} \quad (48)$$

$$O_2 + (-C) + (-CN) \rightarrow (-CO) + (-CNO) \quad (49)$$

$$(-CNO) \rightarrow NO + (-C) \quad (50)$$

$$NO + (-C) \rightarrow 0.5N_2 + (-CO) \quad (51)$$

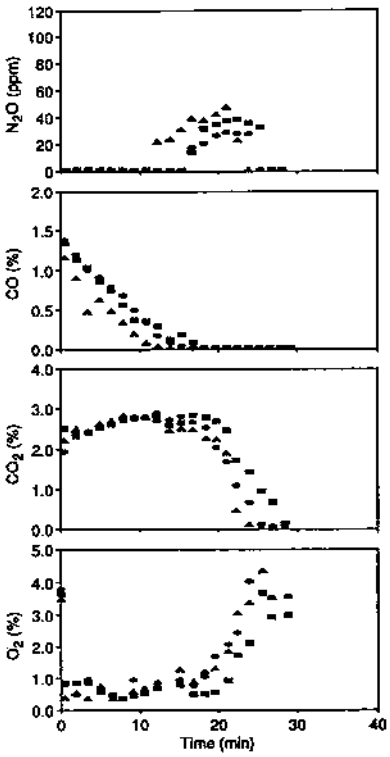

FIG. 20. Emissions as a function of time from the batch combustion of Datong char showing the influence of inlet NO concentrations: ● NO = 300 ppm, ▲ NO = 700 ppm, ■ NO = 900 ppm, 3.5% O_2 in N_2, 800 °C, 800 ml/min (adapted from Mochizuki *et al.*[129]).

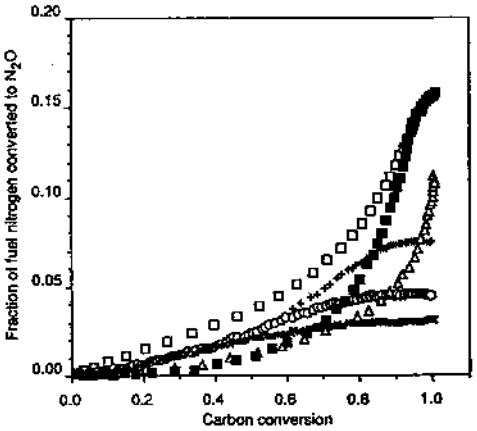

FIG. 21. Correlation of carbon oxidation with the conversion of fuel nitrogen to N_2O at 1073 K, 15% O_2, for petroleum coke △ and petroleum coke char that has undergone varying degrees of devolatilization: □ 873 K, ■ 973 K, + 1073 K, ○ 1173 K, × 1273 K (adapted from Suzuki *et al.*[133]).

$$(-CN) + (-CNO) \rightarrow N_2O + 2(-C) \quad (52)$$

$$N_2O + (-C) \rightarrow N_2 + (-CO). \quad (53)$$

Since only small amounts of N_2O were formed when NO was exposed to the char, de Soete concludes that the following reaction is probably of minor importance:[120]

$$NO + (-CN) \rightarrow N_2O + (-C) \quad (54)$$

although, as mentioned in the previous section, the depletion of surface nitrogen when oxygen is not available to expose new surface may have limited the effectiveness of this reaction in de Soete's experiments.

Transient experiments were performed in which the flow of oxygen–argon was rapidly replaced with pure argon. These experiments showed that the number of available sites occupied by oxygen was only a fraction of the total available sites. This indicates that Eq. (46) is rate controlling. Above 800 K the measured rate of Eq. (46) is such that pore diffusion within the char influences the rate. Thus, the overall rate measured for Eq. (46) includes an effectiveness factor that is a function of the structure of the particular char under consideration.

At the present time one cannot easily use this information to accurately assess the relative role of char-nitrogen conversion to overall N_2O emission. However, some bounds can be placed on the potential contribution. One approach is to use de Soete's observation[120] that up to 6% of the char-nitrogen will react to form N_2O. This value can be used in the pulverized coal example developed earlier (with the additional assumption that half the original coal nitrogen content of 1% remains with the char following devolatilization). The results suggest a maximum emission of 18 ppm. It must, however, be borne in mind that much of this N_2O would be formed above 1500 K, where homogeneous reactions would almost immediately destroy it.[71] Thus, although the ultimate heterogeneous conversion of char-nitrogen to N_2O ranges from 1 to 6%, only a fraction of this would be expected to result in emission.

Mochizuki *et al.*[129] used a small-scale fluidized bed to study N_2O formation from char. They argue that the fluidized bed format gives them better control over particle temperature overshoot than the fixed bed system. Figure 20 shows that N_2O does not begin to break through the bed until the later stages of char combustion, when CO emissions have dropped to zero and O_2 has begun to rise from its original level of about 0.5%. This appears to contradict the results of de Soete,[120] who found that heterogeneous formation of N_2O paralleled carbon burnout. The ultimate analysis of the raw char shows that it is not as strongly devolatilized as the char used by de Soete (it contains over three times as much hydrogen). Thus, the results suggest that N_2O may be formed in the bed through the reactions described by de Soete, but that emission is suppressed by homogeneous activity until the bed no longer emits CO. This is supported by the observation that the addition of CO in the gaseous reactants suppressed N_2O emissions. Oxidation of CO via CO +

$OH \rightarrow CO_2 + H$ could form hydrogen atoms that would remove N_2O via the reaction $N_2O + H$.

The data of Suzuki *et al.*[133] give support to this mechanism. They examined N_2O formation from petroleum coke that had been subjected to different degrees of devolatilization. Figure 21 shows that, for the highly devolatilized cokes, the formation of N_2O was proportional to carbon burnout, as was found in de Soete's experiments.[120] For poorly devolatilized chars, however, the fractional conversion of char-nitrogen to N_2O was suppressed at low carbon conversion, and increased markedly near the end of burnout.

Tullin *et al.*[127] performed a similar experiment in which small amounts of coal were added to a laboratory-scale externally heated fluidized bed to provide time-resolved batch reactor data. Unlike the results of Suzuki *et al.*,[133] they find that N_2O formation proceeds almost linearly with carbon burnout during the char combustion stage for a range of reactor temperatures and oxygen concentrations. This points to a fuel dependent effect that will be discussed in more detail in Section 7.3.4. They also found that doping the fluidized bed with additional NO significantly increased N_2O production during the char oxidation portion of their experiments. This suggests that the dominant mechanism is the production of NO during char oxidation, followed by the reduction of NO at the char surface to yield N_2O. As noted above, the reduction reaction occurs only in the presence of oxygen, possibly because continued char oxidation is needed to expose fresh char-nitrogen for reaction with NO.[129,131]

Thomas *et al.*[134] oxidized ^{13}C materials that were artificially doped with various nitrogen compounds. They observed much higher levels of N_2O release when NH_3 was the doping agent. While it can be easily argued that their material differs significantly from coal char, the data strongly suggest that nitrogen functionality within the char strongly influences the yield of N_2O from char combustion.

Coupled with the data of Suzuki *et al.*,[133] Mochizuki *et al.*,[129] and de Soete,[119,120] these data support the following observations.

(1) For a well-devolatilized char where care has been taken to minimize competing homogeneous reactions, the ultimate yield of N_2O as a fraction of fuel-nitrogen is in the range of approximately 1–6%.
(2) For strictly heterogeneous oxidation, the oxidation process is nonselective (i.e., the formation rates for N_2O formation and char oxidation are proportional).
(3) For poorly devolatilized oil coke, competing gas-phase reactions appear to suppress N_2O during the early stages of combustion.
(4) The final conversion of char-nitrogen to N_2O is, however, higher for poorly devolatilized cokes. One explanation is that the nature of the poorly devolatilized coke lends itself to higher heterogeneous formation rates. The N_2O is, however, suppressed at early times because of homogeneous destruction.
(5) Coals exposed to an environment similar to that of the coke show N_2O growth that parallels the carbon burnout.

Points (4) and (5) are in critical need of resolution. Since devolatilization occurs *in situ* in fluidized beds, during much of its lifetime the coke will more closely resemble the partially devolatilized material of Suzuki *et al.*[133] than the highly devolatilized char (prepared under an inert atmosphere at long times) used by de Soete.[119,120] Accelerated conversion of fuel-nitrogen to N_2O occurs at late times for poorly devolatilized coke, but does not appear to do so for coal char.[127] These points will require resolution to understand the actual emission mechanism in fluidized beds. These topics will be explored further in Section 7.

Another fundamental question is to differentiate between (1) the generation of N_2O by direct char oxidation, and (2) the generation of NO by char oxidation, followed by its conversion to N_2O at the char surface in the presence of O_2. One approach is to observe the response of N_2O as additional NO is doped into the system. Here, the data conflict, and are likely to be dependent on experimental format; thus, discussion is deferred to Section 7.

5.5. *Heterogeneous Generation of HCN from Char-Nitrogen*

Cyano species such as HCN have been shown to be precursors for N_2O under oxidative pyrolysis conditions,[102–104,112] and if HCN is introduced into the post-primary flame gases at an appropriate temperature.[71] The source of HCN in coal flames is thought to be secondary reactions of the nitrogen-containing tars that are one of the primary products of coal devolatilization.[135] Extensive reviews of the overall rate of nitrogen release, the mechanisms of release and conversion, and the influence of parent coal properties are available.[136] No attempt will be made to summarize the literature here.

At temperatures where HCN is converted permanently to N_2O (1100–1500 K) most, but not all, devolatilization is complete in pulverized coal flames.[132] However, char-nitrogen can be converted to N_2O via gasification reactions.[137] In furnaces HCN would probably have such a short lifetime that none would be observed in gas samples. Instead, HCN would be rapidly converted to products, including N_2O. Thus, failure to measure HCN under these postflame conditions does not necessarily indicate the absence of a homogeneous pathway to N_2O that involves HCN.

5.6. *Nitrogen Reactions Over Alkaline Surfaces*

An integral part of combustion fluidized bed technology is the use of limestone sorbents within the bed to capture SO_2. Several studies have suggested that N_2O may be catalytically destroyed over calcium compounds. Also, certain alkaline materials appear to be capable of catalytically forming N_2O from NH_3. Pulverized limestone is used as the raw material for sulfur capture in fluidized beds. This $CaCO_3$ is rapidly decomposed to CaO, which captures SO_2 via the reaction:

$$CaO + SO_2 + 0.5\,O_2 \rightarrow CaSO_4. \qquad (55)$$

Thus, the alkaline surface that is actually exposed for reaction in the bed may be either CaO or $CaSO_4$.

The high catalytic activity of CaO surfaces towards N_2O decomposition is well-documented.[121-123,133,138-142] Figure 18 illustrates that all CaO surfaces are not equivalent in their catalytic activity. First, CaO prepared from calcined limestones will have varying surface areas, depending on the properties of the parent stones, and on the degree of sintering that is allowed to occur following calcination.[143] Hansen *et al.*[141] found that calcined limestones that have a high activity for N_2O destruction also are the most reactive towards SO_2. In the past, high reactivity towards SO_2 has been associated with (1) the development of high porosity during calcination, and (2) the resistance of this structure to porosity loss during sulfation.[144]

Catalytic removal proceeds with a rate that appears to be independent of the presence of a number of other species (NO, HCN, NH_3, O_2).[138] In the experiments of Hansen *et al.*,[141] the failure of added NO to influence the N_2O removal rate was also noted. Since NO was also reduced in these experiments, this indicates that NO and N_2O were not competing for the same sites on the CaO surface.

In practice, the CaO that is present in fluidized beds is rapidly coated with a sulfate product layer. Miettinen *et al.*[122] found that reagent grade $CaSO_4$ showed little reactivity towards N_2O destruction. This low activity has been confirmed by several researchers.[139,141,142] In contrast, others have reported higher activities.[121,145] It appears that chemically pure $CaSO_4$ has little activity towards N_2O, but that sulfated limestone may, under some circumstances, be more reactive. In general, sulfated limestone consists of a sulfate coating over unreacted CaO. Depending on the nature of the surface (i.e., the presence of surface defects), the free-stream gases may have greater or lesser degrees of contact with the more reactive CaO core. Also, the limestones contain varying amounts of impurities, which may promote the destruction reaction.

Little work has been done to measure N_2O decomposition over reduced calcium surfaces. In his study of fluidized bed sulfation, Hansen[146] found that $CaSO_4$ could be reduced to CaS, CaO, and S_2 in fluidized beds. Hansen *et al.*[141] found that CaS was at least as active as CaO towards N_2O destruction when CO was present. This suggests another means by which sulfated limestone could act as an N_2O removal catalyst in fluidized beds: the partial reduction of the unreactive $CaSO_4$ into reactive CaO and CaS.

Klein *et al.*[142] and Mietinen *et al.*[122] found that MgO was almost as reactive as CaO as an N_2O decomposition catalyst. Both were deactivated by sulfation.[142] However, the ability of MgO to capture sulfur is limited in practical systems by (1) a lower decomposition temperature for the sulfate product, and (2) a lower reaction rate with SO_2 due to the lower product layer diffusivity of SO_2 through $MgSO_4$.[147] Thus, Klein *et al.*[142] suggest that MgO may be an appropriate additive to fluidized bed combustors for controlling N_2O since it is resistant to deactivation through sulfation.

Limited studies have been undertaken on other materials. Coal and peat ash have been found to be much less reactive than CaO.[145,148] Miettinen *et al.*[122] examined Fe_2O_3 and Fe_3O_4, and found them to be almost as reactive as CaO.

de Soete studied the catalytic formation of N_2O over a reduced calcium sulfate that was prepared by reaction with graphite.[44] The introduction of 1240 ppm of NO into this fixed bed experiment generated additional N_2O between 1200 and 1400 K, although the maximum yield was only 4 ppm. Although the composition of the reduced $CaSO_4$ is not known, in light of the discussion in Hansen,[146] it seems likely to contain CaO or CaS. Since both of these are potent N_2O reducing agents, it is possible that additional N_2O was formed, but immediately removed. The short gas-phase residence time in de Soete's experiments is designed to minimize competing homogeneous reactions (the empty-bed nominal residence time is ~75 ms).

Iisa *et al.*[145] examined N_2O formation from NH_3 over beds of CaO and $CaSO_4$. N_2O was detected only when CaO was the bed material. Both NH_3/O_2 and $NH_3/NO/O_2$ initial compositions were capable of generating N_2O. In the latter case, a maximum of 300 ppm N_2O was generated from 2000 ppm each of NO and NH_3 at 850 °C, a nitrogen conversion of 15%. The practical importance of this reaction remains uncertain, however. Since $CaSO_4$ was totally unreactive in this situation, one could conclude that normal sulfated limestone would also be unreactive because it always presents a sulfated surface for reaction. Alternatively, the preceding discussion shows that wide variations exist in reported rates for N_2O destruction on sulfated materials. This suggests that some sulfated limestones may have enough CaO "character" to act as catalysts for NH_3–N_2O conversion.

5.7. *Heterogeneous Kinetics Summary*

With few exceptions, the relative importance of

various heterogeneous pathways involving N_2O during combustion has been defined. Quantitative prediction from the fundamental data is still beyond our reach, however. The critical problems include: (1) the great variability in starting materials, and (2) the difficulty in removing the effects of homogeneous chemistry from experiments designed to resolve heterogeneous issues.

The destruction of N_2O on char surfaces has been well characterized, and the products do not appear to include significant NO. Likewise, the reduction of NO on char surfaces does not appear to yield N_2O unless oxygen is present. Oxidation of bound nitrogen from highly devolatilized chars provides an ultimate conversion to N_2O in the range 1–6%, although in practical systems a significant portion of this would probably be homogeneously reduced. In practical systems, it is difficult to differentiate experimentally between N_2O that arises directly from char oxidation, and N_2O that arises due to oxidation of char nitrogen to NO, followed by the reduction of NO to N_2O at the char surface in the presence of oxygen.

Another problem is the difficulty of separating the role of homogeneous chemistry from heterogeneous chemistry in experiments. In particular, the oxidation of poorly devolatilized coke appears to cause reduced N_2O yields at early times and enhanced yields near burnout. This difference in behavior compared to the behavior of well-devolatilized chars is of considerable interest because partially devolatilized coals are more likely to be representative of the chars found in combustion fluidized beds.

The alkaline sorbent CaO is a catalyst for N_2O destruction. Pure $CaSO_4$, however, does not appear to have catalytic activity. Sulfated limestone occasionally appears to have an intermediate activity, which may be the result of variable amounts of reactive CaO being exposed during sulfation. Another source of scatter may be the variable amounts of impurities present in limestone samples. CaO also appears to be a catalyst for the conversion of NH_3 to N_2O.

6. BEHAVIOR IN PULVERIZED COAL FLAMES

Pulverized coal flames were among the first industrial combustion sources to be characterized for N_2O emissions. The widespread use of pulverized coal, coupled with the relatively high amounts of fuel-nitrogen contained in the fuel, suggested that this class of sources was worthy of attention.

The initial measurements on utility boilers were reported in 1976.[26,27] This was followed by a limited number of studies through 1986–1987. As discussed in Section 3, it was later found that large amounts of N_2O could be formed within the flasks that were used for sample storage in many studies. Subsequent studies either modified the storage technique to avoid N_2O formation, or used on-line methods where the samples had little time to age. These later studies have shown very low emissions from pulverized coal or oil-fired units, generally less than 5 ppm. However, there have been several studies of time-resolved N_2O behavior in coal flames, which indicate that much higher N_2O concentrations exist early in the flame. These studies are valuable for their mechanistic insight.

6.1. *Early Coal Studies*

Pierotti and Rasmussen[26] reported three measurements (32.7, 32.8, and 37.6 ppm) from a pulverized coal-fired university power plant. They used 6 l, electropolished stainless-steel flasks for their samples; the subsequent analysis was by GC/ECD. Nominally, these samples would have been subject to the sampling artifact, although the concentrations measured were much lower than those reported in later studies. One reason for this might have been the fact that the source and the analytical laboratory were in close proximity, and the time between sampling and analysis may have been short. Alternatively, the stainless-steel surface may have moderated the pH of the material absorbed on the walls and helped to slow the conversion of NO to N_2O.

Weiss and Craig[27] used 2 l Pyrex sample flasks to collect stack gas from the Mohave coal-fired station in Nevada. These were preconcentrated by freezing in a liquid-nitrogen bath. The concentrated sample was then evaporated and dried. These concentrated gases (containing mainly N_2O and CO_2) were analyzed by an ultrasonic phaseshift detector. Thus, these samples would have also been subject to in-container N_2O formation. The reported N_2O emission was 25.8 ppm, which is also low compared to subsequent studies where the sampling artifact was active.

Kramlich *et al.*[107] measured N_2O emissions from a small-scale tunnel furnace. The goal was to identify whether the use of air staging for NO_x control would lead to enhanced N_2O emissions. These samples were obtained by an on-line preconcentration procedure similar to that of Weiss and Craig (i.e., the samples withdrawn from the reactor were immediately frozen in a liquid-nitrogen trap and then evaporated, dried, and analyzed on-site by thermal conductivity gas chromatography). Although the results were insensitive to the stoichiometry of the rich zone, increased reactor cooling increased N_2O emissions, and premixed coal flames yielded more N_2O than diffusion coal flames. Although the elevated N_2O emissions (20–90 ppm) could be due to sample system chemistry, it is possible that the reduced combustion temperatures in this small facility caused more of the volatile HCN to oxidize in the 1200–1500 K window where N_2O emissions can be formed.[71]

Castaldini *et al.*[149] examined a series of sources associated with NO_x abatement operations. Hao *et*

TABLE 14. Survey of recent N_2O data from combustion systems*

Andersson *et al.*†	Several European plants
Dahlberg *et al.*†	17 combustion plants
Electric Power Research Institute†	14 utilities
Laird and Sloan[151]	3 corner-fired, 2 opposed-fired (1 low-NO_x)
	3 wall-fired coal, 3 wall-fired oil (2 low-NO_x)
Linak *et al.*[33]	6 coal-fired
Muzio *et al.*[113]	2 oil-fired
	7 coal-fired
Persson[152]	1 coal-fired
Sage[153]	2 stokers
Sloan and Laird[46]	4 wall-fired, 3 corner-fired, both normal burners and low-NO_x burners
Soelberg[154]	11 plants
Vitovec and Hackl[116]	9 coal-fired plants, including pulverized coal, lignite, stoker-firing, and briquettes
	11 oil-fired plants
	4 petroleum-coke plants
Yokoyama *et al.*[117,118]	7 coal-fired
	21 oil-fired

* Pulverized-coal fired unless otherwise indicated.
† As reported in Mann *et al.*[24]

al.[25] surveyed nine oil-fired and three coal-fired furnaces in northeastern USA, as well as measurements on a pilot-scale furnace.[150] For both Castaldini and Hao a correlation was noted in which the apparent N_2O emissions (obtained using sample flasks and remote analysis) were about 25% of the NO_x emissions measured on-line at the site (see Fig. 5). As discussed in Section 3, this apparent proportionality was due to the conversion of NO_x within the sample flasks to N_2O at an approximate 4:1 ratio. Following the identification of this artifact, both measurement methods development (see Section 3) and retesting of combustion sources have been priority activities.

6.2. *Recent Database on Pulverized Coal Emissions*

Extensive recent surveys of N_2O emissions from pulverized coal and oil-fired furnaces have been reported. Table 14 summarizes sources of these data.[24,33,46,113,116–118,151,153,154] It is clear from reviewing this very large database that the majority of measurements from industrial combustion systems yield very little N_2O. Emissions in excess of 5 ppm are very rare, with the exception of combustion fluidized beds, which are discussed in Section 7. One general trend is that higher emissions tend to be associated with oil-fired units, although the emission levels are still quite low. The reason for this is not known.

As discussed in Section 3, at these very low emission levels, the care taken in measurement becomes critical. Simple drying or SO_2 scrubbing will prevent the formation of large amounts of N_2O. However, measurement studies show that residual moisture, SO_2, and/or long sample lines will still allow a few ppm of N_2O to form. Thus, the preponderance of the data suggest very low values, and the few outliers warrant close examination to determine if unusual combustion conditions exist, or if sampling procedures were adequate.

6.3. *Mechanistic Studies of Pulverized Coal Combustion*

In spite of the fact that emissions from industrial pulverized coal furnaces are low, several recent studies indicate that higher concentrations exist early in the flame zone. The relation between the fast formation and destruction chemistry early in these pulverized coal flames has become an area of interest that may have some relevance in combustion fluidized beds.

Smart *et al.*[155] obtained time-resolved data in the large axial IFRF pulverized coal flame. The firing rate was 2500 kW and the maximum temperature was about 1600 °C. In this flame, N_2O peaks early in the flame zone at 12 ppm, and decays to an exhaust concentration of about 4 ppm.

Abbas *et al.*[156] performed time-resolved measurements within a moderately swirled pulverized coal flame. This smaller flame (ca 130 kW) yielded a lower maximum flame temperature (1270 °C) than in the experiments of Smart *et al.*[155] In spite of the differences in scale and temperature, Abbas saw similar behavior: an early peak at 9 ppm followed by decay to the exhaust concentration at 4.5 ppm. Both groups interpreted their data as indicating that the N_2O emission was the result of flame-zone N_2O which failed to be fully destroyed before exiting the furnace.

Some valuable insight was provided by the experiments of Aho *et al.*[157] who added dilute suspensions of coal and peat to hot flue gas in a plug-flow reactor operating between 750 and 970 °C. The overall residence time was approximately 370 ms for most of the

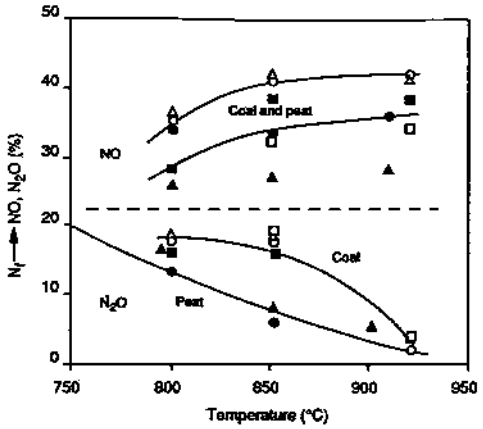

FIG. 22. Conversion of fuel nitrogen into N_2O and NO from a dilute suspension of various coals and peats at 18% O_2: ● S H3 peat, ▲ C H5 peat, ■ English coal, ○ U.S. coal, △ Colombian coal, □ Australian coal (adapted from Aho *et al.*[157]).

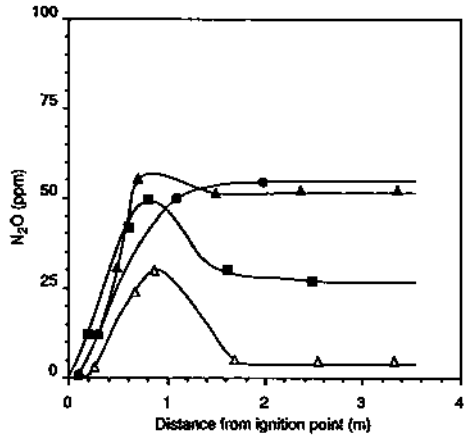

FIG. 23. Effect of maximum combustion temperatures on the time-resolved behavior of N_2O in a pulverized coal flame. Taiheiyo coal, SR = 4.96, d_p = 63 – 105 μm: ● T_{max} = 800 °C, ▲ T_{max} = 900 °C, ■ T_{max} = 1000 °C, △ T_{max} = 1100 °C (adapted from Okazaki *et al.*[160]).

runs. Figure 22 shows the conversion of fuel-nitrogen to NO and N_2O as a function of temperature. Over this residence time, they saw maximum conversion of fuel-nitrogen to N_2O (ca 20%) at the lowest temperature. By 970 °C, essentially no N_2O was found in the exhaust. One could argue, in light of the preceding data[155,156] that at the highest temperatures an N_2O transient was present at short times, but the N_2O was destroyed before exiting. Unfortunately, no time-resolved data were presented at the higher temperature conditions. They also examined the yield of N_2O at 800 °C for a coal and various peats.[158] They found that N_2O yields decreased with increasing fuel oxygen:nitrogen ratio. This suggests less N_2O formation from lower rank fuels, and mirrors the results for fluidized bed combustion presented in Section 7.

In another experiment, Aho *et al.*[157] measured the decay of N_2O added through the coal injector. At 970 °C and 18% O_2, only about half the N_2O was removed before exiting the reactor. Alternatively, if the O_2 concentration was decreased to about 1% and 500 ppm CO was added with the N_2O, the N_2O was fully destroyed in under 50 ms. The suggestion is that the oxidizing CO provided hydrogen atoms to rapidly remove the N_2O. Interestingly, the co-addition of a small amount of peat with the N_2O failed to increase N_2O destruction.

In light of this, there appear to be at least two plausible reasons why N_2O emissions were not noted during the high-temperature coal injection tests shown in Fig. 22: (1) no significant N_2O may have formed, and (2) if N_2O were formed, it could have been removed by the burning volatiles. The failure of injected peat to remove N_2O could have been due to the small amount used, or the fact that the peat volatile combustion may have been concentrated around the particles, and thus in poor contact with the free-stream N_2O.

Hein[159] examined time-resolved N_2O behavior in a 700 kW facility burning German brown coal. These data also showed an early peak (maximum value 40 ppm) which decayed to zero before exiting the reactor. An interesting additional observation is that higher N_2O transient peaks were obtained when the primary zone stoichiometry was restricted towards fuel-rich conditions.

Okazaki *et al.*[160] present a very valuable set of time-resolved pulverized coal measurements in which the temperature of the furnace is varied. As shown in Fig. 23, at low temperatures, N_2O rises to its final value early in the flame zone, and then remains frozen at that value through the remainder of the furnace. At high temperatures, the data strongly resemble the larger-scale coal data: a small peak early in the flame, followed by a decay.

In staged and unstaged oil flames, N_2O was also observed as an early intermediate.[161] Like the other time-resolved data, it rapidly decayed with distance along the flame axis. Like the data of Hein,[159] higher N_2O concentrations were seen early in the flame during staged operation (i.e., when the primary flame was restricted towards fuel-rich conditions).

It is likely that the source of the early N_2O peak is the oxidation of the high flux of HCN arriving in the gas phase from devolatilization. The relationship between this early peak and the N_2O that is actually emitted is less clear, however. Kinetic modeling[71] suggests that N_2O has a very short lifetime under flame condtions. In particular, the 1600 °C flame temperatures of Smart's experiment[155] yield a very short predicted half life. How, then, can N_2O be measured consistently within the flame zones of pulverized coal flames? Also, what is the actual source of the emission measured at the exhaust?

One train of thought is that the N_2O formed in the primary flame is due to a very high flux rate of volatile nitrogen (as HCN) entering the gas phase. Here, it partially reacts to form N_2O, which is also subject to rapid removal reactions. Thus, the N_2O

can be considered to be in pseudo steady state; it is rapidly formed and destroyed, and the exact concentration depends on the local balance between these fluxes.[71] Due to the speed of the reactions, the N_2O will disappear almost immediately if the source flux is removed. Thus, according to this interpretation, the N_2O that appears in the exhaust is not the N_2O that is present in the transient peak. The early N_2O has been completely destroyed, and the exhaust N_2O was actually formed downstream.

An alternative view is based on the fact that coal flames are not well mixed, and the N_2O measured in the early region could be the result of formation in low-temperature, fuel-lean pockets. Here, kinetics suggest that conditions favour N_2O formation. Persistence of these unmixed pockets out of the flame zone and into the exhaust could lead to a flame zone contribution to N_2O emission. In light of what is known, detailed kinetic modeling would likely resolve these issues.

7. COMBUSTION FLUIDIZED BEDS

Among fossil fueled combustion systems, combustion fluidized beds have consistently shown the highest N_2O emissions in field measurements. Although this unwelcome finding has become widely recognized only during the last 6 years, it has spawned a large research effort. The work has focused on (1) formation mechanisms, (2) emissions as a function of combustion parameters, and (3) control strategies.

One response to this high level of interest is the recent appearance of two in-depth reviews of the behavior of N_2O in combustion fluidized beds.[24,162] Major sources for these reviews are the 11th International Fluidized Bed Conference in 1991, as well as the International Workshops on N_2O Emissions that were held in France in 1988[115] and Portugal in 1990. Section 7.2 summarizes the major conclusions of these reviews. Section 7.3 provides a more detailed discussion of papers that have recently appeared. This includes results from the N_2O Workshop that was held in Tsukuba, Japan, in July 1992,[163] as well as a discussion of the controlling mechanisms. The influence of NO_x (and N_2O) abatement strategies on emissions from fluidized beds is discussed in Section 8.

7.1. *Field Data*

Field measurements on various full-scale fluidized bed systems have been reported primarily at the 3rd, 4th, and 5th International Workshops on N_2O Emissions, and at the 11th FBC Conference. Table 15 summarizes some of the features of these measurements.[113,115,116,130,152,153,164–169] It must be borne in mind that the measurements reported at the 3rd International Workshop on N_2O Emissions[115] were made before the sample container artifact was discovered, although the vast majority of these measurements were made under procedures that minimized the in-container generation of N_2O (i.e., most of the samples were dried before storage). The field tests consistently indicate emissions substantially above those found from pulverized coal flames or fuel oil flames.

Attempts to draw general conclusions from the field data are very difficult due to the wide variation in combustor configurations, operating parameters, and fuel types. In spite of this, certain trends are clear from the data. First, N_2O emissions uniformly decrease with increasing bed temperature. At the same time, NO_x emissions increase. In general, lower rank fuels deliver lower N_2O emissions. Most other operating parameters (excess air, addition of limestone) appear to have a weak influence on N_2O. Carefully obtained subscale data have been the means of advancing our understanding beyond that available from field data.

7.2. *Summary of Major Trends*

The following presents the major observations reported in the reviews by Mann *et al.*[24] and Hayhurst and Lawrence.[162] First, it cannot be overemphasized how difficult it is to extract mechanistic information from fluid bed experiments. In general, a wide variety of experimental designs and scales have been used to study N_2O formation in fluidized beds. In addition, enough information is frequently not provided to fully rationalize these data.[162] In fluidized beds many of the parameters are coupled in actual experiments (e.g., excess air and bed temperature), which makes it difficult to cleanly extract the influence of a single variable. These observations show the highly empirical nature of the fluidized bed database, and suggest that much care must be taken in data analysis to develop general conclusions. In spite of these difficulties, considerable progress has been made in understanding this complex phenomenon.

The most pronounced trend is that of temperature. Reduced bed temperatures almost universally cause higher N_2O emissions, as the measurements presented on Fig. 24 show.[167] As discussed in Section 7.3, a number of mechanisms describe the temperature effect. Figure 24 also shows that NO increases with bed temperature, suggesting that higher operating temperature is not the best means of controlling N_2O.[170] In addition, higher operating temperatures reduce SO_2 capture by limestone.

The influence of fuel type is less significant than that of temperature. In general, lower rank fuels tend to yield lower N_2O emissions. This has been attributed to the tendency of the lower rank fuels to favor NH_3 release over HCN release.[108,109] HCN is acknowledged to be more efficiently converted to N_2O.[71,162] Alternatively, the higher surface area of

TABLE 15. Summary of field data for combustion fluidized beds

Åmand and Lechner[164] Åmand *et al.*[130,165]	One 8 and one 12 MW CFB. Detailed parametric variations of excess air, lime addition, and char loading
Braun *et al.*[166]	One 4 MW_T AFBC used for plant heating. Examined influence of bed temperature, fuel-type, and NO_x control strategies
Brown and Muzio[167]	One AFBC and one CFBC were examined in detail. Variations included bed temperature, excess air, and sorbent feed. Also more limited parametric variations at three cogeneration CFBC sites
Gustavsson and Leckner[168]	Examined gas injection for N_2O control at a 12 MW_T CFBC. Emissions range from 80 to 250 ppm as a function of temperature. Examined a number of parameters
Hiltunen *et al.*[169]	Measurements from 8 CFBCs. Results correlated in terms of mean furnace temperature and fuel type. Emissions range from 10 to 140 ppm
Muzio *et al.*[114]	Three CFBCs with N_2O ranging from 26 to 84 ppm at 3% O_2. One unit at 3 loads: 55, 75, 100% of full load, yielding 126, 93, 84 ppm N_2O, respectively
Persson[152]	One 15 MW PFBC and one 40 MW CFB. Varied bed temperature in the larger unit and looked at NO_x control agents
Ryan and Srivastava[115]	Summary of Third International N_2O Workshop; data presented on 4 Swedish units and 6 Finnish units
Sage[153]*	Two AFBCs: 30, 22–77 ppm; one CFBC: 91 ppm
Vitovec and Hackl[116]*	Austrian measurements. Four CFBCs, three AFBCs. CFBC results showed strong dependence on fuel type: bituminous coal = 24 ppm, lignite = 7.5, bark/sewage sludge/bituminous coal = 3.3, bark/sewage sludge = 0.8

*Converted from mg/m^3 to ppm.

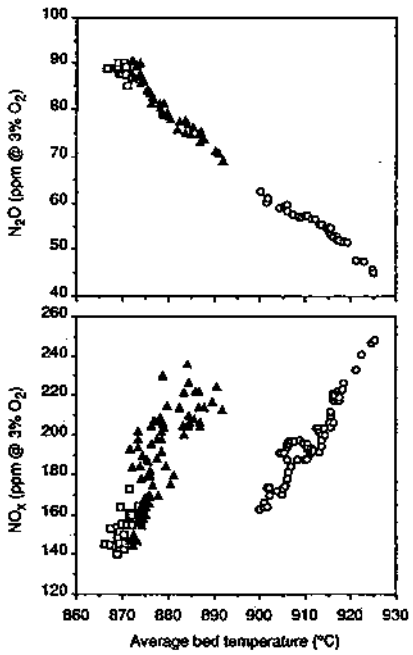

FIG. 24. Comparison of NO_x and N_2O emissions for various combustion temperatures from a full-scale combustion fluidized bed: Nuncia ▲ 56 MW, □ 57 MW, ○ 110 MW (adapted from Brown and Muzio[167]).

lower rank fuels may promote more complete heterogeneous N_2O destruction.[170]

Other correlations have been observed, including an inverse relationship between the oxygen:nitrogen ratio of the fuel and N_2O,[24,126] and an increase with the carbon content of the coal.[164] Although the specific mechanisms underlying these correlations are unclear, both the oxygen:nitrogen ratio and coal carbon content can, within limits, be indirect indicators of coal rank.

Excess air has been an unusually difficult parameter to distingish from temperature because they are so closely coupled in fluidized bed operation. In experiments where the temperature effect was removed, higher excess air generally increases N_2O emissions. Mann *et al.*[24] examined the coupling between temperature and excess air, and found that, at higher temperatures, excess air has less of an effect on N_2O emissions, as shown in Fig. 25.

There appears to be considerable disparity in the effects of limestone addition on N_2O emissions.[24,162,171] In all cases, the change in emission was small, whether the trend was up or down. The results reported in Section 5 show that CaO is an N_2O removal catalyst, although it is also a catalyst for the formation of N_2O from NH_3. In either case, the limestone sorbent is actually coated with $CaSO_4$ due to the absorption of SO_2 during the experiments. As discussed in Section 5, $CaSO_4$ showed much less activity for both formation and destruction. Thus, issues such as the degree of sulfation of the sorbent, the amount of NH_3 released by the coal, and the amount of limestone used (set by the sulfur content of the coal) can be expected to interact to determine the net influence on N_2O. The reader is referred to Mann *et al.*[24] and Hayhurst and Lawrence[162] for a complete discussion of the details.

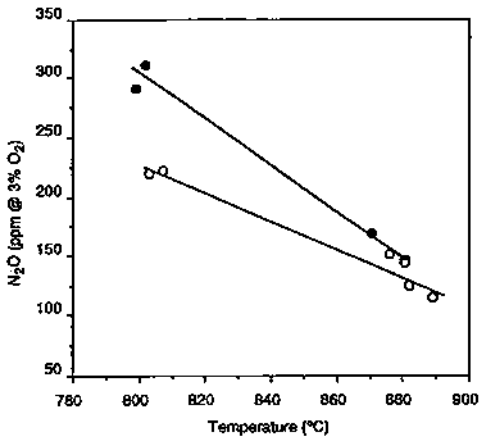

FIG. 25. Influence of excess air on N_2O emissions from a 1 MW pilot-scale circulating fluidized bed combustor: ○ 19% excess air, ● 43% excess air (adapted from Mann *et al.*[24]).

Wallman *et al.*[172] saw an increase in both NO_x and N_2O with pressure. Although the authors attribute this to increased reduction of NO to N_2O over char, the results of de Soete[119] do not support this as a major pathway unless oxygen is present.[127–129] Other results show an increase in N_2O with pressure for bituminous coal, but little change for peat or brown coal.[173] At present, the effect of pressure does not appear to be well understood.

7.3. *Recent Results and Mechanistic Interpretation*

Results which have appeared since the reviews of Mann *et al.*[24] and Hayhurst and Lawrence[162] have further verified trends. These results are largely from the 5th International Workshop on N_2O Emissions which was held at Tsukuba, Japan in July 1992, which was notable for the number of mechanistic studies presented.[163]

In spite of the large number of results, the ongoing controversy over the relative contribution of homogeneous vs heterogeneous N_2O formation in fluidized beds has not been settled. This is really part of a larger question concerning the general mechanisms that are active in fluidized beds. It may well turn out that there is no single answer to these questions, but rather various answers depending on the type of fluidized bed (bubbling vs circulating), fuel type, and operating conditions. Fortunately, much of the recent data have been obtained with the goal of developing an improved mechanistic understanding.

7.3.1. *Temperature*

The tendency of N_2O emissions to decrease with higher bed temperatures is verified by additional results.[174–182] The source of this temperature effect is still an area of controversy. Wallman *et al.*[172] show, through laboratory-scale fluidized bed experiments, that N_2O is formed at the lowest bed temperatures (< 725 °C), but that many solid materials will catalyze decomposition at these low temperatures. They propose that the temperature effect is due to increased catalytic decomposition activity as the temperature increases rather than increased homogeneous removal via $N_2O + H$. The latter reaction is argued to be too slow to contribute at these lower temperatures.[170,172]

Alternately, both Naruse *et al.*[183] and Kilpinen and Hupa[91] have been able to reproduce the fluidized bed temperature behavior (down to 727 °C) based entirely on homogeneous chemistry. For Kilpinen and Hupa the decreasing N_2O at higher temperatures comes about not because of the increasing rate of $N_2O + H$ or increased heterogeneous removal. Instead, the kinetics suggest that higher temperatures promote the oxidation of NCO to NO via:

$$NCO + O \rightarrow NO + CO \qquad (34)$$

$$NCO + H \rightarrow NH + CO \qquad (36)$$

with the NH being eventually oxidized to NO. These reactions compete for the available NCO pool, and reduce the amount of NCO available for N_2O formation via:

$$NCO + NO \rightarrow N_2O + CO. \qquad (29)$$

At high temperatures (> 950 °C) the $N_2O + H$ reaction begins to contribute to N_2O removal. The relative importance of these various pathways are illustrated in Fig. 26 for a high and low bed temperature. Note that these predictions were made with a mechanism that used the earlier, faster rate for Eq. (29). The revised data for this reaction, and the potential that not all the products branch into $N_2O + CO$, may modify the conclusions drawn in Fig. 26. Note also that the figure does not suggest a highly significant role for the $N_2O + OH \rightarrow N_2 + HO_2$ reaction. Thus, the reduced rate for this reaction suggested by Glarborg *et al.*[62] should not affect the calculations.

Kinetics allow the resolution of one apparent discrepancy in the temperature behavior of fluidized beds. In fluidized beds, the N_2O yield increases as the temperature is reduced throughout the normal operating range down to 700 °C. However, when HCN or urea is injected into flue gases for NO_x control, N_2O yields peak at 980 °C.[71,91] This difference is explained by homogeneous chemistry. At lower temperatures, HCN and NH_3 by themselves do not provide enough chain branching to sustain a self-propagating decomposition. In fluidized beds, however, volatile oxidation provides sufficient excess radicals to allow HCN oxidation and N_2O formation to proceed at lower temperatures. With N_2O formation removed as a rate-controlling step, the concentration becomes controlled by other factors as the temperature is increased: (1) the decrease in the

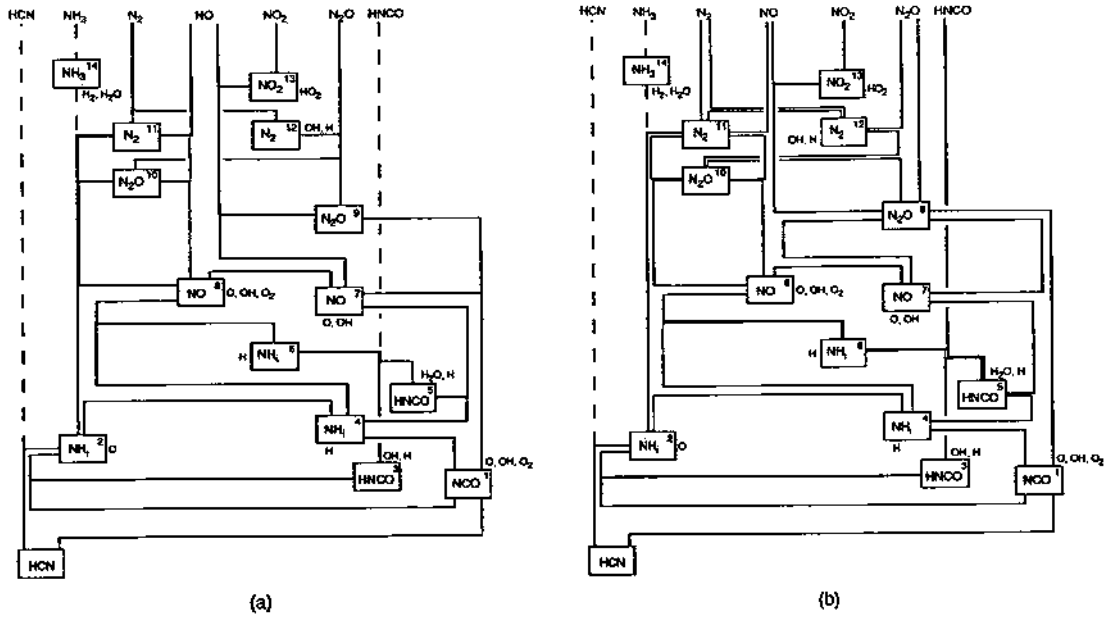

FIG. 26. Critical homogeneous pathways for nitrogen in fluidized bed combustion: (a) 1200 K, (b) 1000 K (adapted from Kilpinen and Hupa[91]).

fraction of NCO that becomes N_2O,[91] (2) the increase in the catalytic destruction rate,[170] and (3) at higher temperatures, the increase in the rate of the N_2O + H reaction.

7.3.2. *Fuel effects*

Numerous studies presented in the reviews[24,162] suggest that higher rank fuels yield more N_2O in fluidized beds. Although several theories have been offered explaining this behavior, none at present appear to be fully consistent with all of the trends within the data. Very likely, several mechanisms are, to greater or lesser degrees, active simultaneously.

Braun *et al.*[166] show that a low-volatile bituminous coal yields more N_2O in a bubbling bed than a high-volatile bituminous coal at the same bed temperature. This trend could be due to higher freeboard temperatures for the high-volatile coal. These higher temperatures promote homogeneous N_2O destruction, and are caused here by the combustion of volatiles in the freeboard. These are released near the top of the bed due to the overbed feeding system. Alternately, Wójtowicz *et al.*[170] suggest that at low bed temperatures homogeneous destruction will be ineffective due to low hydrogen atom concentrations and also the high activation energy of the N_2O + H reaction (although they do suggest that higher freeboard temperatures may be responsible for the behavior). These general trends correlating high coal rank with high N_2O emissions have been observed by other investigators.[179,181,184] The trend for higher N_2O from low-volatile coals also holds for circulating beds.[180]

Another approach has been to correlate the behavior through differences in the bed solids characteristics. Although it is difficult to rationalize a large difference in bed solids between the low- and high-volatile bituminous coals used by Braun *et al.*,[166] differences between bituminous coals and lignites could be important. Wójtowicz *et al.*[170] suggest that the unusual mineral matter content of lignites (e.g., high calcium content) could be partly responsible for suppressing N_2O emissions through heterogeneous destruction. An alternative thought follows similar lines. Lignites tend to generate more ash in the aerosol mode (0.1–0.2 μm) through a vaporization–condensation mechanism.[185] Once released, this aerosol presents a very large surface area for potential catalytic N_2O reduction.

A third difference between low- and high-rank fuels is the tendency of low-rank coals to yield their fuel nitrogen as NH_3 rather than as HCN.[108,109] Several experimental and modeling studies have shown that NH_3 is much less efficiently converted to N_2O than HCN under fluidized bed conditions.[71,91]

7.3.3. *Combustor configuration*

As stated above, one cannot necessarily expect that the same N_2O formation–destruction mechanisms will have the same importance in both circulating and bubbling beds. Naruse *et al.*[174] introduced coal into a bubbling fluidized bed at two locations. In the first configuration the coal was placed on the upper surface of the bed. As shown in Fig. 27, N_2O profiles through the bed indicate that most of the formation takes place in the freeboard. When the coal was introduced at the air distributor, the figure shows that the N_2O formed deep within the bed. This suggests that, at least in bubbling beds, a significant

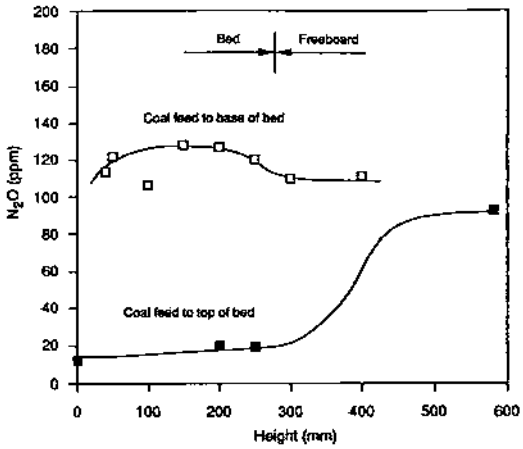

FIG. 27. Influence of location of coal feed on N_2O profile through a bubbling fluidized bed (adapted from Naruse *et al.*[174]).

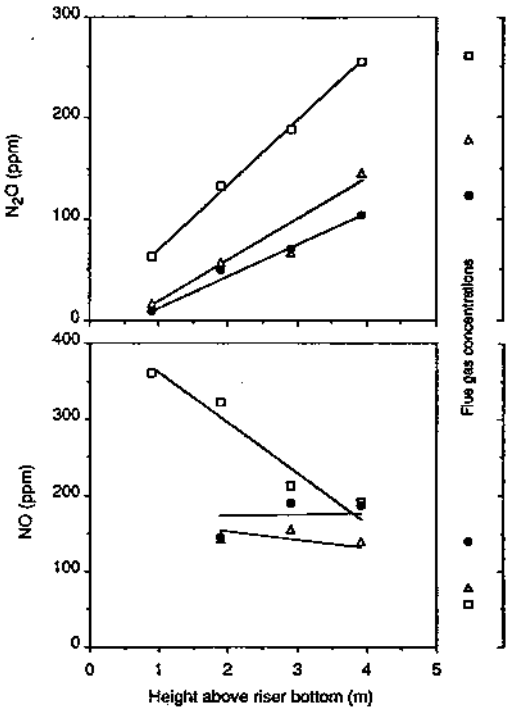

FIG. 28. Concentration profiles for NO and N_2O through a circulating fluidized bed riser at 1073 K for three different coals: ● Taiheiyo high volatile bituminous, △ Datong high volatile bituminous, □ unnamed medium volatile bituminous (adapted from Moritomi and Suzuki[180]).

fraction of the N_2O is formed rapidly, on a time frame similar to that of devolatilization.

In circulating beds, the N_2O formation appears to be more well distributed. Figure 28 shows profiles taken through a circulating fluidized bed by Moritomi and Suzuki.[180] Here, N_2O concentrations increase uniformly throughout the riser section of the combustor, while the NO concentration simultaneously decreases. This has been taken as evidence

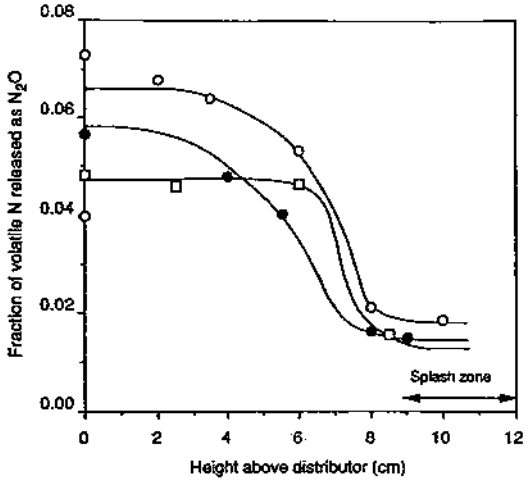

FIG. 29. Yield of N_2O from coal particles that are restrained to burn at a specific height in an externally heated fluidized bed: ○ anthracite, ● lignite, □ bituminous (adapted from Hayhurst and Lawrence[162]).

by some that NO is formed early from volatile nitrogen and is then converted slowly to N_2O through heterogeneous reactions. However, increased excess air increases both NO and N_2O, which suggests that NO is not the only source of N_2O.[180] Åmand *et al.*[165] measured little HCN within the riser of a CFBC, which has been taken as evidence of lack of homogeneous formation. Under these conditions, however, rapid consumption of HCN suggests that low measured HCN concentrations do not necessarily rule out homogeneous formation.

Hirama and Hosoda[186] compared a circulating bed with a bubbling bed operating at the same temperature. They found that the circulating bed generated substantially more N_2O than the bubbling bed. The same trend can be seen in the field data; although not unexpectedly, there is more variation in these results.

The role of combustor configuration has also been addressed by comparing results in which the reaction environment is varied. Hayhurst and Lawrence[162] suspended a coal particle within an electrically heated bubbling bed, and measured the final N_2O emissions as the location (i.e., height) of the particle was varied within the bed. They found, as shown in Fig. 29, that the highest N_2O emissions were obtained with the particle located deep in the bed. As the particle was moved towards the surface, the N_2O emissions decreased. This decrease was associated with the appearance of a luminous volatile flame above the bed. The lowest emissions occurred when the particle was freely burning in the freeboard region. Hayhurst and Lawrence attribute this behavior to a suppression of the N_2O destruction reactions by the bed material. In particular, the hydrogen atoms that are critical for destroying N_2O may be preferentially destroyed by catalytic reactions on the bed material.

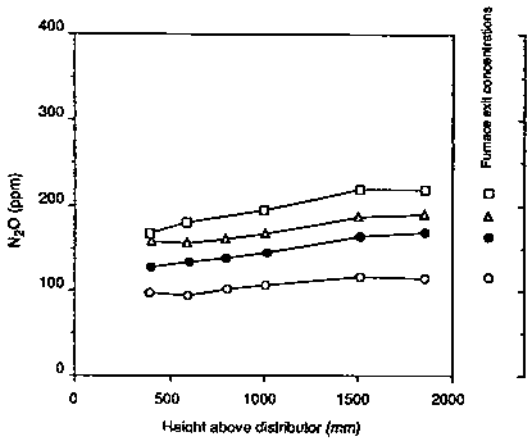

FIG. 30. Influence of bed material size on N_2O from a bubbling fluidized bed: ○ 0.66 mm, ● 0.58 mm, △ 0.45 mm, □ 0.37 mm, bed temperature = 800 °C, excess air = 6.2%, bed material = sand, static bed height = 130 mm, fluidizing velocity = 2.0 m/s (adapted from Fujiwara *et al.*[176]).

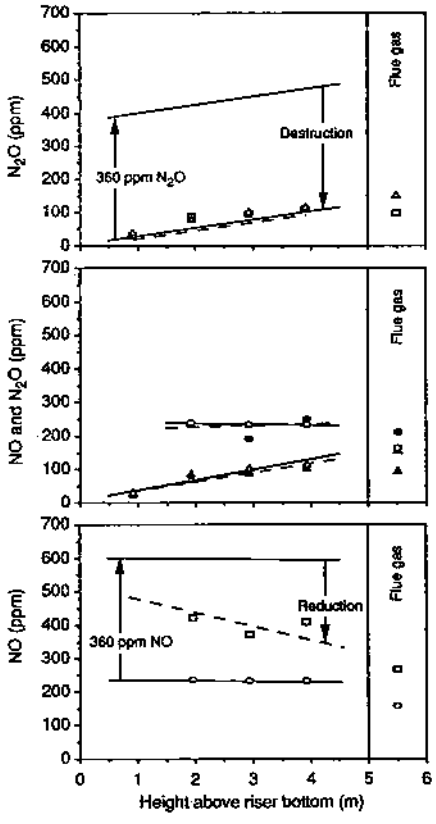

FIG. 31. Changes in concentration profiles of NO and N_2O when NO and N_2O are added to the base of the riser in a combustion fluidized bed burning bituminous coal: Panel 1: △ N_2O before addition, □ N_2O after addition of 360 ppm N_2O; Panel 2: △ N_2O before addition, ▲ N_2O after addition of 360 ppm NO, ○ NO before addition, ● NO after addition of 360 ppm N_2O; Panel 3: ○ NO before addition, □ NO after addition of 360 ppm NO (adapted from Moritomi and Suzuki[180]).

This overall destruction may be accelerated by the high diffusivity of these hydrogen atoms within the dense bed. An alternative interpretation along the lines of Kilpinen and Hupa[91] would suggest that more of the volatile nitrogen is processed into N_2O within the bed because (1) the presence of the bed material moderates the volatile combustion temperature, and (2) the bed material provides a surface for the catalytic recombination of free radicals from volatile combustion. Both of these effects act to restrict NCO oxidation as an alternative to N_2O formation. As the particle height increases and more of the combustion occurs in the freeboard, the temperature and radical concentrations increase and more of the NCO is converted to NO.

Another approach to this was taken by Fujiwara *et al.*[176] They varied the mean diameter of their bed support material while holding all other parameters constant. In this case, *decreasing* the size of the bed material *increased* the fraction of the bed volume occupied by voids (i.e., bubbles). As illustrated by Fig. 30, this had the effect of increasing the N_2O emissions. This suggests that more N_2O is formed within the bubbles than is formed in the dense phase. Initially, this appears to contradict the results of Hayhurst and Lawrence,[162] who saw more N_2O formed when the reactions occurred within the dense parts of the bed. While the results of Fujiwara *et al.* cannot be explained at present, it may be possible that the bubbles provide a vehicle for speeding the removal of volatile nitrogen from the bed.

7.3.4. *Homogeneous vs heterogeneous N_2O*

One of the most important mechanistic issues in fluidized beds is the relative contribution of homogeneous vs heterogeneous N_2O formation reactions. This problem has been extremely difficult to decouple experimentally. In a fluidized bed combustor, both the solid phase and the gas phase act to modify the environment experienced by the other. Thus, fixed bed data where no homogeneous chemistry occurs must be interpreted cautiously in a fluidized bed context. Likewise, strictly homogeneous models may not include critical features describing the interaction between the gas-phase species and the bed material. One approach to obtaining mechanistic data has been to perturb the fluidized bed environment and monitor the result. Several recent studies have used this approach with considerable success.

One attempt to directly define the homogeneous vs heterogeneous contributions is the work of Moritomi and Suzuki.[180] In their experiment, a circulating fluidized bed was fired on either petroleum coke or bituminous coal. Both NO and N_2O were separately injected into the bed to determine (1) the incremental destruction of each of these species, and (2) the degree to which each was converted to the other in the process of being destroyed. Figure 31 shows that,

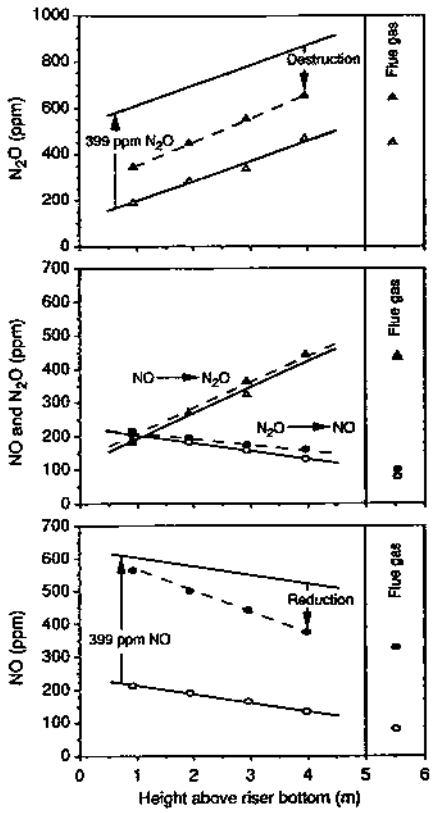

FIG. 32. Changes in concentration profiles of NO and N_2O when NO and N_2O are added to the base of the riser in a combustion fluidized bed burning petroleum coke: Panel 1: △ N_2O before addition, ▲ N_2O after addition of 399 ppm N_2O; Panel 2: △ N_2O before addition, ▲ N_2O after addition of 399 ppm NO, ○ NO before addition, ● NO after addition of 399 ppm N_2O; Panel 3: ○ NO before addition, ● NO after addition of 399 ppm NO (adapted from Moritomi and Suzuki[180]).

for bituminous coal, the injected N_2O was essentially completely destroyed. Figure 31 also shows that essentially none of the injected N_2O was converted to NO during the destruction reaction. When NO was the injected species, only part of the added stream was destroyed, although (again) none of the destroyed NO was converted to N_2O.

These results show that the bituminous coal bed possesses a very strong reducing power towards N_2O. The injection of an additional 360 ppm of N_2O failed to perturb the existing N_2O profile through the bed. This suggests that the N_2O formed within the bituminous coal bed is the result of the balance between a fast formation reaction and a fast destruction reaction. The speed of the destruction reaction is such that the appearance of an additional 360 ppm of N_2O failed to perturb the balance. This further suggests that the formation reactions, in order to develop the amount of N_2O measured, must be supplying a flux that considerably exceeds that corresponding to the 360 ppm of added N_2O. The fact that little of the added NO appeared as N_2O is inconclusive because, even if it were converted to N_2O at 100% efficiency, no increased N_2O emission would be expected, considering that 360 ppm of N_2O injected directly into the bed did not cause an increase.

Wallman *et al.*[172] present a similar experiment, except they used a bubbling bed burning bituminous coal. In contrast to Moritomi and Suzuki,[180] however, the addition of 400 ppm of N_2O to the combustion air resulted in a small increase in N_2O emissions.

Another apparent contradiction is found in the data of Tullin *et al.*[127] In these laboratory-scale measurements the addition of 250 ppm of NO to the bed resulted in an increase from 15 to 24% in the overall conversion of fuel-nitrogen to N_2O. In contrast, the measurements of Moritomi and Suzuki[180] found no change in N_2O when NO was doped into their bed. Thus, it appears that the capability of the bed of Tullin *et al.*[127] for reducing N_2O, which was so strongly noted in the experiments of Moritomi and Suzuki,[180] was diminished. With the relatively light loading and batch operation, N_2O destruction could be reduced due to (1) reduced heterogeneous N_2O destruction, or (2) reduced homogeneous destruction once the coal was devolatilized in these batch experiments. Note that in both experiments, the conversion of NO to N_2O could proceed, but for Moritomi and Suzuki[180] the additional N_2O would have been destroyed by the bed.

The results for the petroleum coke portion of the Moritomi and Suzuki[180] experiment are, however, difficult to rationalize in terms of homogeneous chemistry. When their previous experiment was repeated, some similar features emerged. One is that when NO was injected and destroyed in the bed, little additional N_2O was formed. Likewise, destroyed N_2O did not appear as NO. The first difference is the much higher N_2O emissions, as shown in Fig. 32. The second major difference is that externally added N_2O was only partially destroyed, rather than completely destroyed as with bituminous coal. This second observation suggests that the destruction reactions are not nearly so active in the case of petroleum coke, something that could be explained by the very low volatile content of this fuel. On the other hand, the high N_2O emissions compared to the bituminous coal (450 vs ca 100–150 ppm) and the very high conversion of fuel-nitrogen to N_2O (22.6%) are difficult to explain. Moritomi and Suzuki propose this as evidence that the direct conversion of coke nitrogen to N_2O is the dominant mechanism, since the coke contains only 5.3% volatile matter. This is difficult to reconcile with the much lower conversions of char-nitrogen to N_2O obtained by de Soete[119] and others (1–6%). The alternative that NO obtained from char oxidation reacts at the char surface to produce N_2O is difficult to reconcile with the fact that externally added NO did not yield any increase in N_2O emissions. As pointed out by Mann *et al.*,[24] one possible explanation is that a gasification reac-

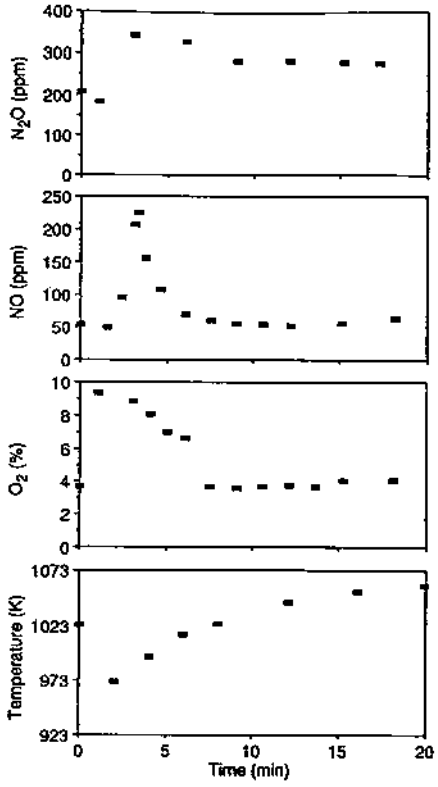

FIG. 33. Changes in the emissions from a fluidized bed burning coal caused by the addition of a spike of petroleum coke at time zero (adapted from Moritomi *et al.*[123]).

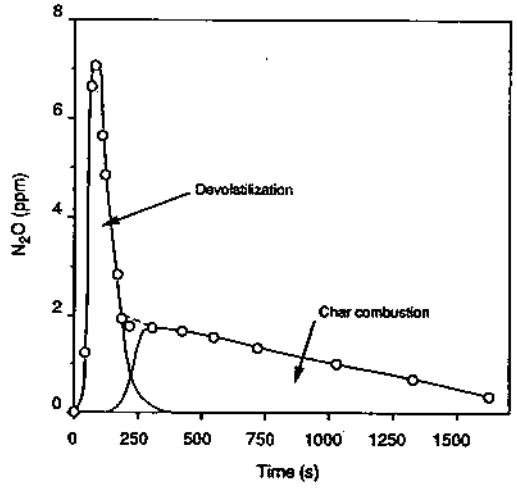

FIG. 34. Emission response of an externally heated fluidized bed to the injection of a small amount of bituminous coal, showing hypothesized reaction regime (adapted from Hayhurst and Lawrence[162]).

tion could provide another means of liberating char-nitrogen and forming N_2O homogeneously. This would not be dependent on the direct formation of N_2O from char-nitrogen, which from de Soete's data appears to give poor yields.

In a similar experiment, Moritomi *et al.*[123] spiked petroleum coke into a CFBC while it was burning

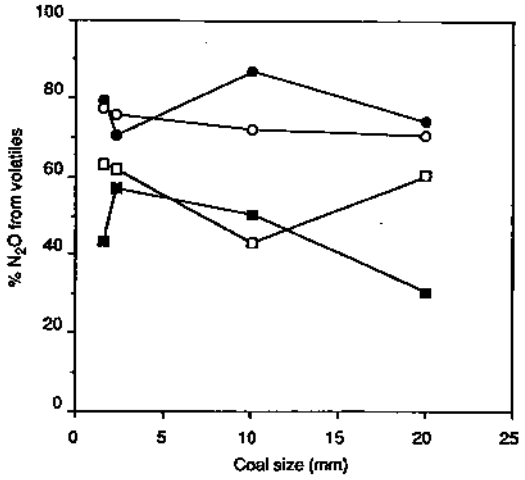

FIG. 35. Resolution of data from spiking experiments to show the fraction of N_2O projected to originate from volatiles as a function of coal type and bed temperature: ■ bituminous at 900 °C, □ bituminous at 800 °C, ● lignite at 900 °C, ○ lignite at 800 °C (adapted from Hayhurst and Lawrence[162]).

bituminous coal. Figure 33 shows that this generated a NO spike, and a long-term increase in N_2O emissions. Simultaneously, however, the temperature decreased and the O_2 concentration increased, both of which tend to increase N_2O. Thus, the higher N_2O could be due to this change in bed conditions, or to the increased conversion efficiency of char-nitrogen into N_2O.

Hayhurst and Lawrence[162] report the results of preliminary experiments where they introduce small batches of coal into an electrically heated bubbling bed. They then follow the N_2O emission with time through devolatilization and char burnout. As shown in Fig. 34, they are capable of resolving an N_2O spike due to devolatilization, and a long-term, slow emission due to char reaction. Integration of these two modes results in an estimate of the total emission that is due to volatile reaction vs that due to char-nitrogen conversion. This is shown in Fig. 35, which shows fairly equal yields of N_2O from both sources for the bituminous coal, and that a preponderance of N_2O arises from the volatiles for the lignite. At least two differences separate these experiments from the actual fluidized bed environments: (1) for the data in Figs 34 and 35, a single 2.5 g piece of coal was inserted into the bed, and (2) because the coal density was much below that found in normal practice, the concentrations of the gas-phase reacting species were much lower than in practice.

Tullin *et al.*[127] conducted a similar experiment in which fresh coal was added to an externally heated fluidized bed. The time-resolved data were similar in form to that of Hayhurst and Lawrence,[162] i.e., a spike in N_2O emissions followed by a long-term release during char combustion. Visual observation during these experiments suggests that devolatilization occurred while the coal particles "floated" on

the surface of the bed, and that this produced a visible flame. As noted earlier, the visible flame condition at the bed surface in the Hayhurst and Lawrence experiments was associated with reduced N_2O yields. Apparently, the bed material moderates volatile combustion temperature and reduces the radicals needed for NCO oxidation to NO. Thus, the experiments of Tullin *et al.*[127] may have understated the volatile N_2O yield compared with the situation where the devolatilization is dispersed throughout the bed material.

Pels *et al.*[184] also attempted to assign fractional conversions of char-nitrogen and volatile nitrogen to N_2O. Their results suggest that the fractional conversions of char-nitrogen were fairly low, while those of the volatile nitrogen were high.

Finally, several studies examined the effect of adding various species to fluidized beds. Gavin and Dorrington[182] examined the effect of doping fuel-nitrogen into a fluidized bed. They found that fuel-nitrogen model compounds (pyridine and pyrrole) strongly stimulated N_2O emissions due to homogeneous conversion. Likewise, Amand and Leckner[187] added CH_3CN to a large circulating fluidized bed and found substantial conversion to N_2O. They also found that the lower portions of their bed exhibited a strong reducing capability for N_2O, similar to that noted by Moritomi and Suzuki.[180] Dam-Johansen *et al.*[188] found that added SO_2 slowed HCN oxidation to N_2O through radical recombination, although the effect was weak. In contrast, Tullin *et al.*[189] also added SO_2 to a laboratory-scale fluidized bed and saw an increase in N_2O emissions. In this case, radical recombination was probably also active but, due to the lack of volatiles at the later stages of this batch experiment, the action was to suppress homogeneous N_2O destruction.

7.4. *Summary*

Clearly, more experimental work and detailed modeling would help to identify the controlling mechanisms in practical fluidized bed combustion. Many results and conclusions are contradictory, and subject to more than one interpretation. Nonetheless, fundamental data have identified two viable mechanisms for N_2O formation in fluidized beds.

(1) Devolatilization of fuel-nitrogen as HCN and NH_3, followed by oxidation to N_2O.
(2) Oxidation of char-nitrogen to NO, followed by the reaction of this NO with char-nitrogen to yield N_2O.

On the surface, homogeneous chemistry seems to be capable of explaining many of the major trends. The release of volatile nitrogen as HCN under fluidized bed conditions yields a known N_2O precursor into an environment where N_2O formation is favored. Lower rank coals are known to yield more of their fuel-nitrogen as NH_3, which does not convert to N_2O as efficiently under fluidized bed conditions. This tentatively explains the lower emissions observed with lower rank fuels. Alternately, low-rank coals may experience greater heterogeneous N_2O reduction due to their different ash composition and morphology. Homogeneous chemistry is capable of reproducing the most prominent characteristic of N_2O behavior in fluidized beds, the decrease in emissions with increasing bed temperature. It does so by showing that the key intermediate, NCO, is increasingly converted to NO rather than N_2O as the bed temperature increases.

Heterogeneous reactions are also capable of generating N_2O. The reduction of NO at a char surface to yield N_2O does not appear to occur if oxygen is not available to expose fresh char-nitrogen.[119] In the presence of oxygen, the effective mechanism appears to be the reaction of NO with exposed char-nitrogen to yield N_2O rather than the absorption of NO on the surface, followed by reaction with a second NO molecule.[127,131]

Extrapolation of these results to practical fluidized beds is more difficult. For example, the data of Tullin *et al.*[127] show that heterogeneous N_2O formation increases with NO doping, a feature used to imply that NO reduction at the char surface is the source of N_2O. Other data for practical beds show no increase in N_2O with NO doping.[180] This implies that strong N_2O destruction reactions are active in the bed that are capable of removing any additional N_2O which may be generated by the reaction of char-nitrogen with NO. Since the bed does generate N_2O emissions in spite of this strong reduction reaction, the actual source flux for N_2O must be many times that represented by the emission. The key question is the identity of this source. The hypothesis is that, in a realistically loaded bed, a large amount of volatile nitrogen passes through N_2O as an intermediate. The emission is only a fraction of the total amount of N_2O formed. The yield of N_2O from char-nitrogen may be masked by this active volatile chemistry in a realistically loaded bed.

An important message from these data is that both the volatile combustion and char oxidation processes involved in N_2O formation are coupled in systems operating under practical conditions. Experimental systems that seek to decouple the process by moving away from practical conditions (e.g., batch processes, light loading of an otherwise inert bed, use of char instead of coal) are expected to generate sound fundamental data. These results cannot, however, be directly extrapolated to describe trends in full-scale units. To do so requires a fully-coupled model that correctly integrates all of the fundamental steps.

8. BEHAVIOR OF N_2O DURING NO_x CONTROL PROCESSES

The goal of NO_x control procedures is to convert NO into N_2 by modifying the combustion environ-

ment, introducing a selective agent, or combining a selective agent with a catalyst. Since all of these processes involve nitrogenous intermediates, there is an opportunity that a portion of these intermediates will react to form N_2O. This possibility was recognized early, at least with respect to combustion modifications.[107,149]

This section will review the influence of the major NO_x control technologies on N_2O emissions, including:

(1) air staging;
(2) reburning or fuel staging;
(3) selective noncatalytic reduction (SNCR), including the thermal DeNO$_x$ process (NH_3 injection), the urea injection process, the RapreNO$_x$ process (cyanuric acid injection), and the use of advanced or promoted agents; and
(4) selective catalytic reduction (SCR).

In addition, we will briefly review the steps that have been taken to specifically control N_2O from combustion fluidized beds.

8.1. *Staged Combustion*

Air staging generally refers to the division of combustion air into at least two streams such that the fuel is initially processed through a region of reduced oxygen availability. Under these conditions, conversion of fuel-nitrogen to N_2 is improved. The second air stream completes fuel burnout. This basic strategy is executed in a number of ways, including fuel biasing and "burners out of service". The low-NO_x burners that are now available from most manufacturers are based on providing staged environments within the burner. The division of the air into two or more streams has been practiced in fluidized beds to create a fuel-rich zone for improved NO_x control.

As discussed in Section 6, it is well established that reducing furnace conditions leads to lower N_2O emissions from pulverized coal combustion. Thus, one might suspect that the early formation of N_2O noted in Section 6 would be reduced during staged combustion. This, however, does not always appear to be the case based on results from brown coal.[159] In spite of the overall fuel-rich conditions in the primary zone, free oxygen still persists early in the flame, and with it, N_2O.

At the point where secondary air is added, the fixed-nitrogen species are nominally distributed among NO, HCN, and NH_3. Thus, the oxidation of at least HCN might be expected to form N_2O. However, the data[159] show no N_2O formation at the staging point. One probable reason for this is the relatively high temperature, above 1000 °C. Another is the concurrent burnout of CO from the primary zone, which will generate hydrogen atoms via $CO + OH \rightarrow CO_2 + H$. Thus, at the staging point, any N_2O which is formed would likely not survive. Earlier work in a smaller furnace[107] failed to find an influence of staging. The emission levels in this facility were elevated (20–90 ppm), which was attributed to the relatively cool combustion temperature. Another study examining air staging in laboratory-scale furnaces[33] found similar N_2O emissions compared to unstaged operation. This study reported N_2O emissions from the staged combustion of natural gas, No. 2 fuel oil, and No. 5 fuel oil all less than 1 ppm. Coal combustion emissions ranged from 1 to 5 ppm.

Air staging can be approached in CFBCs by dividing the air injection location. Mann *et al.*[24] performed a brief examination and found no influence on N_2O emissions. Likewise, Hiltunen *et al.*[169] found no direct influence of air staging beyond that attributable to temperature changes. Jahkola *et al.*[173] found a weak increase in N_2O with staging, while Shimizu *et al.*[190] and Bramer and Valk[191] all saw a concurrent decrease in NO_x and N_2O with increased staging. Hayhurst and Lawrence[162] attribute the latter results to both increasing temperature in the flue gas and the creation of a rich zone at the bottom of the bed. It is clear from the varying results that staging appears to have only a weak influence on N_2O, and its effect is difficult to separate from other parameters.

8.2. *Reburning*

Reburning or fuel staging involves the addition of a second fuel stream after the primary fuel burnout is completed. For example, a low-NO_x burner can be used to complete the burnout of the primary fuel. Secondary fuel is added above these burners to create a moderately fuel-rich zone. Within this zone, radicals generated by the secondary fuel decomposition attack NO to produce N_2, HCN, and NH_3. A final air stream is added to burn out the secondary fuel and convert any remaining reduced nitrogen to NO or N_2. Both coal (containing fuel-nitrogen) and natural gas (nitrogen-free) have been proposed as reburning fuels. Process descriptions and development history are available in the literature.[192]

For coal reburning, the fuel is introduced under a reduced temperature compared to a normal industrial coal flame. This suggests that higher conversions of volatile nitrogen to N_2O may occur than would be normally expected. At present, only very limited measurements have been reported in the open literature. In one subscale study, application of coal reburning to a gas-fired primary increased N_2O emissions from less than 1 to 11–13 ppm.[71] Although in terms of concentration this increase appears to be small, it represents a 6.5% conversion of fuel-nitrogen to N_2O. This is about an order of magnitude greater than the conversion found in coal-fired primary flame (0.7%). This is a little surprising because, according to the discussion on air staging in Section

8.1, one would expect that the N_2O would be destroyed at the final air staging point. Whether this trend for increased N_2O formation extrapolates to large-scale is yet to be seen. In contrast, reburning with natural gas over a coal-fired primary yielded a greater than 50% N_2O reduction.[71]

In their kinetic modeling study, Kilpinen *et al.*[193] studied natural gas reburning. They find no N_2O formation in the fuel-rich zone. If, however, the final air addition temperature is reduced below 1200 K then some of the HCN from the fuel-rich zone is irreversibly converted to N_2O. Such an air injection temperature is, however, too low for practical boiler operation since CO burnout times would become unacceptably long. They did not attempt to simulate coal reburning, in which such a temperature is far too low to provide adequate char burnout. They do find that the performance is strongly transport influenced, so it is difficult to extrapolate the findings to the coal case. It is, however, clear that gas reburning should be a good tool against primary zone N_2O, and that coal reburning may either form or destroy N_2O, depending on the initial primary zone concentration.

An approach similar to reburning has been attempted in fluidized beds, where natural gas was injected into the cyclone of a CFBC.[168] At substantial firing rates (of the order of 10% of the heat input), N_2O reductions of the order of 50% were achieved, compared with kinetic predictions of 90%. The difference was attributed to the effects of imperfect or finite-rate mixing, possible with a contribution due to heat loss. Alternately, the recent data of Glarborg *et al.*[62] suggest that the rate of the critical $N_2O + OH$ destruction reaction may be much slower than that used in the model. This may account for the discrepancy.

8.3. *Selective Noncatalytic Reduction*

Selective noncatalytic reduction (SNCR) had its origins in the observation that NH_3 would selectively react with NO under appropriate temperatures to yield N_2.[194] Many years of work have resulted in an excellent understanding of this process, which is summarized by Miller and Bowman.[57] The following reactions are important:

$$NH_3 + OH \rightarrow NH_2 + H_2O \quad (56)$$

$$NH_2 + NO \rightarrow N_2 + H_2O \quad (57)$$

$$NH_2 + NO \rightarrow NNH + OH \quad (58)$$

$$NNH + M \rightarrow N_2 + H + M \quad (59)$$

$$H + O_2 \rightarrow OH + O. \quad (60)$$

This reaction sequence is self-propagating under the correct conditions. The NH_2 that is consumed by Eq. (58) leads to the generation of OH radicals (via both Eqs (58) and (60)) needed to facilitate Eq. (56). The only significant acknowledged means for generating N_2O is the reaction

$$NH + NO \rightarrow N_2O + H. \quad (32)$$

Both modeling and experimental studies indicate that, while some N_2O is formed, it is a very minor product.[71-73,91] Faster oxidation reactions effectively compete for the NH under these conditions.

Alternative agents have been proposed to avoid the handling problems associated with NH_3 and to improve NO_x removal performance. The principal competitor for NH_3 is urea, $CO(NH_2)_2$.[195] The urea is injected as either an aqueous solution or a dry powder. Some controversy has surrounded the products of the initial thermal decomposition reaction. Arguments based on consistency between data and modeling suggest that the products are NH_3 + HNCO,[72,166] which has been confirmed by experiment.[73]

Once released into the gas phase, the HNCO reacts primarily according to the following sequence:

$$HNCO + OH \rightarrow NCO + H_2O \quad (40)$$

$$NCO + NO \rightarrow N_2O + CO \quad (29)$$

$$HNCO + H \rightarrow NH_2 + CO. \quad (61)$$

In the absence of other reactions, the chain branching associated with NH_2 and N_2O consumption must support the decomposition of HNCO. Other reactions (e.g., concurrent wet CO oxidation) can also provide the radicals needed to drive Eq. (40). The key difference between urea and NH_3 is that urea can generate HNCO, NCO, and N_2O as major products of reaction, NH_3 does not. Thus, as is well-known, urea generates substantially more N_2O emissions when used as an SNCR agent.[72,91] Typically, less than 5% of the NO reduced is converted to N_2O when NH_3 is used. This compares to conversions greater than 10% for urea (see Table 4).

The RapreNO_x process is another SNCR process based on the use of cyanuric acid as an agent.[196,197] The cyanuric acid thermally decomposes to yield HNCO, which reacts according to Eqs (40), (29), and (61) to destroy NO, in the course of which N_2O is formed as a by-product.[198]

Comparison of urea and cyanuric acid as agents shows that urea generates less N_2O under equivalent conditions. This is expected since only half of the nitrogen contained in the urea becomes associated with HNCO following injection. The other half forms NH_3 which does not yield significant N_2O. In the case of cyanuric acid injection, all of the nitrogen initially becomes HNCO, and thus final N_2O yields are increased.[72]

A major limitation of SNCR is the relatively narrow temperature window over which the agents are active at removing NO_x. Also, in large-scale facilities, NO removal at the optimum temperature is

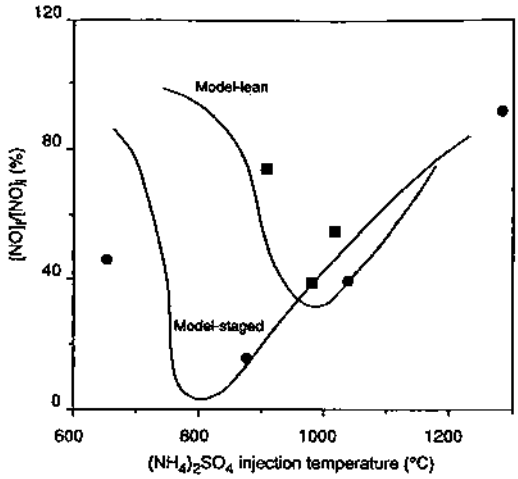

FIG. 36. Influence of promotion on SNCR performance. In this case, the promoter was provided by mild staging of the combustion process: ● SR_1 = 0.99, ■ SR = 1.25, SR_T = 1.02 (adapted from Chen *et al.*[199]).

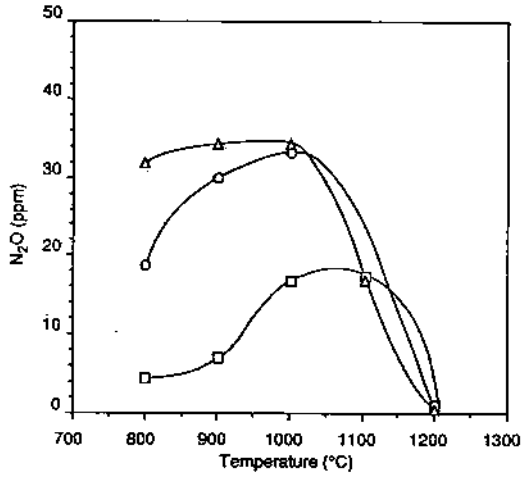

FIG. 37. Influence of CO promotion on N_2O emissions from urea injection, for initial NO = 125 ppm and additive at N/NO = 2: □ 0 ppm CO, ○ 500 ppm CO, △ 1000 ppm CO (adapted from Teixeira *et al.*[200]).

not complete. Thus, a considerable research effort has been expended to enhance performance. One approach is the co-injection of combustible promoting compounds (e.g., CO or H_2) with the agents. As shown in Fig. 36,[199] this has the effect of shifting the optimum temperature window to lower temperatures (in this case, the introduction of the combustible was achieved by staging). Depending on the amount of free oxygen present and the amount of combustible, the performance at the new optimum temperature can be either better or worse than the original unpromoted system. The temperature shifts because the oxidation of the combustible generates excess free radicals that are needed to initiate the reaction of the agent. Without the reaction of the combustible, the agent would not react at the lower temperature be-

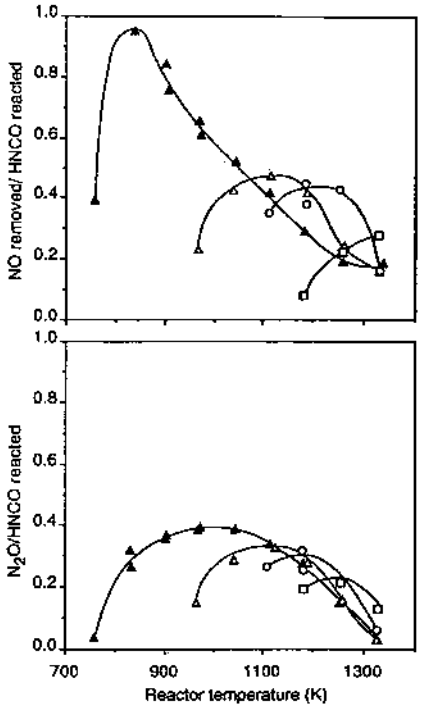

FIG. 38. Influence of hydrogen promotion on NO removal performance and N_2O formation during HNCO reaction: □ 0 ppm H_2, ○ 300 ppm H_2, △ 600 ppm H_2, ▲ 2950 ppm H_2 (adapted from Caton and Siebers[74]).

cause it cannot supply sufficient radicals through chain branching.

Figure 37 illustrates the effect of CO on urea performance.[200] Increased amounts of CO lead to a shift in the NO_x reduction window to lower temperatures, but do not dramatically change the width of the window. The N_2O formation window, however, is seen to increase in width with increasing CO. In another experiment, H_2 was used as a combustible promoter for the HNCO reaction.[74] In this case, as shown in Fig. 38, the combustible both promoted the NO_x removal performance and increased the N_2O emissions.

Kinetic modeling shows that the combustible acts to generate free radicals. These radicals promote agent decomposition: $HNCO + OH \rightarrow NCO + H_2O$. Next, N_2O forms via NCO + NO. At higher temperatures, the N_2O is destroyed by $N_2O + H$. At lower temperatures, the hydrogen atom is still available, but the relatively high activation energy prevents the $N_2O + H$ reaction from being effective. Thus, as the temperature window for NO removal is shifted to lower temperatures by the combustible, most of the reactions "follow" the window due to their weak temperature sensitivity. The $N_2O + H$ reaction is the exception due to its strong temperature dependence, and the N_2O produced from the agent reaction fails to react further.

The conclusion is that the presence of a combustible may or may not widen the SNCR window for

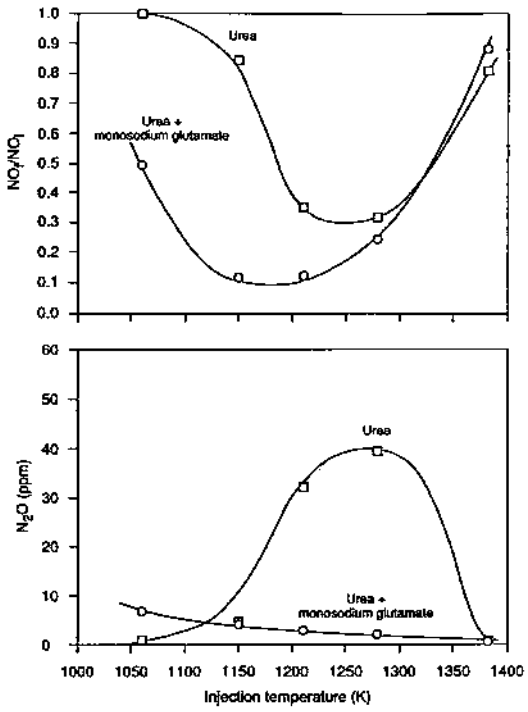

FIG. 39. Tunnel furnace results for NO reduction and N_2O formation for injection of urea and urea + monosodium glutamate (MSG). Conditions: NO_i = 300 ppm, urea injection ratio = 1.5 (expressed as N/NO), and MSG equivalent to 50 ppm sodium in the reactor gas (adapted from Chen *et al.*[201]).

urea injection, but that it appears to (1) reduce the temperature at which peak N_2O emissions are observed, and (2) increase these peak emissions. Note the similarity between this situation and that within a FBC. In a FBC, fuel-nitrogen in the form of HCN is released by the coal. This reacts in the presence of oxidizing coal volatiles. Thus, the combustibles within the volatiles can be viewed as "promoters", which tend to reduce the optimum temperature for NO reduction and N_2O formation. With sufficient combustibles present, as would be the case in a FBC, this optimum temperature would be reduced to < 700 °C. Thus, as temperature is increased, N_2O emissions would be expected to be reduced, and NO emission would increase, which is the normal characteristic of FBCs.

Recent experimental work suggests that sodium additives may be one effective means of reducing N_2O formation in SNCR. Chen *et al.*[201] performed tunnel furnace experiments in which a variety of sodium compounds were co-injected with urea. Figure 39 shows NO_x reduction and N_2O emissions as a function of urea injection temperature. The figure shows that urea promoted by monosodium glutamate gave both an increase in NO_x removal performance and a substantial reduction in N_2O emissions. Other sodium compounds, such as Na_2CO_3, also reduced N_2O emissions, although SO_2 tended to reduce effectiveness. This could be due to the formation of a nonreactive sulfate coating on the sodium particles, or through suppression of sodium volatility due to sulfate formation.

Use of NH_3 for NO_x reduction in FBCs has been extensively examined. The results indicate that little N_2O is generated until NH_3 is added in high stoichiometric excess over NO.[166,173,202] Urea injection, however, is strongly correlated with increased N_2O emissions.[166] However, fixed bed studies using quartz, clay, and ash show that, even with urea injection, N_2O yields are sharply depressed.[203] This suggests that appropriate inorganic surfaces can be used to suppress N_2O formation when urea is used as an SNCR agent.

8.4. *Selective Catalytic Reduction*

In the present context, selective catalytic reduction (SCR) refers to the reduction of NO by added NH_3 over a catalyst. This distinguishes it from processes involving other agents, such as CO, H_2, and CH_4. The process is, at present, applied only to stationary sources of NO_x, with mobile sources being dominated by direct catalytic reduction without the use of an agent such as NH_3. Selective catalytic reduction is currently being applied to industrial systems in Japan and Germany, and is being increasingly used in other parts of the world.

The formation of N_2O during SCR was noted in the early 1970s (e.g., Otto *et al.*[204]). A very detailed review of the fundamentals of SCR, including the problem of N_2O production, is available.[205] In addition, a general review of the application of catalysts to environmental problems is also available, which includes SCR and other topics.[206]

Most SCR systems are based on either noble metal catalysts or vanadium in combination with other metals and various substrates. Laboratory work suggests that N_2O can be a major product of SCR over noble metal catalysts.[207] The amount of N_2O formed depends on the state of the surface, and also on the nature of the substrate.[205] The formation appears to be due to a reaction through a Langmuir–Hinshelwood mechanism between two adsorbed NO molecules.[204] The nature of the platinum surface seems to have an effect, with single crystals not yielding significant N_2O. We were unable to find published field measurements on noble metal catalysts, although unpublished information suggests that a significant portion of the reduced NO can be converted into N_2O in practical installations on gas turbine sets.[208]

In addition to the general review of Bosch and Janssen,[205] the problem of N_2O formation over vanadium has been specifically reviewed by Odenbrand *et al.*[209] In earlier work, the proposed mechanism involved the reoxidation of the vanadium surface by adsorbed NO to yield reduced N_2O.[205] Recent work

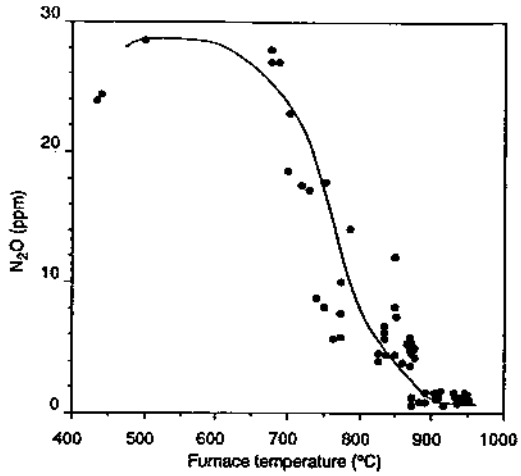

FIG. 40. Relationship between furnace temperature and emissions for a MSW incinerator (adapted from Iwasaki *et al.*[114]).

suggests that N_2O arises directly from the reaction of NH_3 and NO at low temperatures, and from direct NH_3 oxidation at high temperatures. Due to this mechanism, the minimum for NO_x emissions falls at a lower temperature than the maximum in N_2O emissions.[205,210] The practical consequence is that, below ~300 °C, only negligible N_2O is formed, while the formation becomes significant at higher temperatures due to NH_3 oxidation.[209] This is supported by long-term, pilot-scale testing of a wide number of vanadium catalysts.[211] Here, no significant N_2O was noted, at least to 400 °C. Since catalyst sintering starts to become a problem above these temperatures,[209] this is unlikely to be a common operating condition. A survey of N_2O emissions from 22 SCR installations in Japan indicated no emissions exceeding 1 ppm.[118]

Review of the data suggests that, within the broad bounds outlined above, the actual yield of N_2O is highly variable. It depends on catalyst type, catalyst treatment (e.g., crystal size), contamination, support, and background gas composition. It will likely depend on catalyst age. The results suggest that vanadium catalysts do not generate significant N_2O under their normal operating conditions, but that noble metal catalysts may.

8.5. *Summary*

In general, NO_x control procedures have led to significantly increased N_2O if they promote the reaction of cyano species under reduced temperature conditions. Thus, coal reburning may, under some conditions, lead to enhanced N_2O due to the release of fuel-nitrogen under reduced temperatures. However, the N_2O yields are somewhat reduced by the concurrent oxidation of volatiles, which leads to N_2O scavenging and competitive oxidation of the NCO intermediate.

The downstream injection of urea and cyanuric acid both lead to N_2O formation. Preliminary data suggest that concurrent injection of combustible promoters (e.g., CO or H_2) leads to increased N_2O formation as agent injection temperatures are reduced. The application of SCR suggests that N_2O emissions are negligible from vanadium catalysts if they are operated at their nominal low temperatures. Noble metal catalysts, however, can convert significant quantitites of NO into N_2O during SCR.

9. THERMAL WASTE REMEDIATION

To date, a limited number of field measurements have appeared describing emissions from thermal waste remediation activities. Almost all of these have dealt with municipal solid waste (MSW) or dried sewage sludge. The limited number of results currently available support only a qualitative description of the trends. Nonetheless, some significant differences between waste incineration and coal combustion are apparent.

Most of the measurements are on MSW units. The following data have been reported:

(1) Iwasaki *et al.*:[114] 10 units (8 stoker, 1 fluidized bed, 1 batch),
(2) Yasuda and Takahasi:[212] 5 units (2 grates, 3 fluidized beds),
(3) Hiraki *et al.*:[213] at least one unit, and
(4) Watanabe *et al.*:[214] 12 units (5 stokers, 5 fluidized beds, 2 rotary kilns).

As illustrated in Fig. 40, the most striking variation is the decrease in emissions with combustion temperature. In spite of the low combustion temperatures, however, the emissions of N_2O rarely exceed 20 ppm. This appears to be due at least partly to the relatively low nitrogen content of the fuel; Iwasaki *et al.*[114] report fuel-nitrogen contents of about 0.5% and emission factors of approximately 70 g N_2O/metric ton waste. This corresponds to a fractional conversion of fuel-nitrogen to N_2O of approximately 1%. Interestingly, none of the data suggest a consistent influence of combustor configuraton (fluidized bed vs stoker–grate) on emissions.

A smaller number of sludge incinerators were also examined, including:

(1) Iwasaki *et al.*:[114] 4 units (2 multistage and 2 fluidized beds),
(2) Yasuda and Takahasi:[212] 5 units (4 fluidized beds and 1 rotary grate), and
(3) Hiraki *et al.*:[213] at least one unit.

These units showed much higher emissions: in the case of Yasuda and Takahasi[212] up to 600 ppm. This appears to be primarily a response to the high nitrogen content of the sludge. Iwasaki *et al.*[114]

TABLE 16. Mobile source N_2O emission rates

(mg N_2O/km (mg N_2O/mi))*	Sigsby[215]†	Prigent and de Soete[216]	Dasch[217]
Noncatalyst auto	3.1–3.7 (5–6)	2.9 (4.8)	1.5–3.0 (2.4–4.8)
Catalyst auto	4.3–85.1 (7–137)	9.3–62.1 (15–100) oxidation or three-way catalyst	1.9–41.0 (3–66) oxidation catalyst 16.2–59.0 (26–95) dual bed catalyst 8.1–62.8 (13–101) three-way catalyst
Diesel trucks/buses	19.3–91.3 (31–147)		
Gasoline trucks	29.8–60.3 (48–97)		55.3 (89) light duty, three-way catalyst

* Numbers in parentheses have units of mg N_2O/mi.
† Compilation of test data from several sources.

report 5–8% fuel-nitrogen, with emission factors corresponding to 400 g N_2O/metric ton sludge. This still represents only a 0.5% conversion of fuel nitrogen. Yasuda and Takahasi[212] evaluated a sufficient number of units at various temperatures to suggest that higher temperatures in fluidized beds can reduce the very high N_2O emissions associated with sludge combustion.

Interestingly, the NO_x emissions were low enough not to be influenced in a significant way by the change in temperature. For MSW incineration, the NO_x levels were much higher.[114,212] Mixed MSW and sludge incineration appeared to take on the characteristics of "diluted" sludge incineration (i.e., increased N_2O emissions in proportion to the increased amount of fuel-nitrogen).

Very little work has been reported on other waste treatment activities. Emissions from liquid injection incineration of high nitrogen wastes have not been reported. The high temperatures that are typical of these units are not expected to support high N_2O emissions. Fume incinerators, however, may operate at much lower temperature. Frequently, the fume represents a relatively inert stream containing dilute fuel-nitrogen compounds. Many of these fumes have low heating values that must be supplemented by gas fuel to obtain a stable flame. For economic reasons, the gas usage is minimized, which can yield a low-temperature flame. Such an environment may favor N_2O emissions.

10. MOBILE SOURCES

While limited, the historical N_2O database for mobile sources appeared not to have been impacted by the sampling artifact. Although mobile source measurements using chassis dynamometers were often made by sample extraction using tedlar sampling bags and seldom performed on-line, SO_2 concentrations in mobile source vehicle emissions are many times smaller than those from stationary coal and heavy oil combustion. Thus, the sampling artifact which dominated measurements from coal-fired utility boilers did not seem to affect measurements from mobile sources. Mobile source emissions levels established in the early and mid-1980s, before the artifact issue was brought to light, compare favourably with measurements made in later years by researchers who were well aware of the potential sampling problems and took care to avoid the sampling artifact. Table 16 presents a comparison of N_2O emission rates for several classes of vehicles.[215–217] Of particular note is the good agreement among the values reported by the three groups, and the fact that catalytically equipped vehicles emit up to 20 times more N_2O than comparable noncatalyst equipped vehicles.

Based on the above results, a conservative estimate of 62.1 mg N_2O/km (100 mg N_2O/mile), and the 1982 estimate for the U.S. vehicle fleet size (115×10^6) and distance traveled (2.6×10^{12} km, 1.6×10^{12} miles),[215] the total U.S. production of N_2O from mobile sources is approximately 1.6×10^5 metric tons/yr (1.6×10^{11} g N_2O/yr, 1.0×10^{11} g N/yr, or 0.1 Tg N/yr). Assuming that the world fleet size and distance driven per year are three times that of the U.S., then worldwide mobile N_2O emissions are approximately 0.3 Tg N/yr. This value compares favorably with the values given in Table 3 and constitutes approximately 8.5% of the total anthropogenic flux. However, in addition to the uncertainties regarding fleet size and distance driven used in the above analysis, many research issues remain, including the applicability of different driving cycles to actual use, engine–emission control malfunction or nonoptimal operation, quantification of the number of vehicles that use catalysts (including type of catalyst), and the influence of ambient conditions.

11. EMISSIONS FROM INDUSTRIAL SOURCES

Few industrial sources have been identified as potential emitters of significant N_2O. One receiving recent attention is the manufacture of adipic acid, used primarily in the manufacture of nylon. By one report[218] the manufacture of adipic acid accounts for ca 10% of the anthropogenic flux to the troposphere, based on adipic acid production. This inven-

tory failed to take into account existing abatement within the industry, and an improved estimate is 5–8% of the anthropogenic flux.[219]

Adipic acid is formed by the reaction of cyclohexanone and cyclohexanol under nitric acid oxidation. The reaction produces an off-gas that contains 1 mol of N_2O by-product for each mole of adipic acid produced, along with some NO_x. This stream, which can contain 30–50 mol.% N_2O, is usually passed through an absorber to recover NO_x, and then vented to the atmosphere. Some plants incinerate the stream in process boilers to reduce NO_x, which coincidentally destroys the N_2O. In 1990, approximately 32% of the off-gas streams were abated in this manner.[219]

Since the recognition of adipic acid as a significant atmospheric source of N_2O, the industry has launched several co-operative projects to evaluate abatement options.[219] Some of these options have the goal of simply eliminating N_2O from the exhaust stream at the lowest cost. Others focus on converting N_2O into NO_x, which can then be used as a nitric acid feedstock. Approaches currently under evaluation include:

(1) N_2O decomposition over a catalyst to yield N_2 or NO_x for by-product recovery,
(2) high temperature N_2O thermal decomposition to yield NO_x as a recovered by product, and
(3) thermal destruction in boilers.

These co-operative projects have as a goal a substantial reduction in emissions from this source by 1996. It is recognized that no one technology is likely to be applicable to all plants because of site specific technical and economic factors.

Other industrial sources that involve the oxidation of nitrogen compounds under moderate temperature conditions are candidates as N_2O emitters. Examples mentioned in the literature are catalytic cracker regenerators.[31] These units are used in gasoline manufacture to regenerate the catalyst used to crack feedstock after it has become coated with nitrogen-rich coke. The coke is burned off the catalyst in a fluidized bed. Temperatures are moderate in the bed, fuel-nitrogen levels are high, and the volatile content of the coke is low. Thus, many of the factors that contribute to high N_2O emissions in fluidized bed coal combustion are present. To date, however, no emissions measurements have been reported.

12. CONCLUDING REMARKS

What we have attempted to do is bring together the widely scattered literature on the relatively new problem of N_2O emissions from energy conversion and industrial equipment, and the influence of these emissions on the environment. This is still an evolving area, where changes in both quantitative and qualitative interpretations are likely. Far from being the last word, this review will likely only act as a starting point for future work.

Within homogeneous chemistry, the principal issues include the products of the NCO + NO reaction, and the rates and products of the reactions consuming HCN and HNCO that give rise to NCO and other species in moderate temperature combustion. A significant amount of modeling effort has used rates for NCO + NO that are likely too high. Thus, the adequacy of homogeneous chemistry to explain N_2O yields in processes such as combustion fluidized beds and in selective noncatalytic reduction needs to be revisited.

A considerable amount of effort has gone into defining the influence of basic operating parameters on N_2O emissions from fluidized beds. While basic operating trends are now known, a clear mechanistic understanding is not yet complete. The relative roles of homogeneous vs. heterogeneous N_2O production are shrouded by the fact that char behavior is strongly dependent on the degree of devolatilization. Since fluidized beds contain chars of widely varying ages, the overall behavior represents an ensemble average. This has clearly complicated the task of identifying mechanistic information from actual fluidized bed data. Clean mechanistic experiments are needed, and these have begun to appear. Particularly useful studies include the examination of simulated differential fluidized bed elements. Another approach is to characterize bed response to perturbations in the gas-phase environment (e.g., the addition of N_2O or HCN into the feed air), or in the solid phase (e.g., the spiking of a well-characterized char into a combustor).

Acknowledgements/Disclaimer—We would like to thank Tom McGrath of the Energy and Environmental Research Corporation and Larry Muzio of the Fossil Energy Research Corporation for providing unpublished information on the generation of N_2O in SCR systems. E. K. Butcher and S. A. Osler aided the production of this work at the University of Washington. Portions of this work were conducted under EPA Purchase Order 2D1449NAEX with J. Kramlich. The research described in this review has been reviewed by the Air and Energy Engineering Research Laboratory, U.S. Environmental Protection Agency, and approved for publication. The contents of this review should not be construed to represent Agency policy nor does mention of trade names or commercial products constitute endorsement or recommendation for use.

REFERENCES

1. Ramanathan, V., *Science* **24**, 293 (1988).
2. Levine, J. S., The global atmospheric budget of nitrous oxide, and supplement: global change: atmospheric and climatic, *5th International Workshop on Nitrous Oxide Emissions*, Tsukuba, Japan (1992).
3. Houghton, J. T., Jenkins, G. J. and Ephraums, J. J., *Climate Change: The IPCC Scientific Assessment*, Cambridge University Press, Cambridge, UK (1990).
4. Levine, J. S., Nitrous oxide: sources and impact on atmospheric chemistry and global climate, Presented at: *LNETI/EPA/IFP European Workshop on the Emission of Nitrous Oxide*, Lisboa, Portugal (1990).

5. JANETOS, A., Overview and update of EPA's stratospheric ozone and global climate program, Presented at: *LNETI/EPA/IFP European Workshop on the Emission of Nitrous Oxide*, Lisboa, Portugal (1990).
6. CHAPMAN, S., *Quart. J. R. Meteorol. Soc.* **3**, 103 (1930).
7. CRUTZEN, P. J., *J. Geophys. Res.* **76**(30), 7311 (1971).
8. LEVINE, J. S., Impacts of N_2O and other trace gases on stratospheric ozone, *EPA/IFP European Workshop on the Emission of Nitrous Oxide from Fossil Fuel Combustion*, Rueil-Malmaison, France, June 1988, EPA-600/9-89-089 (NTIS PB90-126038) (1989).
9. WEISS, R. F., *J. Geophys. Res.* **86**, 7185 (1981).
10. RASMUSSEN, R. A. and KHALIL, M. A. K., *Science* **232**, 1623 (1986).
11. National Oceanic and Atmospheric Administration (NOAA), *Geophysical Monitoring for Climate Change*, Vol. 16, pp. 67, B. A. Bodhaine and R. M. Rosson (Eds), U.S. Dept of Commerce, Washington, DC (1988).
12. PRINN, R., CUNNOLD, D., RASSMUSSEN, R. A., SIMMONDS, P., ALYEA, R., CRAWFORD, A., FRASER, P. and ROSEN, R., *J. Geophys. Res.* **95**(18), 369 (1990).
13. KHALIL, M. A. K. and RASMUSSEN, R. A., *J. Geophys. Res.* **97**(D13), 14,651 (1992).
14. PEARMAN, G. I., ETHERIDGE, D., DE SILVA, F. and FRASER, P. J., *Nature* **320**(20), 248 (1986).
15. KHALIL, M. A. K. and RASMUSSEN, R. A., *Ann. Glaciol.* **10**, 73 (1988).
16. ETHRIDGE, D. M., PEARMAN, G. I. and DE SILVA, F., *Ann. Glaciol.* **10**, 28 (1988).
17. ZARDINI, D., RAYNAUD, R., SCHARFFE, D. and SEILER, W., *J. Atmos. Chem.* **8**, 198 (1989).
18. RAYNAUD, D., JOUZEL, J., BARNOLA, J. M., CHAPPELLAZ, J., DELMAS, R. J. and LORIUS, C., *Science* **259**, 926 (1993).
19. DE SOETE, G. G., General discussion, conclusions, and need for future work, Presented at: *LNETI/EPA/IFP European Workshop on the Emission of Nitrous Oxide*, Lisboa, Portugal (1990).
20. Intergovernmental Panel on Climate Change (IPCC, 1990), taken from Minami, K., N_2O emissions from soils and agro-environment, *5th International Workshop on Nitrous Oxide Emissions*, Tsukuba, Japan (1992).
21. Intergovernmental Panel on Climate Change (IPCC, 1992), taken from Minami, K., N_2O emissions from soils and agro-environment, *5th International Workshop on Nitrous Oxide Emissions*, Tsukuba, Japan (1992).
22. ELKINS, J. W., State of the research for atmospheric nitrous oxide (N_2O) in 1989, Intergovernmental Panel on Climate Change, National Oceanic and Atmospheric Administration (1989).
23. ELKINS, J. W., Current uncertainties in the global atmospheric nitrous oxide budget, Presented at: *LNETI/EPA/IFP European Workshop on the Emission of Nitrous Oxide*, Lisboa, Portugal (1990).
24. MANN, M. D., COLLINGS, M. E. and BOTROS, P. E., *Prog. Energy Combust. Sci.* **18**, 447 (1992).
25. HAO, W. M., WOFSY, S. C., MCELROY, M. B., BEER, J. M. and TOQAN, M. A., *J. Geophys. Res.* **92**(D3), 3098 (1987).
26. PIEROTTI, D. and RASMUSSEN, R. A., *Geophys. Res. Lett.* **3**, 265 (1976).
27. WEISS, R. F. and CRAIG, H., *Geophys. Res. Lett.* **3**, 751 (1976).
28. MUZIO, L. J. and KRAMLICH, J. C., *Geophys. Res. Lett.* **15**, 1369 (1988).
29. DE SOETE, G. G., Parametric study of N_2O formation from sulphur oxides and nitric oxide during storage of flue gas samples. Institut Français du Pétrole, Report No. 36 732-40 ex. (1988).
30. MUZIO, L. J., TEAGUE, M. E., KRAMLICH, J. C., COLE, J. A., MCCARTHY, J. M. and LYON, R. K., *J. Air Pollut. Control Assoc.* **39**, 287 (1989).
31. LYON, R. K. and COLE, J. A., *Combust. Flame* **77**, 139 (1989).
32. LYON, R. K., KRAMLICH, J. C. and COLE, J. A., *Environ. Sci. Technol.* **23**, 392 (1989).
33. LINAK, W. P., MCSORLEY, J. A., HALL, R. E., RYAN, J. V., SRIVASTAVA, R. K., WENDT, J. O. L. and MEREB, J. B., *J. Geophys. Res.* **95**(D6), 7533 (1990).
34. KHALIL, M. A. K. and RASMUSSEN, R. A., *J. Geophys. Res.* **97**(D13), 14,645 (1992).
35. CRAIG, H. and GORDON, L. I., *Geochim. Cosmochim. Acta* **27**, 949 (1963).
36 BOCK, R., and SCHUTZ, K. *Z. Anal. Chem.* **237**, 321 (1968).
37. LAHUE, M. D., AXELROD, H. D. and LODGE, J. P., Jr., *Anal. Chem.* **43**, 1113 (1971).
38. GOLDAN, P. D., BUSH, Y. A., FEHSENFELD, F. C., ALBRITTON, D. L., CRUTZEN, P. J., SCHNELTEKOPF, A. L. and FERGUSON, E. E., *J. Geophys. Res.* **83**, 935 (1978).
39. CICERONE, R. J., SHETTER, J. D., STEDMAN, D. H., KELLY, T. J. and LIU, S. C., *J. Geophys. Res.* **83**(C6), 3042 (1978).
40. SINGH, H. B., SALAS, L. J. and SHIGEISHI, H., *Tellus* **31**, 313 (1979).
41. WEISS, R. F., KEELING, C. D. and CRAIG, H., *J. Geophys. Res.* **86**(C8), 7197 (1981).
42. RYAN, J. V. and KARNS, S. A., Recommended operating procedure No. 56: collection of gaseous grab samples from combustion sources for nitrous oxide measurement, EPA-600/R-92-141 (NTIS PB92-216928) (1992).
43. RYAN, J. V. and KARNS, S. A. Development of sampling and analytical methods for the measurements of nitrous oxide from fossil fuel combustion sources, EPA-600/R-93-088 (NTIS PB93-194330) (1993).
44. DE SOETE, G. G., Formation of nitrous oxide from NO and SO_2 during solid fuel combustion, *In: 1989 Proc.: Joint Symposium on Stationary NO_x Control*, EPA-600/9-89-062b (NTIS PB89-220537) (1989).
45. DE SOETE, G. G., Heterogeneous N_2O and NO formation from bound nitrogen atoms during coal char combustion, *9th Members Conference of the International Flame Research Foundation*, Noordwijkerhout, The Netherlands (1989).
46. SLOAN, S. A. and LAIRD, C. K., *Atmos. Environ.* **24A**, 1199 (1990).
47. LANIER, W. S. and ROBINSON, S. B., EPA workshop on N_2O emission from combustion (Durham, NC, February 13–14, 1986), EPA-600/8-86-035 (NTIS PB87-113742) (1986).
48. BRIDEN, F. E., NATSCHKE, D. F. and SNODDY, R. B., The practical application of tunable diode laser infrared spectroscopy to the monitoring of nitrous oxide and other combustion process stream gases, *1991 Joint Symposium on Stationary Combustion NO_x Control*, Vol. 3, EPA-600/R-92-093c (NTIS PB93-212868) (1992).
49. MONTGOMERY, T. A., SAMUELSEN, G. S. and MUZIO, L. J., *J. Air Pollut. Control Assoc.* **39**(5), 721 (1989).
50. FORD, J. S., Recommended operating procedure No. 45; analysis of nitrous oxide from combustion sources, EPA-600/8-90-053 (NTIS PB90-238502) (1990).
51. RYAN, J. V. and LINAK, W. P., On-line measurement of nitrous oxide from combustion sources by automated gas chromatography, *5th International Workshop on Nitrous Oxide Emissions*, Tsukuba, Japan (1992).
52. BAULCH, D. L., DRYSDALE, D. D., HORNE, D. G. and LLOYD, A. C., *Evaluated Kinetic Data for High Temperature Reactions: Homogeneous Gas Phase Reactions of the H_2-N_2-O_2 System*, Vol. 2, CRC Press, Cleveland, OH (1973).
53. HANSON, R. K. and SALIMIAN, S., Survey of rate constants in the N/H/O system, *Combustion Chemistry*, W.

C. Gardiner (Ed.), Springer-Verlag, New York,. NY (1984).
54. Tsang, W. and Herron, J. T., *J. Phys. Chem. Ref. Data* **20**, 609 (1991).
55. Dindi, H. Tsaj, H.-M. and Branch, M. C., *Combust. Flame* **87**, 13 (1991).
56. Johnsson, J. E., Glarborg, P. and Dam-Johansen, K., Thermal dissociation of nitrous oxide at medium temperatures, *24th International Symposium on Combustion*, p. 917, The Combustion Institute, Pittsburgh, PA (1992).
57. Miller, J. A. and Bowman, C. T., *Prog. Energy Combust. Sci.* **15**, 287 (1989).
58. Hulgaard, T., Nitrous oxide from combustion, Ph.D. Dissertation, Technical University of Denmark, Lyngby, Denmark (1991).
59. Fujii, N., Sagawai, S., Sato, T., Nosaka, Y. and Miyana, H., *J. Phys. Chem.* **93**, 5474 (1989).
60. Malte, P. C. and Pratt, D. T., *Combust. Sci. Technol.* **9**, 221 (1974).
61. Michaud, M. G., Westmorland, P. R. and Feitelberg, A. S., Chemical mechanism of NO_x formation for gas turbine conditions, *24th International Symposium on Combustion*, p. 879, The Combustion Institute, Pittsburgh, PA (1992).
62. Glarborg, P., Johnsson, J. E. and Dam-Johansen, K., Kinetics of nitrous oxide decomposition, *Combust. Flame*, in press.
63. Hidaka, Y., Takuma, H. and Suga, M., *Bull. Chem. Soc. Jpn* **58**, 2911 (1985).
64. Davidson, D. F., DiRosa, M. D. Chang, A. Y. and Hanson, R. K., Shock tube measurements of the major products channels of $N_2O + O$, *18th International Symposium on Shock Waves* (1991).
65. Marshall, P., Fontijn, A. and Melius, C. F., *J. Chem. Phys.* **86**, 5540 (1987).
66. Marshall, P., Ko, T. and Fontijn, A., *J. Phys. Chem.* **93**, 1922 (1989).
67. Martin, R. J. and Brown, N. J., *Combust. Flame* **82**, 312 (1990).
68. Biermann, H. W., Zetzsch, C. and Stuhl, F., *Ber. Bunseng, Phys, Chem.* **80**, 909 (1976).
69. Chang, J. S. and Kaufmann, F., *Geophys. Res. Lett.* 4, 192 (1977).
70. Schofield, K., Comment to paper by Bian, J., Vandooren, J. and Van Tiggelen, P. J. Experimental study of the structure of ammonia-oxygen flame, *21st International Symposium on Combustion*, p. 953, The Combustion Institute, Pittsburgh, PA (1987).
71. Kramlich, J. C., Cole, J. A., McCarthy, J. M., Lanier, W. S. and McSorley, J. A., *Combust. Flame* **77**, 375 (1989).
72. Muzio, L. J., Martz, T. D., Montomery, T. A., Quartucy, G. C., Cole, J. A. and Kramlich, J. C., N_2O formation in selective non-catalytic NO_x reduction processes, *American Flame Research Committee 1990 Fall International Symposium* (1990).
73. Caton, J. A. and Siebers, D. L., *Combust Sci. Technol.* **65**, 277 (1989).
74. Caton, J. A. and Siebers, D. L., Effects of hydrogen addition on the removal of nitric oxide by cyanuric acid, *23rd International Symposium on Combustion*, p. 225, The Combustion Institute, Pittsburgh, PA (1991).
75. Lyon, R. K. and Cole, J. A., *Combust. Flame* **82**, 435 (1990).
76. Miller, J. A. and Bowman, C. T., *Int. J. Chem. Kinet.* **23**, 289 (1991).
77. Perry, R. A., *J. Chem. Phys.* **82**, 5485 (1985).
78. Atakan, B. and Wolfrum, J., *Chem. Phys. Lett.* **178**, 157 (1991).
79. Mertens, J. D., Dean, A. J., Hanson, R. K. and Bowman, C. T., A shock tube study of the reactions of NCO with O and NO using NCO laser absorption, *24th International Symposium on Combustion*, p. 701, The Combustion Institute, Pittsburgh, PA (1992).
80. Fifer, R. A. and Holmes, H. E., *J. Phys. Chem.* **88**, 2935 (1982).
81. Cookson, J. L., Hancock, G. and McKendrick, K. G., *Ber. Bunsenges. Phys. Chem.* **89**, 335 (1985).
82. Cooper, W. F. and Hershberger, J. F., *J. Phys. Chem.* **96**, 771 (1992).
83. Zahniser, M. S., McCurdy, K. and Kolb, C. E., Data reported in Miller, J. A. and Bowman, C. T., *Prog. Energy Combust. Sci.* **15**, 287 (1989).
84. Baulch, D. L., Cox, R. A., Just, T., Kerr, J. A., Pilling, M. J., Troe, J., Walker, R. W. and Warnatz, J., *J. Phys. Chem. Ref. Data* **21**, 411 (1992).
85. Becker, K. H., Kurtenbach, R. and Wiesen, P., Investigation of the N_2O formation in the NCO + NO reaction by Fourier-transform infrared spectroscopy, *5th International Workshop on Nitrous Oxide Emissions*, Tsukuba, Japan (1992).
86. Miller, J. A. and Melius, C. F., The reactions of imidogen with nitric oxide and molecular oxygen, *23rd International Symposium on Combustion*, p. 719, The Combustion Institute, Pittsburgh, PA (1992).
87. Mertens, J. D., Chang, A. Y., Hanson, R. K. and Bowman, C. T., *Int. J. Chem. Kinet.* **23**, 173 (1991).
88. Glarborg, P., Miller, J. A. and Kee, R. J., *Combust. Flame* **65**, 177 (1986).
89. Bian, J., Vandooren, J. and Van Tiggelen, P. J., Experimental study of the formation of nitrous and nitric oxides in H_2-O_2-Ar flames seeded with NO and/or NH_3. *23rd International Symposium on Combustion*, p. 379, The Combustion Institute, Pittsburgh, PA (1991).
90. Morley, C., The mechanism of NO formation from nitrogen compounds in hydrogen flames studied by laser fluorescence, *18th International Symposium on Combustion*, p. 23, The Combustion Institute, Pittsburgh, PA (1981).
91. Kilpinen, P. and Hupa, M., *Combust. Flame* **85**, 94 (1991).
92. Gaydon, A. G. and Wolfhard, H. G., Spectroscopic studies of low-pressure flames, *3rd Symposium Combustion, Flame and Explosion Phenomena*, p. 504, Williams and Wilkins, Baltimore, MD (1949).
93. Wolfhard, H. G. and Parker, W. G., Spectra and combustion mechanism of flames supported by the oxides of nitrogen, *5th International Symposium on Combustion*, p. 718, Reinhold, New York, NY (1955).
94. Anderson, W. R., Decker, L. J. and Kotlar, A. J., *Combust. Flame* **48**, 178 (1982).
95. Vanderhoff, J. A., Beyer, R. A., Kotlar, A. J. and Anderson, W. R., *Combust. Flame* **49**, 197, (1983).
96. Habeebullah, M. B., Alasfour, F. N. and Branch, M. C., Structure and kinetics of CH_4/N_2O flames, *23rd International Symposium on Combustion*, p. 371, The Combustion Institute, Pittsburgh, PA (1991).
97. Zabarnick, S., *Combust. Sci. Technol.* **83**, 115 (1992).
98. Roby, R. J. and Bowman, C. T., *Combust. Flame* **70**, 119 (1987).
99. Di Julio, S. S. and Knuth, E. L., *Combust. Sci. Technol.* **66**, 149 (1989).
100. Martin, R. J. and Brown, N. J., *Combust. Flame* **80**, 238 (1990).
101. Borghi, R., *Prog. Energy Combust. Sci.* **14**, 245 (1988).
102. Houser, T. J. and Lee, P. K., *Combust. Sci. Technol.* **23**, 177 (1980).
103. Houser, T. J., McCarville, M. E. and Houser, B. D., *Combust. Sci. Technol.* **27**, 183 (1982).
104. Houser, T. J., McCarville, M. E. and Zhuo-Ying, G., *Fuel* **67**, 642 (1988).
105. Wolfrum, J., *Chemie Ingenieur Technik* **44**, 656 (1972).

106. DRAKE, M. C., RATCLIFFE, J. W., BLINT, R. J., CARTER, C. D. and LAURENDEAU, N. M., Measurements and modeling of flamefront NO formation and superequilibrium radical concentrations in laminar high-pressure premixed flames, *23rd International Symposium on Combustion*, p. 387, The Combustion Institute, Pittsburgh, PA (1991).
107. KRAMLICH, J. C., NIHART, R. K., CHEN, S. L., PERSHING, D. W. and HEAP, M. P., *Combust. Flame* **48**, 101 (1982).
108. CHEN, S.-L., HEAP, M. P., PERSHING, D. W. and MARTIN, G. B., *Fuel* **61**, 1218 (1982).
109. CHEN, S.-L., HEAP, M. P., PERSHING, D. W. and MARTIN, G. B., Influence of coal composition on the fate of volatile and char nitrogen during combustion, *19th International Symposium on Combustion*, p. 1271, The Combustion Institute, Pittsburgh, PA (1983).
110. KRAMLICH, J. C., SEEKER, W. R. and SAMUELSEN, G. S., *Fuel* **67**, 1182 (1988).
111. AXWORTHY, A. E., DAYAN, V. H. and MARTIN, G. B., *Fuel* **57**, 29 (1978).
112. AXWORTHY, A. E., KAHN, D. R., DAYAN, V. H. and WOOLERY, D. O., Fuel decomposition and flame reactions in conversion of fuel nitrogen to NO_x, EPA-600/7-81-158 (NTIS PB82-108358) (1981).
113. MUZIO, L. J., MONTGOMERY, T. A., SAMUELSEN, G. S., KRAMLICH, J. C., LYON, R. K. and KOKKINOS, A., Formation and measurement of N_2O in combustion systems, *23rd International Symposium on Combustion*, p. 245, The Combustion Institute, Pittsburgh, PA (1990).
114. IWASAKI, Y., TATSUICHI, S. and UENO, H., N_2O emissions from stationary sources, *5th International Workshop on Nitrous Oxide Emissions*, Tsukuba, Japan (1992).
115. RYAN, J. V. and SRIVASTAVA, R. K., *EPA/IFP European Workshop on the Emission of Nitrous Oxide from Fossil Fuel Combustion*, Rueil-Malmaison, France, June 1988, EPA-600/9-89-089 (NTIS PB90-126038) (1989).
116. VITOVEC, W. and HACKL, A., Pyrogenic N_2O emissions in Austria—measurement at 45 combustion sources, *5th International Workshop on Nitrous Oxide Emissions*, Tsukuba, Japan (1992).
117. YOKOYAMA, T., NISHINOMIYA, S. and MATSUDA, H., N_2O emissions from fossil fuel fired power plants. *5th International Workshop on Nitrous Oxide Emissions*, Tsukuba, Japan (1992).
118. YOKOYAMA, T., NISHINOMIYA, S. and MATSUDA, H., *Environ. Sci. Technol.* **25**, 347 (1991).
119. DE SOETE, G. G., Heterogeneous N_2O and NO formation from bound nitrogen atoms during coal char combustion, *23rd International Symposium on Combustion*, p. 1257, The Combustion Institute, Pittsburgh, PA (1991).
120. DE SOETE, G. G., Heterogeneous N_2O reactions related to combustion, *5th International Workshop on Nitrous Oxide Emissions*, Tsukuba, Japan (1992).
121. SANTALA, P., IISA, K. and HUPA, M., Report 90-6, Abo Akademi, Turku, Finland (1990).
122. MIETTINEN, H., STRÖMBERG, D. and LINDQUIST, O., The influence of some oxide and sulphate surfaces on N_2O decomposition, *Fluidized Bed Combustion: ASME 1991*, 999 (1991).
123. MORITOMI, H., SUZUKI, Y., KIDO, N. and OGISU, Y., NO_x formation mechanism of circulating fluidized bed combustion, *Fluidized Bed Combustion: ASME 1991*, 1005 (1991).
124. KHAN, T., LEE, Y. Y. and YOUNG, L., Heterogeneous decomposition of nitrous oxide in the operating temperature range of circulating fluidized bed combustors, *1991 Joint Symposium on Stationary Combustion NO_x Control*, Vol. 3, EPA-600/R-92-093c (NTIS PB93-212868) (1992).
125. GULYURTLU, I., ESPARTEIRO, H. and CABRITA, I., N_2O reactions with char in a fluidized bed combustor, *5th International Workshop on Nitrous Oxide Emissions*, Tsukuba, Japan (1992).
126. AHO, M. J. and RANTANEN, J. T., *Fuel* **68**, 586 (1989).
127. TULLIN, C. J., SAROFIM, A. F. and BEÉR, J. M., *J. Inst. Energy* **66**, 207 (1993).
128. KRAMMER, G. F. and SAROFIM, A. F., *Combust. Flame* **97**, 118 (1994).
129. MOCHIZUKI, M., KOIKE, J. and HORIO, M., The mechanisms of N_2O formation from fluidized bed char combustion, *5th International Workshop on Nitrous Oxide Emissions*, Tsukuba, Japan (1992).
130. ÅMAND, L.-E., LECHNER, B., ANDERSSON, S. and GUSTAVSSON, L., N_2O from circulating fluidized bed boilers-present status. Presented at *LNETI/EPA/IFP European Workshop on the Emission of Nitrous Oxide*, Lisboa, Portugal (1990).
131. TULLIN, C. J., GOEL, A., MORIHARA, A., SAROFIM, A. F. and BEÉR, J. M., *Energy Fuels* **7**, 796 (1993).
132. SONG, H. H., BEÉR, J. M. and SAROFIM, A. F., *Combust. Sci. Technol.* **28**, 177 (1982).
133. SUZUKI, Y., MORITOMI, H., KIDO, N., IKEDA, M., SUZUKI, K. and TORIKAI, K., N_2O formation from char and heterogeneous reactions with char and CaO, *5th International Workshop on Nitrous Oxide Emissions*, Tsukuba, Japan (1992).
134. THOMAS, K. M., GRANT, K. and TATE, K., *Fuel* **72**, 941 (1993).
135. FRIEHAUT, J. D. and PROSCIUA, W. M., *Energy Fuels* **3**, 625 (1989).
136. ELLIOTT, M. A. (Ed.), *Chemistry of Coal Utilization: 2nd Suppl. Volume*, Wiley, New York, NY (1981).
137. KASOAKA, S., SASOLOKA, E. and OZAKI, A., *Nenryo Kyokai Shi* (*Fuel Association Journal*) **62**, 669 (1983).
138. DE SOETE, G. G. and NASTOLL, W., *10th Members Conference of the IFRF*, Noordwijkerhout, The Netherlands (1992).
139. KHAN, T., LEE, Y. Y. and BROWN, R. A., N_2O bench scale studies, *5th International Workshop on Nitrous Oxide Emissions*, Tsukuba, Japan (1992).
140. JOHNSSON, J. E., Nitrous oxide formation and destruction in fluidized bed combustion—a literature review of the kinetics, *23rd IEA Meeting*, Firenze, Italy (1991).
141. HANSEN, P. F. B., DAM-JOHANSEN, K., JOHNSSON, J. E. and HULGAARD, T., *Chem. Eng. Sci.* **47**, 2419 (1992).
142. KLEIN, M., KÖSER, H. and ROTZOLL, G., Catalytic N_2O destruction by alkaline earth oxides in flue gases and fluidized-bed combustors, *5th International Workshop on Nitrous Oxide Emissions*, Tsukuba, Japan (1992).
143. BORGWARDT, R. H., *Chem. Eng. Sci.* **44**, 53 (1989).
144. NEWTON, G. H., CHEN, S.-L. and KRAMLICH, J. C., *AIChE J.* **35**, 988 (1989).
145. IISA, K., SALOKOSKI, P. and HUPA, M., Heterogeneous formation and destruction of nitrous oxide under fluidized bed combustion conditions, *Fluidized Bed Combustion: ASME 1991*, 1027 (1991).
146. HANSEN, P. F. B., Sulfur capture under fluidized bed conditions, Ph.D. Dissertation, The Technical University of Denmark; Lyngby, Denmark (1991).
147. KOCAEFE, D., KARMAN, D. and STEWARD, F. R., *AIChE J.* **33**, 1835 (1987).
148. IVARRSON, E. V., NO_x and N_2O emissions from a pressurized bench-scale fluidized bed reactor, Licentiate of Engineering Thesis, Chalmers Technical University, Göteborg, Sweden (1990).
149. CASTALDINI, C., DEROSIER, R., WATERLAND, L. R. and MASON, H. B., Environmental assessment of industrial process combustion equipment modified for low-

NO_x operation, *1982 Joint Symposium on Stationary Combustion NO_x Control*, EPA-600/9-85-022b (NTIS PB85-235612) (1985).
150. Hao, W. M., Wofsy, S. C., McElroy, M. B., Farmayan, W. F., Toqan, M. A., Beér, J. M., Zahniser, M. S., Silver, J. A. and Kolb, C. E., *Combust. Sci. Technol.* 55, 23 (1987).
151. Laird, C. K. and Sloan, S. A., *Atmos. Environ.* 27A, 1453 (1993).
152. Persson, K., N_2O emissions from coal fired boilers during thermal NO_x reduction tests: Experiences from SWEDCO-supported projects, Presented at: *LNETI/-EPA/IFP European Workshop on the Emission of Nitrous Oxide*, Lisboa, Portugal (1990).
153. Sage, P. W., Nitrous oxide emissions from coal-fired plant: An update on the Joule collaborative project, *5th International Workshop on Nitrous Oxide Emissions*, Tsukuba, Japan (1992).
154. Soelberg, N. R., Characterization of NO_x in utility flue gases, Test Report for Canadian Electrical Association, Energy and Environmental Research Corp., Irvine, CA (1989).
155. Smart, J. P., Roberts, P. A. and de Soete, G. G., *J. Inst. Energy* 63, 131 (1990).
156. Abbas, T., Costa, M., Costen, P. and Lockwood, F., *Combust. Flame* 87, 104 (1991).
157. Aho, M. J., Rantanen, J. T. and Linna, V. L., *Fuel* 69, 957 (1990).
158. Aho, M. J., Hämäläinen, J. P. and Tummauuori, J. L., *Fuel* 72, 837 (1993).
159. Hein, K. R. G., N_2O emissions from the combustion of low calorie coals—research and large scale experience, *5th International Workshop on Nitrous Oxide Emissions*, Tsukuba, Japan (1992).
160. Okazaki, K., Niwa, T. and Verma, S. S., N_2O formation and destruction behaviors in pulverized coal combustion at low temperatures, *5th International Workshop on Nitrous Oxide Emissions*, Tsukuba, Japan (1992).
161. Hampartsoumian, E., Nimmo, W., Clarke, A. G. and Williams, A., *Combust. Flame* 85, 499 (1991).
162. Hayhurst, A. N. and Lawrence, A. D., *Prog. Energy Combust. Sci.* 18, 529 (1992).
163. Moritomi, H. (Ed.), *Proc. 5th International Workshop on Nitrous Oxide Emissions*, Tsukuba, Japan (1992).
164. Åmand, L.-E. and Lechner, B., *Combust. Flame* 84, 181 (1991).
165. Åmand, L.-E., Lechner, B. and Andersson, S., Formation of N_2O in circulating fluidized bed boilers, *2nd Nordic Conference on Control of SO_2 and NO_x Emissions from Combustion of Solid Fuels*, Lyngby, Denmark (1990).
166. Braun, A., Bu, C., Renz, U., Drischel, J. and Köser, H. J. K., Emission of NO and N_2O from a 4 MW fluidized bed combustor with NO reduction, *Fluidized Bed Combustion: ASME 1991*, 709 (1991).
167. Brown, R. A. and Muzio, L. J., N_2O emissions from fluidized bed combustion, *Fluidized Bed Combustion: ASME 1991*, 719 (1991).
168. Gustavsson, L. and Leckner, B., N_2O reduction with gas injection in circulating fluidized bed boilers, *Fluidized Bed Combustion: ASME 1991*, 677 (1991).
169. Hiltunen, M., Kilpinen, P., Hupa, M. and Lee, Y., N_2O emissions from CFB boilers: experimental results and chemical interpretation, *Fluidized Bed Combustion: ASME 1991*, 687 (1991).
170. Wójtowicz, M. A., Oude Lohuis, J. A., Tromp, P. J. J. and Moulijn, J. A., N_2O formation in fluidized-bed combustion of coal, *Fluidized Bed Combustion: ASME 1991*, 1013 (1991).
171. Shimazu, T., Tachiyama, Y., Kuroda, A. and Inagaki, M., *Fuel* 71, 841 (1992).
172. Wallman, P. H., Ivarsson, E. L. and Carlsson, R. C. J., NO_x and N_2O formation in pressurized fluidized-bed combustion tests, *Fluidized Bed Combustion: ASME 1991*, 1021 (1991).
173. Jahkola, A., Lu, Y. and Hippinen, I., The emission and reduction of NO_x and N_2O in PFB-combustion of peat and coal, *Fluidized Bed Combustion: ASME 1991*, 725 (1991).
174. Naruse, I., Imanari, M., Koizumi, K. and Ohtake, K., N_2O formation and destruction characteristics in bubbling fluidized bed combustion, *5th International Workshop on Nitrous Oxide Emissions*, Tsukuba, Japan (1992).
175. Kimura, N., N_2O emission levels at Wakamatsu 50 MW AFBC plant and N_2O control technologies, *5th International Workshop on Nitrous Oxide Emissions*, Tsukuba, Japan (1992).
176. Fujiwara, N., Yamamoto, M., Nishiyama, A. and Kimura, N., Experimental study on the formation of N_2O from bubbling fluidized bed combustion. *5th International Workshop on Nitrous Oxide Emissions*, Tsukuba, Japan (1992).
177. Andries, J. and Hein, K. R. G., N_2O emissions from pressurized fluidized bed combustion of coal, *5th International Workshop on Nitrous Oxide Emissions*, Tsukuba, Japan (1992).
178. Lu, Y., Hippinen, I. and Jahkola, A., A comparison of different parameters in reducing of N_2O emissions in pressurized fluidized bed combustion, *5th International Workshop on Nitrous Oxide Emissions*, Tsukuba, Japan (1992).
179. Lu, Y., Jahkola, A., Hippinen, I. and Jalouaara, J., *Fuel* 71, 693 (1992).
180. Moritomi, H. and Suzuki, Y., N_2O emissions from circulating fluidized bed combustion, *4th China–Japan Fluid Bed Symposium* (1991).
181. Oude Lohuis, J. A., Tromp, P. J. J. and Moulijn, J. A., *Fuel* 71, 9 (1992).
182. Gavin, D. G. and Dorrington, M. A., *Fuel* 72, 381 (1993).
183. Naruse, I., Yamamoto, Y., Imanari, M., Yuan, J.-W. and Ohtake, K., Study on N_2O formation/destruction characteristics in coal combustion under wide temperature range, *24th International Symposium on Combustion*, p. 1415, The Combustion Institute, Pittsburgh, PA (1992).
184. Pels, J. R., Wójtowicz, M. A. and Moulijn, J. A., *Fuel* 72, 373 (1993).
185. Linak, W. P. and Peterson, T. W., Mechanisms governing the composition and size distribution of ash aerosol in a laboratory pulverized coal combustor, *21st International Symposium on Combustion*, p. 399, The Combustion Institute, Pittsburgh, PA (1986).
186. Hirama, T. and Hosoda, H., N_2O emissions from bubbling and circulating fluidized bed combustors, *5th International Workshop on Nitrous Oxide Emissions*, Tsukuba, Japan (1992).
187. Åmand, L.-E. and Lechner, B., *Energy Fuels* 7, 1097 (1993).
188. Dam-Johansen, K., Åmand, L.-E. and Lechner, B., *Fuel* 27, 565 (1993).
189. Tullin, C. J., Sarofim, A. F. and Beér, J. M., *Ind. Eng. Chem. Res.*, in press (1994).
190. Shimizu, T., Tachiyama, Y., Souma, M. and Inagaki, M., Emission control of NO_x and N_2O of bubbling fluidized bed combustor, *Fluidized Bed Combustion: ASME 1991*, 695 (1991).
191. Bramer, E. A. and Valk, M., Nitrous oxide and nitric oxide emissions by fluidized bed combustion, *Fluidized Bed Combustion: ASME 1991*, 701 (1991).
192. Chen, S.-L., McCarthy, J. M., Clark, W. D., Heap, M. P., Seeker, W. R. and Pershing, D. W., Bench and pilot scale process evaluation of reburning for in-

furnace NO_x reduction, *21st International Symposium on Combustion*, p. 1159, The Combustion Institute, Pittsburgh, PA (1987).
193. KILPINEN, P., GLARBORG, P. and HUPA, M., *Ind. Eng. Chem. Res.* **31**, 1477 (1992).
194. LYON, R. K., Method for the reduction of the concentration of NO in combustion effluents using ammonia, U.S. Patent 3,900,544 (1975).
195. ARAND, J. K., MUZIO, L. J. and SOTTER, J. G., Urea reduction of NO_x in combustion effluents, U.S. Patent 4,208,386 (1980).
196. PERRY, R. A. and SIEBERS, D. L., *Nature* **324**, 657 (1986).
197. PERRY, R. A., NO reduction using sublimation of cyanuric acid, U.S. Patent 4,731, 231 (1988).
198. SIEBERS, D. L. and CATON, J. A., *Combust. Flame* **79**, 31 (1990).
199. CHEN, S.-L., COLE, J. A., HEAP, M. P., KRAMLICH, J. C., MCCARTHY, J. M. and PERSHING, D. W., Advanced NO_x reduction processes using –NH and –CN compounds in conjunction with staged air addition, *22nd International Symposium on Combustion*, p. 1135, The Combustion Institute, Pittsburgh, PA (1989).
200. TEIXEIRA, D. P., MUZIO, L. J., MONTGOMERY, T. A., QUARTUCY, G. C. and MARTZ, T. D., Widening the urea temperature window, *1991 Joint Symposium on Stationary Combustion NO_x Control*, Vol. 3, EPA-600/R-92-093c (NTIS PB93-212868) (1992).
201. CHEN, S.-L., SEEKER, W. R., LYON, R. K. and HO, L., N_2O decomposition catalyzed in the gas phase by sodium, *1993 ACS Meeting*, Denver, CO (1993).
202. ÅMAND, L.-E. and ANDERSSON, S., Emission of nitrous oxide (N_2O) from fluidized bed boilers, *Proceedings 10th Int. Conf. on FBC*, San Francisco, CA (1989).
203. WALLMAN, P. H. and CARLSSON, R. C. J., *Fuel* **72**, 187 (1993).
204. OTTO, K., SHELEF, M. and KUMMER, J. T., *J. Phys. Chem.* **75**, 875 (1971).
205. BOSCH, H. and JANSSEN, F., *Catal. Today* **2**, 369 (1988).
206. ARMOR, J. N., *Appl. Catal. B.* **1**, 221 (1992).
207. MEIER, H. and GUT, G., *Chem. Eng. Sci.* **33**, 123 (1978).
208. MUZIO, L. J., Fossil Energy Research Corp., personal communication (1993).
209. ODENBRAND, C. U. I., GABRIELSSON, P. L. T., BRANDIN, J. G. M. and ANDERSSON, L. A. H., *Appl. Catal.* **78**, 109 (1991).
210. DE SOETE, G. G., Nitrous oxide formation and destruction by industrial NO abatement techniques, including SCR, Institut Français du Pétrole, Report No. 37 755-10 ex., Presented at the Spring 1990 AFRC Meeting, Tucson, AZ (1990).
211. MCGRATH, T., Energy and Environmental Research Corp., personal communication (1993).
212. YASUDA, K. and TAKAHASI, M., Emissions of nitrous oxide from waste management system, *5th International Workshop on Nitrous Oxide Emissions*, Tsukuba, Japan (1992).
213. HIRAKI, T., SHOGA, M., TAMAKI, M. and OTA, S., N_2O emission factor of stationary combustion sources and N_2O removal effect by ordinary flue gas treatment, *5th International Workshop on Nitrous Oxide Emissions*, Tsukuba, Japan (1992).
214. WATANABE, I., SATO, M., MIYAZAKI, M. and TANAKA, M., Emission rate of N_2O from municipal solid waste incinerators, *5th International Workshop on Nitrous Oxide Emissions*, Tsukuba, Japan (1992).
215. SIGSBY, J. E., N_2O emission rates from mobile sources, Session III, *EPA Workshop on N_2O Emissions from Combustion*, Durham, NC, February 1986, EPA-600/8-86-035 (NTIS PB87-113742) (1986).
216. PRIGENT, M. F. and DE SOETE, G. G., Nitrous oxide (N_2O) in engines exhaust gases. A first appraisal of catalyst impact, *1989 SAE International Congress and Exposition* (890492), Detroit, MI (1989).
217. DASCH, J. M., *J. Air Waste Manage. Assoc.* **42(1)**, 63 (1992).
218. THIEMENS, M. H. and TROGLER, W. C., *Science* **251**, 932 (1991).
219. REIMER, R. A., PARRETT, R. A. and SLATEN, C. S., Abatement of N_2O emissions produced in adipic acid manufacture, *5th International Workshop on Nitrous Oxide Emissions*, Tsukuba, Japan (1992).